

**SYNTHESIS OF A GANGLIOSIDE GM1 ANCHOR FOR MEMBRANE TETHERED LIGANDS OF
G-PROTEIN COUPLED RECEPTORS**

A SENIOR HONORS THESIS WRITTEN BY

ERIENE-HEIDI SIDHOM

TUFTS UNIVERSITY

MAY 2013

ADVISOR: PROFESSOR KRISHNA KUMAR

ABSTRACT

G-protein coupled receptors, as a class of proteins, are most important therapeutically. It is estimated that over 50% of prescription drugs target these receptors.¹ At nearly 1000 proteins, this family is divided into 5 classes, or families. The largest of these is Class A, the Rhodopsin family. This class is identifiable by conserved sequences which are critical for membrane activation. Among these receptors is Chemokine-like Receptor 1 (CMKLR1 or Chem32), which is most highly expressed on leukocytes. Its natural ligand, chemerin, is shown to have chemoattractant capabilities and other pro-inflammatory characteristics.²⁻⁶ However, therapeutically promising are the short C-terminal peptides, naturally derived from the bioactivation of chemerin, which show potent antagonist and anti-inflammatory properties.⁷ Learning more about this receptor could be important, especially for its therapeutic implications.

Classically, the targeting of GPCRs has been done through soluble ligands which bind to extracellular orthosteric or allosteric binding sites. However, in 2002, a new method of targeting receptors, termed pepducins, was presented by Covic et al.^{8,9} They targeted various Class A GPCRs by taking advantage of the critical third inner loop which shifts significantly during activation due to movement of the sixth transmembrane domain.¹⁰⁻¹² The method was reliant on the usage of palmitic acid to tether the peptide to the plasma membrane and localize it specifically to the cytoplasmic leaflet. This concept of membrane-tethered ligands was applied to the extracellular leaflet in 2009 by Fortin et al., in which they targeted Class B GPCRs using peptide anchors mimicking the transmembrane domain of GPCRs to ensure accurate polarity.¹³ They later moved to a lipid anchor, specifically GM1.¹⁴

Here, we present the synthesis and purification of a maleimide functionalized GM1 (mGM1) on the terminal sialic acid from natural GM1. Additionally, the synthesis and

purification of a biostable chemerin peptide (sChem9-PEG8-MPA), linked to a polyethylene glycol polymer (PEG₈) and functionalized with a thiol, to be reactive with the maleimide on GM1. Future experiments will need to optimize the reaction and purification of the mGM1 and sChem9-PEG8-MPA. Following successful purification of the compound, cell experiments using a luciferase assay and cells expressing CMKLR1 can determine the efficacy of the GM1-tethered ligand versus soluble ligands. If this method can be generalized to targeting other GPCR receptors it could potentially be a valuable therapeutic and investigative tool.

ACKNOWLEDGEMENTS

I would first like to thank Professor Krishna Kumar, for being both my major advisor and research mentor over the past five semesters and two summers. He has been a source of valuable advice both in research, in academics, and in pursuing my future after Tufts. His willingness to meet regularly and accommodate my schedule has been of great benefit to me over the last two and a half years and was critical in my ability to complete this thesis. Additionally, thank you to Professor Joshua Kritzer and Professor Mitch McVey for being on my committee and advising me through this process. Your advice and encouragement have been invaluable.

Thank you to the Summer Scholars Program and Robert R. Dewald Summer Scholarship for funding my research over the summer. The ability to work full time in lab over two summers and to maintain continuous work on my project has been one of the largest influences on selecting my future career path in research. These last two summers have taught me both the technical and intellectual skills required in research.

I would next like to thank Dr. Zhao Liu and Dr. Subrahmanian Tarakkad Krishnaji for being the best graduate student mentors anyone could hope for. Thank you for staying until midnight with me in the lab; thank you for coming in on the weekends for me; thank you for being so patient with me and helping me to refine my organic synthesis skills, my critical thinking skills, and my presentation skills. Through their guidance, mentorship, encouragement and friendship they have taught me so much both scientifically and personally.

Additionally, I would like to give a special thanks to Cristina Zamora and Venkat Raman for being so willing to give me advice and help me whenever I asked. Thank you, for being patient with me when I was frustrated and taking time from your own projects to help me with

my own. Thank you as well for coming into lab on the weekends and working with me through experimental problems. Also, to Suzanne Shapira and Alexander Sakers, thank you for your friendship, scientific and career advice; Pearson Hall was so much more enjoyable because of you. To all other members of the Kumar lab, past and present, I would also like to extend my thanks: Sophia Wei-En Lin, Gizem Akçay, Emel Adaligil, Zachary Fang, Judah Gruen, Kanupriya Tewari, Edward Rodionov, and Tao Xu.

Next, I would like to extend infinite thanks to my housemates and friends for listening to me talk about my research, even when you had no idea what I was talking about. Thank you for always being willing to give advice, or simply lending an ear. I would not have been able to maintain my sanity through this without you. Thank you!

Finally, but most definitely not least, thank you to my family, Mom, Dad, John and Mary-Joy for their love, patience and support over the past twenty-one years. Thank you for supporting me in my research, even when it meant missing family events. Thank you for helping me to maintain perspective and for always looking out for my best interest.

Thank you, all.

TABLE OF CONTENTS

CHAPTER 1: AN INTRODUCTION TO THE CELL MEMBRANE.....	1
1.1 The composition of the cell membrane.....	1
1.1.1 Lipids.....	1
1.1.2 Cholesterol.....	2
1.1.3 Proteins.....	3
1.2 Theoretical descriptions of the structure of the cell membranes.....	4
1.2.1 The Fluid Mosaic Model.....	5
1.2.2 Lipid Rafts and Lipid Microdomains.....	6
1.3 Maintenance and dynamics of the cell membrane: Endocytosis.....	9
1.3.1 Introduction to endocytosis and clathrin-dependent endocytosis.....	9
1.3.2 Clathrin Independent Endocytosis.....	10
1.3.3 Caveolae structure and composition.....	11
1.3.4 Biological function of caveolae and caveolar endocytosis.....	12
1.4 Ganglioside GM1.....	14
1.4.1 Introduction to gangliosides and glycosphingolipids.....	14
1.4.2 Metabolism and catabolism of ganglioside GM1.....	14
1.4.3 Biological function of gangliosides.....	16
1.4.4 Trafficking of Cholera Toxin B by ganglioside GM1.....	17
CHAPTER 2: AN INTRODUCTION TO G-PROTEIN COUPLED RECEPTORS AND THEIR DRUG TARGETS.....	19
2.1 An Introduction to GPCRs.....	19
2.1.1 Classification of GPCRs and their ligands.....	19
2.1.2 Signal Transduction Pathways of GPCRs.....	20
2.1.3 Structure and function relationships of family A GPCRs and GPCR associated proteins.....	23
2.2 Membrane-tethered ligands of GPCRs.....	26
2.2.1 Pepducins.....	26
2.2.2 Orthosteric Membrane-Tethered Ligands.....	29
2.3 Chemokine Receptor Like 1 (CMKLR1) & Chemerin.....	31
2.3.1 Biological Importance of CMKLR1 and chemerin.....	31
2.3.2 Chemerin peptides as CMKLR1 antagonists.....	32
CHAPTER 3: EXPERIMENTAL PROCEDURES AND FUTURE DIRECTIONS.....	35
3.1 General Synthesis, Detection and Purification Conditions.....	35
3.2 Final synthesis and purification procedures.....	36

3.2.1 Synthesis and Purification of <i>N</i> -(ϵ -Maleimidocaproyloxy) succinimide ester (EMCS)	37
3.2.2 Synthesis and Purification of Deacyl-Lyso GMI	38
3.2.3 Synthesis and Purification of Deacyl-GMI	39
3.2.4 Synthesis and Purification of Maleimide-GMI (mGMI)	40
3.2.6 Synthesis and Purification of <i>s</i> -Chemerin9-PEG8-3-Mercaptopropionic Acid (<i>s</i> Chem9-PEG8-MPA)	42
3.2.7 Spectral Data of Compounds	44
3.3 Optimization of Reactions	45
3.3.1 Optimization of purification of Deacyl-Lyso GMI	45
3.3.2 Optimization of overall synthesis of Maleimide-GMI (mGMI)	46
3.3.2 Optimization of synthesis and purification of Deacyl-GMI	49
3.3.3 Optimization of synthesis and purification of Maleimide-GMI (mGMI)	50
3.3.4 Optimization of overall synthesis of Chemerin9-PEG8-3-Mercaptopropionic Acid (<i>s</i> Chem9-PEG8-MPA)	51
3.3.5 Optimization of maleimide-thiol coupling reaction	52
3.4 Future Directions	54
APPENDIX	55
BIBLIOGRAPHY	75

CHAPTER 1: AN INTRODUCTION TO THE CELL MEMBRANE

All mammalian and living cells are surrounded by a lipid bilayer plasma membrane. Thus, in any therapeutics quest to affect cellular processes, the cell membrane must be approached. Whether the therapeutic acts merely on receptors on the cell membrane, is internalized via endocytosis, or passively enters through channels, the design and administration of drugs are all highly dependent on cell membrane structure, composition, and function. Thus, decades have been devoted to studying the cell membrane; understanding this critical structure of living cells is the first step in modulating cellular processes.

1.1 The composition of the cell membrane

The composition of these membranes varies both with time and between cells. As Davson and Danielli said in their 1952 paper, “It can truly be said of living cells, that by their membranes ye shall know them”.¹⁵ Due to the hydrophobic effect, the cell membrane forms a bilayer in which lipids and proteins can diffuse. Unlike liquid hydrocarbons, the hydrophobic core of membranes has been described as “liquid crystalline” due to its ordered nature.¹⁶ The major lipid components of the cell membrane are phospholipids, sphingolipids, cholesterol, and proteins.¹⁷⁻¹⁹

1.1.1 Lipids

The major class of structural lipids in the cell membrane is phospholipids. Of these, there are five constitutive phospholipids found in plasma membranes: phosphatidylcholine (PC), phosphatidylethanolamine (PE), phosphatidylserine (PS), phosphatidylinositol (PI), phosphatidic acid (PA).^{17,19} All of these lipids share diacylglycerol (DAG) as their hydrophobic domain.¹⁹ In addition to phospholipids, there are sphingolipids whose hydrophobic domain is ceramide. The dominant sphingolipids are sphingomyelin (SM) and glycosphingolipids, including gangliosides, which have terminal sialic acids. Sphingolipids are different from phospholipids in that they pack

more tightly and are thought to be, along with cholesterol, the major component of microdomains of the cell membrane, known as lipid rafts.¹⁹

A key characteristic of cell membranes is asymmetry, in particular asymmetry of phospholipid composition on the cytoplasmic and extracellular faces of the plasma membrane. In general, choline-containing lipids (PC and SM) are found on the extracellular face while amine-containing lipids (PE and PS) are found on the cytoplasmic face.^{16,18} This asymmetry is established in the Golgi through P4ATPases which selectively translocate PS and PE to the cytosolic face. SM, however, is synthesized on the luminal side from ceramide and is not transported by the P4ATPases, and thus ends up on the extracellular face of the plasma membrane.¹⁹ The composition of phospholipids affects the polarity and stability of plasma membranes. For example, phospholipids with polar head groups (PC, PI, and PS) allow for water and ions to bind and result in a hydrated and charged membrane surface. PE-rich surfaces, however, are hydrophobic and this instability can result in cellular processes such as membrane fusion and the formation of alternate structures due to the hydrophobic effect.¹⁸

1.1.2 Cholesterol

After phospholipids, cholesterol is the most abundant lipid in plasma membranes. Like phospholipids, there is asymmetry to cholesterol distribution, and the concentration of cholesterol has long been known to play a significant role in membrane protein function. The effects of cholesterol can be traced back to its physical effects on cell membranes. The effect of cholesterol on membrane fluidity has been termed the “condensing effect” in that it reduces lateral diffusion within the lipid bilayer.²⁰ At high concentrations, cholesterol inhibits membrane protein function; this universal effect is thought to be due to the reduction in “free volume,” and thus cholesterol prevents conformational changes necessary for function. However, at low

concentrations, increases in cholesterol can increase activity of certain membrane proteins, such as Na⁺-K⁺-ATPase. This effect is perhaps due to direct binding of cholesterol to membrane proteins, which would result in both activation and inhibition.²¹

1.1.3 Proteins

Proteins can be associated with the membrane through two distinct mechanisms: they can be embedded in the lipid bilayer, known as integral proteins, or they can be associated with the membrane. Integrated proteins must have a region of hydrophobic amino acids, the transmembrane region, which spans the lipid bilayer.¹⁶ The twentieth century saw many leaps in the understanding of the structure of the plasma membrane and the integration of proteins within this structure.

1.2 Theoretical descriptions of the structure of the cell membranes

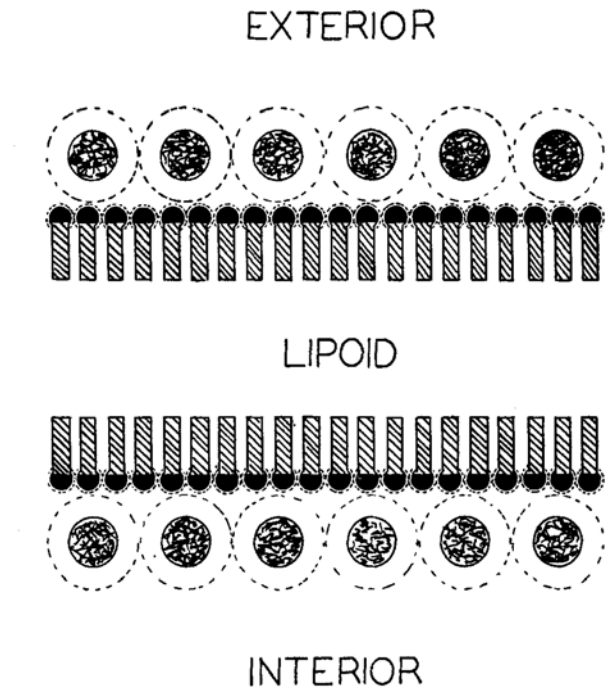


Figure 1. The Davson and Danielli Model of the Cell Membrane in which the lipid bilayer is sandwiched between membrane proteins.²² [Reprinted with permission from John Wiley and Sons.]

Much of the current knowledge of the cell membrane has come in the last century. Before the twentieth century, without the tools to image the membrane, it was characterized based on its functions. For example, the plasma membrane was hypothesized to be made from lipids due to the ease with which nonpolar molecules crossed the membrane relative to water soluble molecules.²³ In 1917, Irving Langmuir showed that lipid films over water were a monomolecular layer, potentially providing the first hint as to the structure of membranes in cells.²⁴ However, soon after in 1925 Gorter and Grendel concluded based on the lipid content of the plasma membranes of red blood cells, that the plasma membrane was in fact arranged in a bilayer configuration, establishing the accepted lipid bilayer model for membranes in living organisms.²⁵ However, the plasma membrane is not comprised of solely lipids and Davson and Danielli, in 1935, showed the presence of proteins in the membrane, proposing a model in which the

globular proteins sandwiched the lipid bilayer.²² While this model was incorrect, it helped to lay the foundation of the fluid mosaic model proposed by Singer and Nicolson in 1972.

1.2.1 The Fluid Mosaic Model

In 1972 Singer and Nicolsen proposed a model for the plasma membrane, and living membranes in general, which they termed the fluid mosaic model.²⁶ The key components of this model were the distinction of integral versus peripheral proteins, the interactions of proteins with lipids, and perhaps most importantly, the fluid nature of the membrane. They began by reconfirming the lipid bilayer model, in which hydrophobic groups, such as lipid tails, are sequestered from the aqueous environment within the lipid bilayer core and the polar and charged groups of lipid heads and proteins, are exposed to the aqueous environment, leading to the most thermodynamically stable configuration. Furthermore, what they refer to as the “trilaminar arrangement” with the bilayer sandwiched between proteins would not be thermodynamically favorable due to hydrophobic amino acids on proteins exposed to the aqueous environment and polar groups on lipids being shielded from the aqueous environment. Thus they proposed that there are both peripheral and integral proteins. The peripheral proteins are those which can be dissociated from the membrane under mild conditions, free of lipids and are relatively soluble in neutral aqueous buffers. The integral proteins require much more drastic treatment to dissociate from the membrane, often still associated with lipids, and are highly insoluble in neutral aqueous solutions; the integral proteins are thus the only proteins important for membrane structure.

The fluid mosaic model was described as such: integral proteins alternate with sections of phospholipid; proteins and phospholipids are amphipathic and their embedding in the membrane is under thermodynamic control; there is no long range order and the lipids are fluid and not a

crystalline structure. This final aspect of the fluid mosaic model, the fluidity of the plasma membrane as often been interpreted as analogous to randomness.²⁷ However, within the 1972 paper, Singer and Nicolson acknowledge that a lack of long-range order does not preclude the presence of short-range order, such as the organization of the components of the electron transport chain. They even mention there are exceptions to long range order, such as synapses of neurons. Describing the presence of short-range order in the cell membrane has been a challenge which led to the hypothesis of lipid rafts and lipid microdomains.

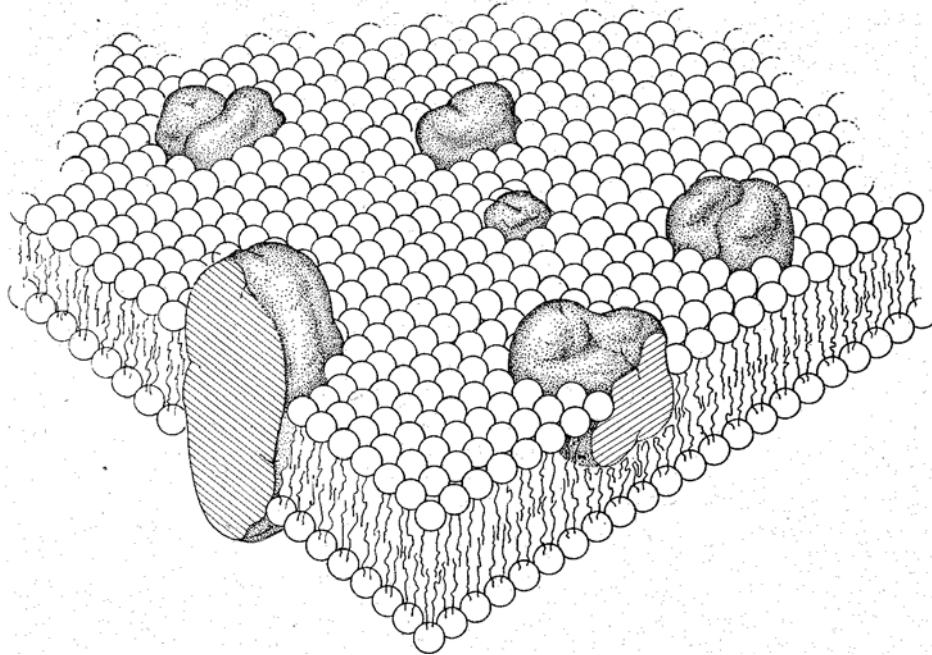


Figure 2. Fluid mosaic model proposed by Singer and Nicolsen in 1972 in which membrane proteins are integrated in the lipid bilayer.²⁶ [Reprinted with Permission from AAAS.]

1.2.2 Lipid Rafts and Lipid Microdomains

At the same time as Singer and Nicolson's paper on the fluid mosaic model, evidence was already being found for the lateral segregation of lipids, implying short-range organization of the plasma membrane. In 1973, Shimshick and McConnell presented evidence of phase separations in model membranes and in 1977 Jain and White, using model membranes, showed

that there were patches of lipids which differed from the average composition of the membrane.^{28,29} The functional purpose of these membrane patches were to aid in the sorting and trafficking of lipids and lipid-bound proteins. Further evidence for the importance of these membrane patches in protein sorting came in 1992 when Brown and Rose presented evidence that Glycosylphosphatidylinositol-anchored proteins (GPI-APs), lipid-anchored proteins, could enter domains of the membrane which were rich in cholesterol and SM. These regions of the membrane could be isolated from the rest of the membrane due to their immiscibility in cold, non-ionic detergents.³⁰ This characterization of such regions as detergent-resistant became a key characterization of such regions, termed “lipid rafts,” and also the basis of much controversy.

In 1997 Simons and Ikonen presented their theory on lipid rafts as sphingolipid and cholesterol enriched domains, which associated via the carbohydrate heads on the sphingolipids and the voids were filled by cholesterol molecules.³¹ These lipid rafts were thought to be the answer to the question of membrane polarization, in that newly synthesized glycosphingolipids would organize on the luminal leaflet of the Golgi membrane and thus were sorting centers for proteins destined for the extracellular side of the plasma membrane. The role of lipid rafts in protein sorting and trafficking was supported by the prior evidence for GPI-APs sorting into cholesterol and sphingolipid-enriched, detergent resistant domains. Additionally, caveolae, invaginations in the plasma membrane involved in endocytosis, were also shown to be enriched in glycosphingolipids and were cholesterol-dependent.^{32,33} Thus, Simons and Ikonen presented their hypothesis on lipid rafts as organized lipid microdomains into which proteins can be selectively included or excluded and thus function as rafts for transport or stations of intracellular signaling.

The experimental methods with which lipid rafts were being identified led to controversy over their existence; were these true biological phenomena or merely the result of tampering with the membrane? For example, experiments to show cholesterol-dependence of protein activity used cyclodextrin to remove cholesterol, but with membrane composition being up to 40% cholesterol, it is not necessarily a surprise that there would be consequences on biological functions, regardless of the presence of lipid rafts.³⁴ Fluorescence techniques were used to try and visualize heterogeneity in membrane organization of protein complexes. However, fluorescence techniques were restricted by optical resolution due to diffraction of light and differing techniques led to differing conclusions on the organization of different proteins.^{34–36} Super-resolution optical microscopy was used to overcome this resolution issue, such as stimulated emission depletion (STED) microscopy which showed that sphingolipids and GPI-APs were transiently located in cholesterol-dependent complexes in living cells.³⁷

With progress in microscopy, the existence of transient nanoscale microdomains, enriched in cholesterol and sphingolipids, has become more widely accepted. The 2006 Keystone Symposium of Lipid Rafts and Cell Function defined lipid rafts as “Membrane rafts are small (10–200 nm), heterogeneous, highly dynamic, sterol- and sphingolipid-enriched domains that compartmentalize cellular processes.”³⁸

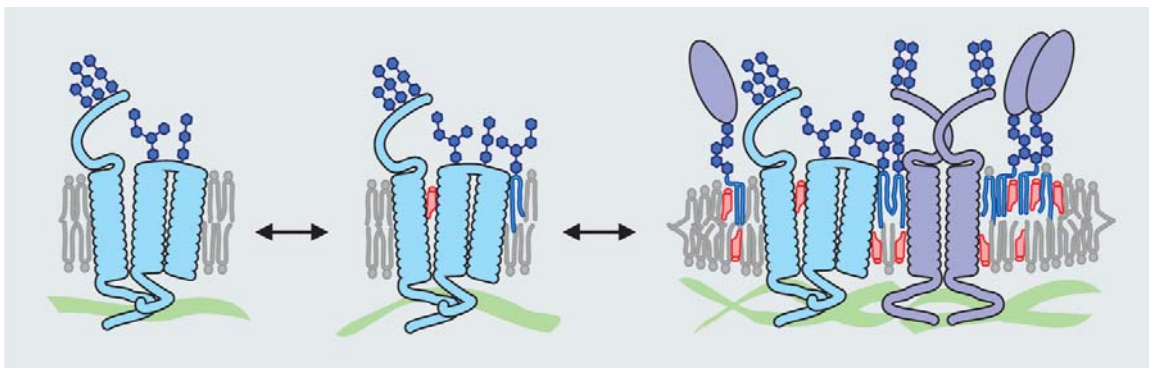


Figure 3. Model of a membrane protein (light blue) associating with sterols and glycosphingolipids to form a lipid microdomain.³⁹ [Reprinted with Permission from AAAS.]

1.3 Maintenance and dynamics of the cell membrane: Endocytosis

1.3.1 Introduction to endocytosis and clathrin-dependent endocytosis

Endocytosis is the mechanism by which cells take up components of their plasma membrane, the associated ligands, and surrounding fluids through the production of internal membranes from the plasma membrane bilayer.^{40,41} This process is constantly happening *in vivo*; it is estimated that cells internalize the equivalent of their cell surface one to five times per hour, and thus this process must be incredibly well regulated.⁴² Endocytosis has many biological functions including regulation of cellular signaling cascades, and pathogens take advantage of endocytic pathways as mechanisms of cell entry.⁴⁰ Once internalized, these new vesicles are delivered to early endosomes where they undergo cargo-specific sorting. From this point, they can be targeted to late endosomes or lysosomes for degradation, or the trans-Golgi network or recycling endosome to return to the plasma membrane.⁴³ Endocytosis occurs via many different mechanisms within the cell and this manifests partially, in the different morphological intermediates of endocytosis. The most studied of these are the clathrin-coated pits, but there are also flask-shaped vesicles, known as caveolae, tubular invaginations, and larger macropinocytic vesicles. However, it is important to note that invaginations in the cell membrane are not themselves diagnostic of endocytic intermediates and that specific cellular mechanisms cannot be directly determined from structural classifications.⁴¹

As previously mentioned, clathrin dependent endocytosis (CDE) is the most studied endocytosis pathway, and until the early 1990s it was even controversial whether clathrin independent endocytic pathways existed. CDE begins with clathrin-coated pits which then develop into clathrin-coated vesicles.⁴⁰ Like many endocytic pathways, CED is cholesterol-sensitive and is mediated by many adaptor proteins which recognize the cytoplasmic domains for

plasma membrane proteins.^{40,43-45} One important protein for both clathrin-dependent and clathrin-independent pathways is the GTPase dynamin which is necessary for the detachment of vesicles from the membrane.^{40,46,47} While CDE is the best studied endocytic pathway it is by no means the only or the dominant mechanism of endocytosis.

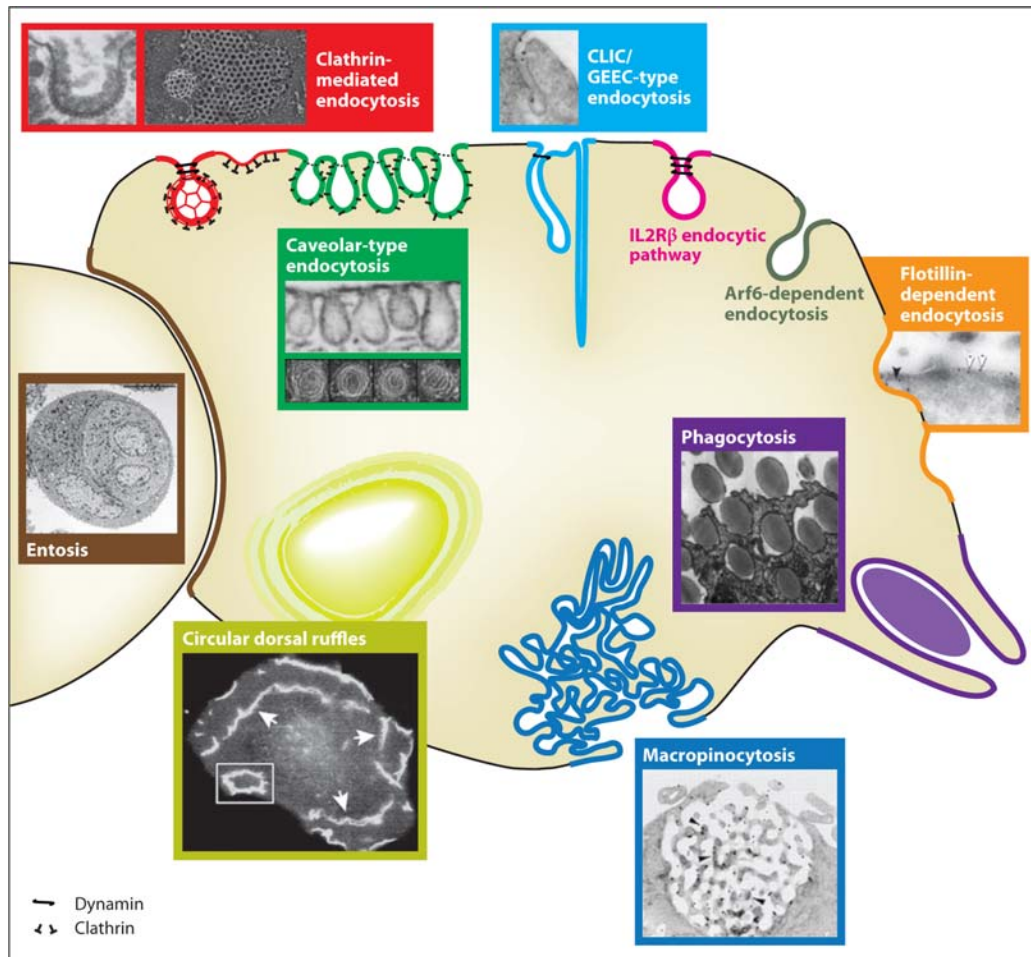


Figure 4. A summary of the different mechanisms of endocytosis.⁴⁰ [Reprinted with permission from ANNUAL REVIEWS, INC.]

1.3.2 Clathrin Independent Endocytosis

Clathrin independent endocytosis (CIE) are endocytosis pathways which undergo internalization via vesicles which are lacking a clathrin coat, identifiable by electron microscopy.⁴⁰ Substantial experimental evidence for clathrin independent pathways only began to accumulate in the 1990s when pharmacological perturbation of CDE did not completely block

the endocytosis of bacterial toxins, even though quantitative approaches could account for all detectable uptake via CDE.^{41,48} This implied that cells had another endocytic mechanism, independent of clathrin. In 1995, more evidence showed that dynamin knockout cells, necessary for CDE, were still able to internalize extracellular fluid, giving further proof for CIE.⁴⁹ Since then, many mechanisms of CIE have been identified, among them caveolar endocytosis, described in detail below, and macropinocytosis. Macropinocytosis allows the uptake of much larger membrane areas than CDE or caveolar endocytosis, as the vesicles can be up to 5 μm in diameter.^{41,50} Morphologically, macropinocytosis is characterized by highly ruffled regions of the plasma membrane that are actin-dependent.⁵⁰ Additionally, endocytosis can occur by irregular invaginations in the cell membranes: glycosphingolipids (GSLs) are often endocytosed in tubular vesicles and the crosslinking of GSLs by bacterial toxins, such as Shiga toxin binding to GM1, can also induce tubular vesicle formation.⁴¹

1.3.3 Caveolae structure and composition

Caveolae were identified in the 1950s by electron microscopy as non-clathrin coated invaginations in the plasma membrane, 50 to 80 nm in diameter.⁵¹ In the 1990s when evidence began to accrue in defense of CIE, caveolae were the first structures to be considered as players in this process. This hypothesis was strengthened when dynamin was found to be recruited to both caveolae and clathrin-coated pits.^{52,53} Three mammalian proteins, caveolin-1, -2 and -3, have been identified as being important for caveolae formation and function. Caveolin-3 appears to be muscle specific, while caveolin-1 and -2 are found in non-muscle cells; neurons and leukocytes appear to entirely lack caveolin.⁴¹

Of these three proteins, caveolin-1 is the major component of caveolae, with about 100 to 200 caveolin-1 monomers per caveolae.⁴⁰ It has also been shown to be necessary for caveolae

biogenesis; in the absence of caveolin-1, caveolae are not observed and caveolae formation can be induced through the reintroduction of caveolin-1.⁵⁴ Caveolin-1 is synthesized in the endoplasmic reticulum as an integral membrane protein and forms a hairpin configuration with both N- and C-terminal cytoplasmic domains.⁵⁵ It begins to form oligomers, and after travelling to the Golgi complex it continues oligomerization. From the Golgi network, caveolin is transported to the plasma membrane.^{56,57} Caveolin-1 plays important roles caveolae structure and is thought to act as a scaffold, as it directly binds cholesterol and the fatty acid tails of GSLs, such as ganglioside GM1.^{40,58} Additionally, cholesterol and ganglioside GM1 are also important for caveolin-1 trafficking from the Golgi network to the plasma membrane.^{59,60} Due to the high concentration of cholesterol and ganglioside GM1 within caveolae, it was initially hypothesized that caveolae and lipid microdomains, or lipid rafts, were synonymous.⁵⁸ However, later studies have identified caveoline-free detergent-insoluble microdomains, and thus caveolae are now thought to be a non-planar subdomain for lipid rafts.⁵⁸

1.3.4 Biological function of caveolae and caveolar endocytosis

Caveolae have been implicated to play a role in many cell functions such as various signaling pathways, mechanosensing and especially endocytosis. Just as caveolin acts as a scaffold in binding cholesterol and GSLs, it is also thought to act as a scaffold in signaling pathways. There is experimental evidence which shows that a class of membrane receptors, G-protein coupled receptors (GPCRs) are enriched in caveolae-containing detergent-resistant membranes. These findings have been supported by spectroscopic techniques like confocal imaging and FRET as well as the co-immunoprecipitation of GPCRs with caveolin, although this does not directly imply interactions on the cell surface.⁶¹ Mechanosensing refers to the

phenomenon of cells sensing and responding to physical stimuli; caveolae have been shown to respond to changes in membrane tension, such as membrane swelling.⁶²

The role of caveolae as a mediator of endocytosis was not always so clear. Video microscopy and FRAP analysis had shown GFP-tagged-caveolin-1 to be relatively immobile at the plasma membrane and to have a relatively low turnover rate.⁵⁸ In fact, there is evidence that caveolin-1 is a negative regulator of endocytosis.⁶³ While, caveolae are thought to be relatively stable structures, endocytosis can be induced by the presence of cargo, and it plays roles in the internalization of GSLs, integrins and bacterial toxins.⁵⁸ Caveolar endocytosis involves the reorganization of the actin cytoskeleton and is mediated by dynamin, Src kinases which phosphorylate caveolin-1 at Tyr14, and PKC.⁶⁴ Due to its role in internalizing integrins, it is thought to play an important role in cell adhesion; the clustering and activation of β 1-integrins can initiate caveolar endocytosis resulting in its removal from the cell surface.⁵⁵ In addition to the presence of cargo, caveolar endocytosis can be stimulated by phosphatase inhibitors or kinase activators, and the activation is accompanied by the activation of Src kinases which phosphorylate caveolin-1 and dynamin.⁵⁸ The role of caveolar endocytosis as it relates to the ganglioside GM1 and lipid trafficking will be discussed further.

1.4 Ganglioside GM1

1.4.1 Introduction to gangliosides and glycosphingolipids

Glycosphingolipids (GSLs) are a class of amphipathic membrane lipids with a sugar head and a ceramide hydrophobic tail, which consists of a long chain amino alcohol linked to a fatty acid via an amide bond. The long chain is most frequently C:18 in vertebrates, with C:20 being less common and there is usually a trans double bond between C4-C5 of the long chain.^{65,66} The fatty acid can vary between two and twenty-eight carbon atoms.⁶⁷ Gangliosides are a subfamily of GSLs which have at least three sugars attached via a β -glycosidic bond to the 1-hydroxy group of the ceramide and at least one sugar must be sialic acid. The sugar heads can be up to 20 residues or more and are composed from combinations of the following monosaccharides: glucose, galactose, N-acetylglucosamine, N-acetylgalactosamine, fucose, sialic acid and glucuronic acid.⁶⁵ GSLs are found predominantly in the exoplasmic leaflet of the plasma membrane. Due to their amphipathic nature, the saccharide head is exposed to the cell surface and the ceramide moiety is embedded in the lipid bilayer. It is also present in minor quantities in other subcellular compartments and organelles where it is synthesized, degraded or involved with intracellular trafficking.⁶⁵

1.4.2 Metabolism and catabolism of ganglioside GM1

The synthesis of GSLs and gangliosides occurs in the lumen of the endoplasmic reticulum (ER) and trans-Golgi network (TGN). It is then transported to the plasma membrane via exocytic transport vesicles.^{65,68} Ceramide is the precursor used for GSL synthesis onto which sugar residues are added to the 1-hydroxy group. There are two hypotheses for the mechanism of synthesis within the TGN. There is evidence of a gradient distribution of glycosyl-transferases, necessary for the synthesis for the sugar head of GSLs, in the TGN, which implicates a flow of

intermediates through the TGN.^{65,69} However, there is also evidence of multiglycosyl-transferase complexes leading to a competing hypothesis that there is an enzyme complex dedicated to the synthesis of each individual ganglioside.⁶⁵ Regardless of which of these two hypotheses is correct, the focus here will be on the individual enzymes required in the biosynthesis of these compounds.

Ceramide is synthesized by serine palmitoyltransferase from serine and palmitoyl CoA, yielding dihydrosphingosine; this reaction occurs on the cytosolic leaflet for the ER.⁷⁰ Dihydrosphingosine is converted to dihydroceramide through N-acylation by dihydroceramide synthase which attaches a fatty acid, usually between 14-28 carbon atoms in length.⁶⁷ Finally, dihydroceramide is reduced to ceramide via dihydroceramide desaturase.⁷¹ All GSLs then go through the same two steps to yield lactosylceramide, which results from the attachment of a glucose and a galactose residue via glucosylceramide synthase and galactosyl transferase I, respectively.⁷² In particular, the ganglioside GM1, is then synthesized through an additional three steps in which sialic acid, N-acetylgalactosamine, and galactose are added sequentially by GM3 synthase, GM2 synthase and GM1 synthase, respectively.⁶⁷

Ganglioside catabolism occurs predominantly in the lysosome by hydrolytic enzymes and proteins known as sphingolipid activator proteins (SAP). SAPs consist of five small nonenzymatic glycoproteins: a GM2 activator protein and SAP A-D. SAPs are required for ganglioside catabolism and are thought to either mediate the interaction between GSLs and the enzyme or activate the enzyme directly.⁶⁷ In the lysosome, the degradation occurs by a sequential removal of sugar residues yielding ceramide. Ceramide can then either leave the lysosome for degradation elsewhere, or it can be degraded to sphingosine and a fatty acid in the lysosome by acid ceramidase with the help of SAP-D.⁷³

1.4.3 Biological function of gangliosides

Gangliosides are located in in all cell types, but they are located in particularly high concentrations in neuronal membranes, constituting 10-12 percent of the total lipid content and 20-25 percent of the lipid content in the exoplasmic leaflet of the plasma membrane.⁶⁵ As previously described, gangliosides, in particular ganglioside GM1, are thought to be important to many endocytic and signaling pathways. Gangliosides are involved in a wide array of biological functions including regulation of the immune system, cell-cell interactions, cell adhesion, and neuronal differentiation.⁶⁵ Due to their biological importance, understanding the movement of gangliosides through the cell has been a topic of intense research. The question has been probed using fluorescent-labeled lipid analogues, labeled toxins and radioactively-labeled lipids. Through all these studies, factors such as the cargo and GSL structure have been identified as factors which affect the trafficking of ganglioside GM1 in the cell.^{68,74} In particular, ganglioside GM1 is the natural receptor for Cholera Toxin (CT), and thus the movement of GM1 through the cell has been studied using CT.⁶⁸

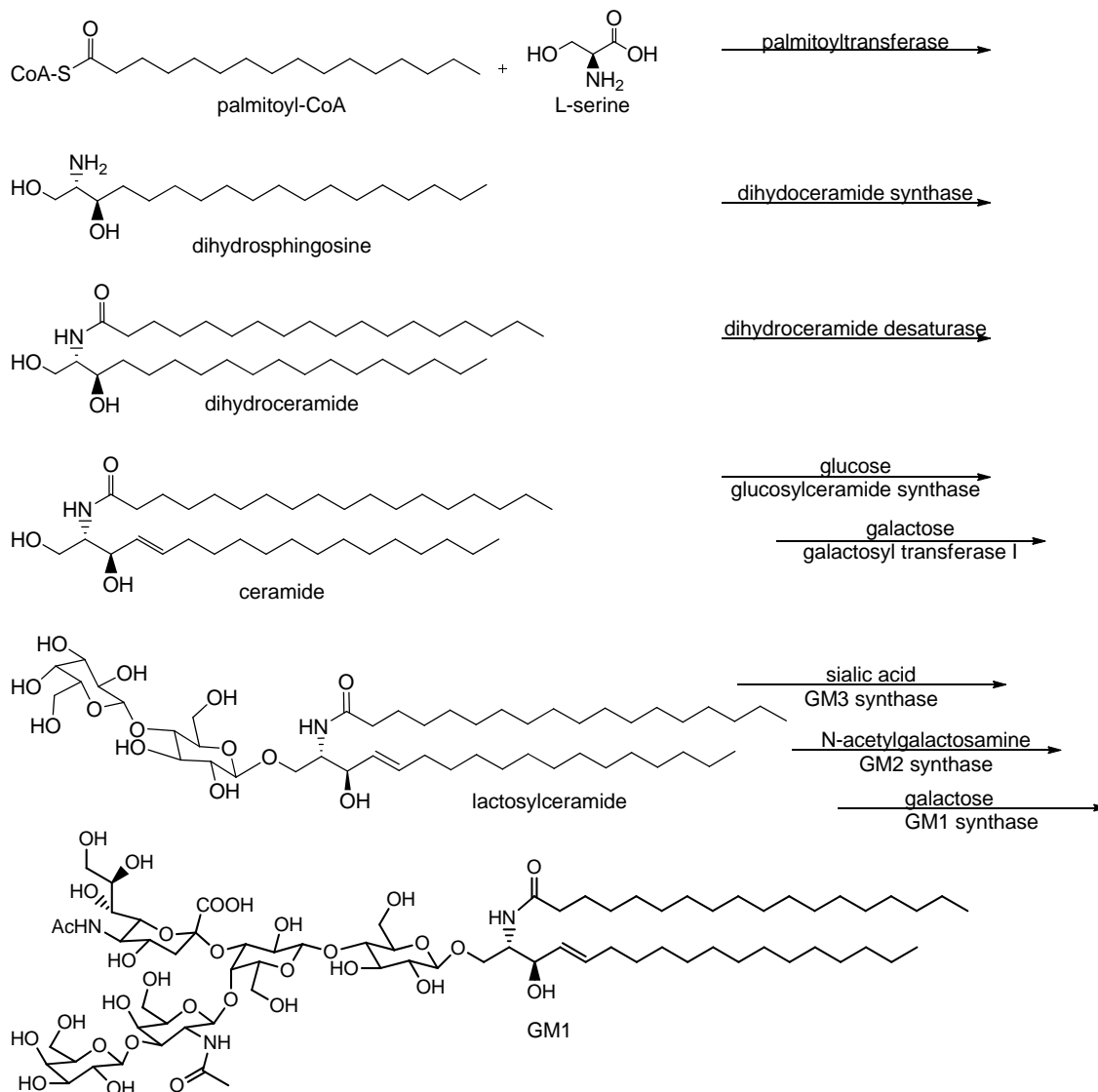


Figure 5. Biosynthesis of ganglioside GM1.

1.4.4 Trafficking of Cholera Toxin B by ganglioside GM1

Cholera toxin is secreted by the Gram-negative bacteria *Vibrio cholerae* and is responsible for the diarrhea associated with Asiatic cholera disease.⁷⁵ It is part of the AB₅ family of toxins, which consist of an A subunit and a pentameric B₅ subunit. The A subunit is catalytic and acts by constitutively activating heterotrimeric G protein which activates adenylate cyclase and leads to constitutively high levels of cyclic-AMP. The net result is massive secretion of chloride and water from intestinal enterocytes.⁷⁶ The B₅ subunit consists of five identical monomers which

can bind up to 5 ganglioside GM1 receptors simultaneously.⁷⁷ The binding of CTB to GM1 is quite strong with a dissociation constant of 5pM to 1 nM based on SPR.⁷⁸ The B subunit's function is solely to transport the A subunit to the endoplasmic reticulum, after which it dissociates from the A subunit, and the A subunit is transported to the cytosol via retro-translocation.⁷⁶

Studies of the intracellular trafficking of CT have shown that it can enter by both CDE and CIE, and that caveolar endocytosis comprises only a minor pathway.^{41,79,80} However, it is important to note that cell membrane composition varies between cell type and this could also affect the degree to which different endocytic pathways are used.⁷⁶ As indicated above, after binding to ganglioside GM1 and the plasma membrane, CT is trafficked to the TGN and then ultimately to the ER.⁶⁸ The internalization of CT, the virus SV40, and labeled gangliosides have all shown to be cholesterol-dependent, as well as actin-dependent; disruption of these two components prevents the internalization of ganglioside GM1 attached to cargo, as well as labeled cargo.^{65,81,82}

Understanding the intracellular trafficking of GM1 and how it is impacted by cargo and its own structure is critical in using it as a mode of drug transport. Using lipids as vehicles to concentrate drugs at cellular membranes is a potent method of targeting drugs to their receptors. The added advantage that GM1 localizes to specific membrane structures and organelles could prove to be a powerful therapeutic tool.

CHAPTER 2: AN INTRODUCTION TO G-PROTEIN COUPLED RECEPTORS AND THEIR DRUG TARGETS

2.1 An Introduction to GPCRs

G protein coupled receptors (GPCRs) are the largest family of proteins in the human proteome.⁸³ They are proteins, characterized by their seven transmembrane (TM) domains. Since the full sequencing of the human genome, it has been determined that GPCRs comprise of 3-4% of human genes and estimates range from 800 to 1300 different receptors.⁸³⁻⁸⁶

2.1.1 *Classification of GPCRs and their ligands*

The first attempt at classifying this family of receptors came in 1993, in which Attwood and Findlay classified receptors based on sequence homology. Today, the most standard classification was presented by Fredricksson in 2001, in which the receptors were classified based on phylogenetic criteria into five families: rhodopsin (class A), secretin (class B), glutamate (class C), adhesion and Frizzled/Taste.^{87,88} The three largest groups are families A, B and C, described below.

Family A, the rhodopsin family, is the largest and most diverse, comprising of approximately 670 proteins.⁸⁸ They are grouped together based on conserved sequences and structural features, discussed at greater length below. Within this group, there are three subgroups: Group 1 are receptors with small ligands and binding sites within the transmembrane domain; group 2 are receptors for peptides and their binding site is located both in the extracellular loops and in the extracellular region of the transmembrane domain; group 3 are receptors for glycoprotein hormones and they are characterized by large extracellular domains where the ligand-binding site is primarily located.⁸⁶ Family B, the secretin family, and Family C, the glutamate family, have approximately 60 proteins and 24 proteins, respectively, and like

group 3 of the rhodopsin family, these receptors have large extracellular domains which are the ligand binding sites for high molecular weight hormones.

As indicated, the ligands for GPCRs range from the tiniest of particles, photons, to large glycoproteins, but most of the ligands are small molecules including, nucleosides, lipids, peptides, and ions.^{83,85,89} These ligands are classified into two general classes: agonists, which promote GPCR activation, and antagonists, which block GPCR activation.⁸⁴ The agonists can then be broken down further into two subcategories: full agonists, which result in maximal receptor stimulation, and partial agonists, which even a saturation, fall short of full activation. Similarly, the antagonists can be subdivided into two categories: neutral antagonists have no effect on the downstream signaling activity, but block the binding of agonists, and inverse agonists, which reduce the level of basal activity of the unbound receptor.⁸⁷ The action of these diverse ligands result in the activation of a plethora of downstream signaling pathways which play a role in nearly all cellular responses, from embryological development, to taste and vision, to the bodies immunological response.

2.1.2 Signal Transduction Pathways of GPCRs

The idea of cell membrane receptors was first proposed by Langley in the early twentieth century to explain the ability of drugs to regulate neuromuscular transmission; a “receptive substance” was described as the mediator between the drug and cellular response.⁸³ During the twentieth century, the class of membrane receptors, GPCRs were identified, and the classical function of this receptor family was thought to couple the binding of ligands to the activation of heterotrimeric G proteins, which in turn led to downstream cellular responses.⁸⁷ A simple model of GPCRs are engines which oscillate between a stable inactive state and a ligand-stabilized active state.⁸⁹ However, structural studies of GPCRs have modified this model, since it is now

known that many receptors have a basal level of activity, they can adopt multiple conformations leading to the activation of differential signaling, and their effect is not limited to G-protein dependent pathways.^{89,90} G-protein independent pathways are described at greater length below, and have been primarily associated with regulation of signaling.

While there are G-protein independent pathways activated by GPCRs, many of the downstream effects are modulated by heterotrimeric G proteins. In general, a ligand binds at the extracellular surface of the GPCR causing a conformational change which mediates a nucleotide exchange reaction, in which the G-protein exchanges GDP for GTP and becomes activated.⁸⁴ Heterotrimeric G proteins are membrane bound and consist of an alpha ($G\alpha$), beta ($G\beta$) and gamma ($G\gamma$) subunits which are found on the cytosolic leaflet of the membrane. In its inactive state, $G\alpha$ is bound to GDP and is associated with the $G\beta\gamma$ heterodimer.⁹¹ Upon agonist binding, the GPCR acts as a guanine nucleotide exchange factor (GEF), facilitating the release of GDP. Due to the relatively higher concentration of GTP within the cell, GTP binding then causes a conformational change in $G\alpha$ and causes its release from $G\beta\gamma$.^{92,93} The freed $G\alpha$ and $G\beta\gamma$ are then both free to activate intracellular signaling pathways. Signaling is arrested due to the intrinsic GTPase activity of $G\alpha$, leading to the conversion of GTP to GDP and the subsequent reassociation with $G\beta\gamma$.^{94,95}

The diversity of G-proteins allows for specificity in GPCR downstream response: In the human proteome, there are 23 $G\alpha$ subunits, 5 $G\beta$ subunits and 12 $G\gamma$ subunits. While it was previously thought that only $G\alpha$ was a mediator of downstream signaling, it is now known that the released $G\beta\gamma$ heterodimer also activates secondary messenger molecules. Among the $G\beta\gamma$ effectors are G-protein regulated inward rectifier K^+ channels (GIRK), neuronal calcium channels, kinases and small G proteins.⁹¹ Among the targets of activated $G\alpha$ is adenylyl cyclase

(AC), which was the first effector identified.^{96,97} However, it was another twenty years before the corresponding G-protein was identified; G proteins which activate AC isoforms are termed $G\alpha_s$ and those which inhibit AC isoforms are termed $G\alpha_i$.⁹⁸ There are other $G\alpha$ proteins which are key in taste and odorant response and $G\alpha_i$ also plays a key role in vision through its effect on GMP-gated Na^+/Ca^{2+} channels. Additionally, $G\alpha_{12/13}$'s effect on the small G protein RhoA is key in cell transformation.⁹¹ Of these downstream targets, AC is one of the best studied. AC catalyzes the conversion of ATP to cyclic-AMP (cAMP). cAMP then acts as a secondary messenger.⁸⁵ Using the β 2-adrenergic receptor (β 2-AR) as a model, the production of cAMP results in the activation of cAMP-dependent protein kinase A (PKA), which leads to the phosphorylation of proteins involved in muscle contractions.⁹⁹

Equally important to activation of signaling is its deactivation and regulation. It was previously thought that GPCR signaling was purely regulated by the intrinsic GTPase activity of the $G\alpha$ subunit and the negative feedback from its effectors.¹⁰⁰ However, in 1996 a family of proteins termed regulators of G protein signaling (RGS) were discovered which accelerate the GTPase activity of $G\alpha$.¹⁰¹ There are now 37 known RGS proteins.⁸⁵ In addition to RGS proteins, one of the best studied G-protein independent pathways is the GPCR kinases (GRKs) and β -arrestins pathway: GRKs phosphorylate the GPCR, resulting in the recruitment of β -arrestin and the deactivation of heterotrimeric G-protein.⁸⁵ Additionally, receptor internalization, recycling, and lysosomal degradation are other methods of GPCR regulation.⁸⁷

2.1.3 Structure and function relationships of family A GPCRs and GPCR associated proteins

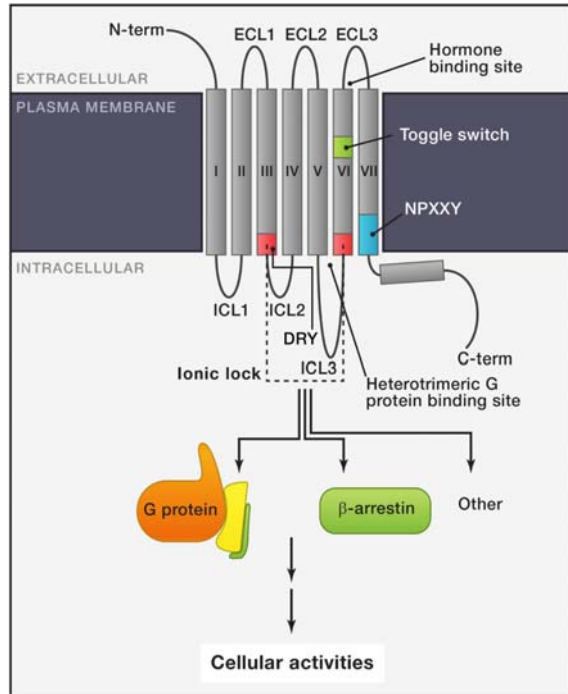


Figure 6. Diagram of the important motifs for GPCR activation.⁸⁴ [Reprinted with permission from Elsevier.]

In 1975 the first three dimensional structure of a transmembrane protein was obtained by electron microscopy, and in 1983 the first structure of a GPCR, rhodopsin, was published.⁸³ It wasn't until 2000 that a the first high-resolution crystal structure of rhodopsin was obtained allowing the determination of side chain configuration and the sequences of transmembrane and intra- and extracellular domains.^{84,89} In 2007, the structures of GPCRs bound to diffusible ligands were determined allowing for the study of the effects of ligand binding on the GPCR configuration and determination of the mechanism of activation.⁸⁴ Progress in methods of crystallization of transmembrane proteins and in Xray diffraction allowed for the crystallization and high resolution structure determination of 47 GPCR structures between 2007 and 2012.⁸⁴ Described below are the mechanisms of ligand binding and GPCR activation in the rhodopsin family of GPCRs.

As previously described, the most characteristic feature of GPCRs are their seven transmembrane domains (TM I-VII), extracellular N-terminal domain, intracellular C-terminal domain, three extracellular loops (ECL 1,2,3) and three intracellular loops (ICL 1,2,3). While this general structure is conserved among all families of GPCRs, there is little sequence homology even within families. However, the class A, rhodopsin, GPCRs have several conserved sequences which play an integral role in ligand binding and activation.

Among rhodopsin family GPCRs there are two methods of ligand binding: there are those ligands which bind parallel to the plane of the plasma membrane, deep within the transmembrane bundle, such as rhodopsin, and there are those ligands which bind perpendicular to the plasma membrane, such as β 1- and β 2-adrenergic receptor (β 1- and β 2-AR). Regardless of the binding mechanism, ECL2 plays in a key role.⁸⁴ In rhodopsin, the ECL2 is a short β -sheet that caps covalently bound 11-cis retinal and prevents Schiff base hydrolysis. Upon photoactivation and Schiff base hydrolysis, retinal is released, allowing Trp265, known as the Toggle switch, to move into the space previously occupied by retinal, this altered configuration also breaks interactions between Lys296 on TMVII and Glu113 on TMIII, allowing the transmembrane bundle pocket to open, which is important in G-protein activation.⁸⁷ In β 1- and β 2-AR the ECL2 has a short alpha-helical structure and ECL1 and 3 aid in directing the ligand towards the binding site.^{84,87} Relative to the rhodopsin binding site of retinal, the binding site for β 1- and β 2-AR are more exposed to the bulk solvent. β 1- and β 2-AR also have corresponding tryptophan residues (Trp303 and Trp303 for β 1-AR and β 2-AR, respectively). Upon ligand binding, they undergo rotation, which is also necessary for agonism.^{102,103}

The two characteristic motifs of the cytoplasmic domain of family A GPCRs are the E/DRY motif, which makes the “ionic lock,” and the NPXXY motif. In the inactive state, the

polar interaction between arginine on TMIII and glutamate on TMVI is called the “ionic lock”.⁸⁴ However, upon activation, this interaction is disrupted leading to the movement of TMVI away from the TM bundle.^{10,11} Simultaneously, the NPXXY motif, located on TMVII bends inwards allowing the tyrosine residue to stabilize the TMVI; the R of the DRY motif juts into the bundle and is stabilized by the C-terminus.⁸⁴ This conformational change is consistent between rhodopsin and β 1- and β 2-AR; in rhodopsin, TMVI shifts 6Å outwards resulting in a cavity between TMIII, V and VI for the binding of the heterotrimeric G-protein.¹⁰⁻¹²

Understanding the activation mechanism of GPCRs can be very informative when designing drugs, either agonists or antagonists. As previously mentioned, GPCRs are the largest family of proteins in the human proteome, and elucidating the general trends in their activation and deactivation can result in generalizable therapeutic tools which can be applied to a wide range of disease states and their related receptors.

2.2 Membrane-tethered ligands of GPCRs

In 2006, Overington et al. carried out a study looking at 21,000 drug products to identify 1,357 unique drugs. From this, they analyzed the drug targets for those whose mode of action was known, resulting in 324 distinct molecular targets. From this they determined that 26.8% of all FDA approved drugs acted on Class A GPCRs.¹⁰⁴ Since then, estimates of greater than 50% of prescribed drugs have been thought to target GPCRs.⁹ Their medicinal relevance has made studying exogenous agonists and antagonists of these receptors a focus of intense study. In the last decade, a new methodology in targeting has been studied using lipidated peptides to target GPCRs both intracellularly and extracellularly. These two methods are discussed below.

2.2.1 Pepducins

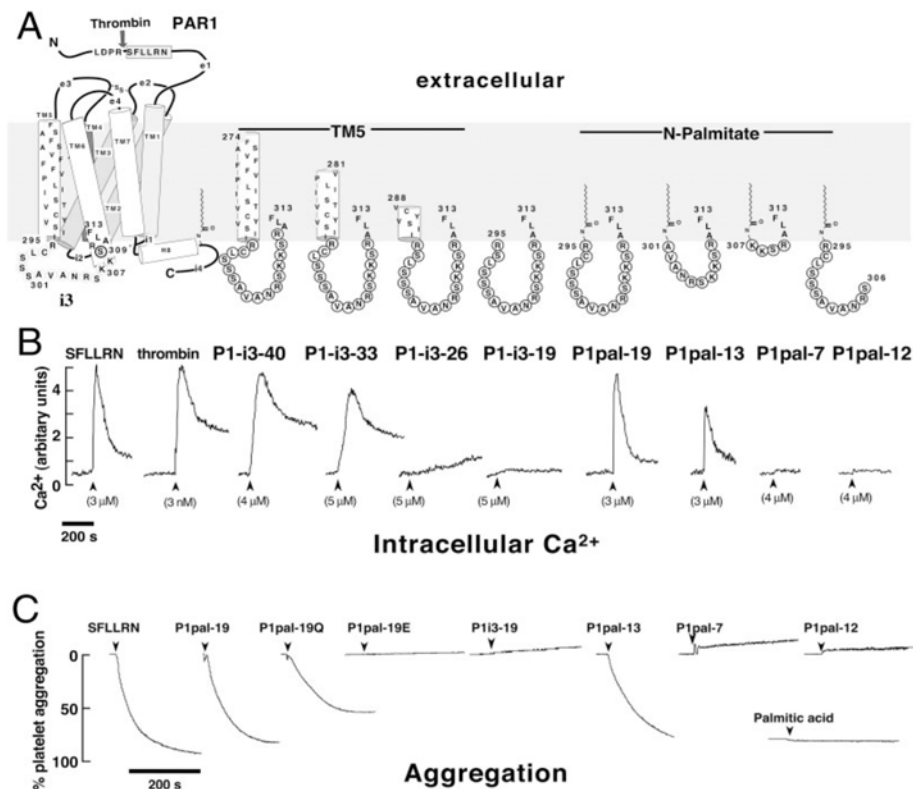


Figure 7. GPCR activation by peptide-anchored and palmitate-anchored pepducins as measured by $[Ca^{2+}]$ and platelet aggregation. Decreasing the size of the transmembrane domain and decreasing the size of the ICL3 mimic result in loss of agonist activity.¹⁰⁵ [Reprinted with permission from the National Academy of Sciences.]

Classically, GPCRs have been targeted by using ligands soluble in the extracellular fluid which bind to either the orthosteric binding site or an allosteric site resulting in either increased or decreased activation. However, in 2002, Covic et al. presented a new method of targeting GPCRs, which they termed pepducins.^{8,9} These novel therapeutics were cell penetrating, palmitate-tethered, peptides derived from the ICL3 of the targeted GPCR. As previously mentioned, a key event in the activation of GPCRs is the movement of TMIII and TMVI which also alter the conformation of the ICLs leading to the activation of G-proteins. Additionally, past mutagenesis studies had showed that ICL3 played a critical role in the coupling between the receptor and the heterotrimeric G proteins.^{1,106} Other studies had shown that when ICL3 is expressed separately, it competes with $\alpha 1B$ -AR for G protein binding.¹⁰⁷

In their first study, Covic et al. worked with protease-activated receptor 1 and 2 (PAR-1,-2) and melanocortin-4.⁹ Their first constructs had the ICL3 loop peptides of PAR-1 with 40 N-terminal, hydrophobic, transmembrane residues from the adjacent TMV (p1-i3-40) to anchor the peptide in the lipid bilayer, to ensure translocation across the lipid bilayer, and to increase the effect molarity by the receptor. Their initial hypothesis, based on the past studies, was that this exogenous peptide would act as an inhibitor, but rather they saw that similar to agonists of PAR-1, resulted in a flux of intracellular Ca^{2+} concentrations. Additionally, these hydrophobic transmembrane amino acids were necessary for the activation; reducing the transmembrane domain to 11-12 amino acids resulted in loss of function. This was hypothesized to be due to a lack of translocation to the inner leaflet. This concept was then modified, using palmitate, also known to translocate to the inner leaflet, as the hydrophobic anchor (p1pal-19); this construct similarly caused a rapid increase intracellular Ca^{2+} concentration.

Upon varying the length of the peptide sequence from ICL3, they determined that certain sequences were ineffective as agonists; they tested these constructs for antagonistic activity. A construct with 12 amino acids, p1pal-12 was found to block activation by the peptide agonist, SFLLRN, for PAR-1, but was selective against the related receptor PAR-4.^{8,9} The difference between agonists and antagonists were hypothesized to be due to a two-site binding model, in which the higher affinity site results in activation, but there is a lower affinity site which results in antagonism. This model was supported by an agonist for PAR-2, p2pal-21 which lost agonist activity at higher concentrations, hypothesized to be due to saturation of the higher affinity agonist binding sites and the subsequent binding to antagonist binding sites.⁸

Pepducin therapies have been shown to be an effective model making antagonists against other GPCRs including CXCR1 and CXCR2, which are implicated in chronic inflammation and whose inhibition is important for neutrophil clearance.¹⁰⁸

2.2.2 Orthosteric Membrane-Tethered Ligands

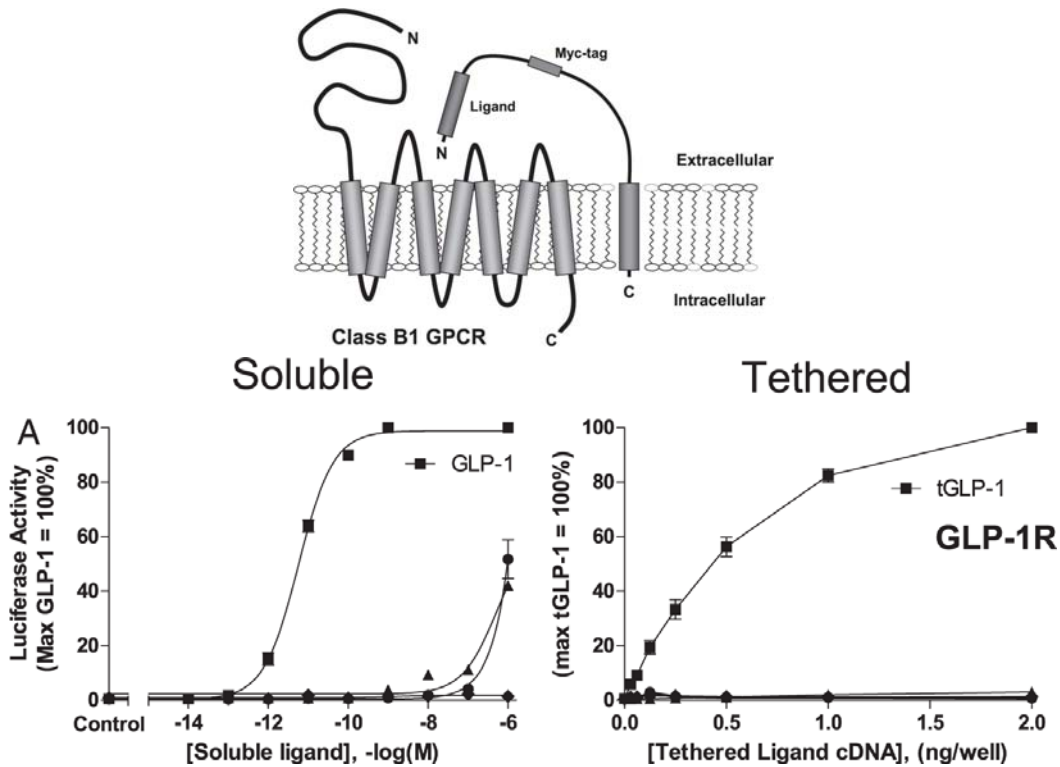


Figure 8. (Top) Model of the activation of a GPCR by a transmembrane-peptide-tethered ligand. (Bottom) The luciferase activity of the soluble versus tethered ligand of GLP-1R and compared to ligands of related receptors. [Taken from ¹³.]

In 2009, Fortin et al. built on the idea of membrane-tethered ligands (MTLs), but instead used modified structures of the natural ligands to target Class B GPCRs, specifically, GLP-1R, extracellularly at the orthosteric site.¹³ This receptor is important for insulin release and there are already drugs on the market for diabetes which target this receptor (the GLP-1 mimic, EXE4, exenatide or BYETTA). The model for binding Class B receptors is that the C-terminus of the ligand binds the N-terminus of the extracellular domain (ECD), which is important for affinity and specificity, and then the N-terminus of the ligand interacts with the transmembrane domain (TMD) and connecting ECLs to initiate receptor activation. These MTLs were comprised of five regions: (1) to ensure the ligand was situated in the proper orientation TMDI was used as the hydrophobic anchor, (2) a flexible peptide linker connected the TMD to the ligand, (3) a myc

epitope tag was incorporated into the linker (4) class B1 receptor ligand (5) a signaling peptide at the N-terminus to ensure localization to the plasma membrane, and is cleaved during peptide processing. A luciferase assay was used to determine activation of the receptor: activation of the GPCR lead to increased levels of intracellular cAMP which bound to a cAMP response element (CRE) upstream of a luciferase reporter gene. The results from these experiments showed that in HEK293 cells which co-expressed a tethered ligand and its corresponding GPCR experienced 35-100% activation relative to the soluble ligand and was able to be selective for its cognate receptor relative to other receptors. Additionally, tethering was shown to overcome the need for C-terminal recognition of the N-terminal ECD; when N-terminal truncated PTH-R1 was tested with both its soluble ligand, PTH and tethered-PTH, the truncated N-terminal receptor only affected the activation by the soluble ligand.

Similar to pepducins, the next step was to use a lipid anchor, instead of a peptide anchor. In a subsequent study, EXE4, the agonist for GLP-1R, was tethered to GM1 ganglioside.¹⁴ The resulting MTL enhanced signaling approximately 50-fold relative to the soluble EXE peptide when assessed against a related receptor GIP-R and was able to retain picomolar potency against GLP-1R ($EC_{50}=48$ pM). Further, the activity of the tethered ligand was retained even after serial washes, which is attributed to the tethering by the ganglioside GM1.

Given the enrichment of GPCRs in lipid rafts, and the importance of GM1, as previously discussed, in signal transduction, endocytosis and lipid rafts, makes the synthesis of peptides tethered to GM1 potentially very important therapeutically and in investigating the function and signaling pathways of GPCRs.⁶¹ The GM1 intracellular trafficking pathway to other organelles, such as the TGN and ER, could potentially make it a vehicle to affect intracellular receptors through similar MTL constructs.

2.3 Chemokine Receptor Like 1 (CMKLR1) & Chemerin

Chemokine-like Receptor 1 (CMKLR1 or Chem32) is an example of a GPCR, which has therapeutic potential, but whose signaling pathway has yet to be fully understood. It was first cloned in 1996 using PCR from human chromosome 12q.24.¹⁰⁹ It was initially identified through sequence homology in TMIII and VI to somatostatin receptors 1-4. The gene product had 371 amino acids and seven transmembrane domains, but only had approximately 40% nucleotide similarity to somatostatin receptors. Instead, CMKLR1 appears to be structurally related to chemoattractant receptors.¹⁰⁹ Finding its agonist proved to be difficult; testing of over 200 bioactive molecules yielded no successful activation of the receptor. Its agonist, termed chemerin, was found through assays of biological fluids.³ Chemerin has since been established as a chemoattractant protein and is implicated in adipogenesis, metabolism and inflammation.²

2.3.1 *Biological Importance of CMKLR1 and chemerin*

Chemerin is expressed predominantly in the placenta, liver, and in particular white adipose tissue (WAT), which is believed to be the main source of circulating chemerin. In healthy individuals, levels vary from 90-200 ng/mL.¹¹⁰⁻¹¹² In the body, chemerin is synthesized as prochemerin with an N-terminal signal sequence (20 amino acids) which is subsequently cleaved prior to secretion, to an 18 kDa biologically inactive protein, prochemerin (Chem-163).³ Most of the chemerin in circulation is believed to be the biologically inactive prochemerin.¹¹³ Cleavage of prochemerin at the C-terminus leads to various isoforms of chemerin with varying levels of bioactivity. The cleavage of 6 amino acids to yield Chem-157 (Met¹-Ser¹⁵⁷) is the most biologically active form of chemerin.^{2,113} Subsequent isoforms, Chem-156,152-158, decrease in biological activity with Chem-152,153 being essentially inactive.² Pathologically, chemerin is elevated in numerous disease states associated with chronic inflammation, including Crohn's

disease, ulcerative colitis, and chronic kidney disease.² It is also positively correlated with high concentrations of other pro-inflammatory molecules such as C-reactive protein (CRP), IL-6, TNF α , and *in vitro* studies show enhanced secretion of pro-inflammatory cytokines upon treatment with chemerin.⁴ It also shows function as a chemoattractant, promoting the chemotaxis of CMKLR1-expressing leukocytes, and the adhesion of macrophages to extracellular matrix proteins and endothelial cells.^{3,5,6}

While CMKLR1 is believed to be the primary receptor for chemerin, it is also of worth noting that two other GPCRs have been found to bind chemerin: GPR1 and chemokine (CC motif) receptor-like 2 (CCRL2). CCRL2 is not believed to transduce a signal upon binding, but rather it is thought to act a means to concentrate chemerin and present it to CMKLR1 and GPR1. Between CMKLR1 and GPR1, signaling of CMKLR1 due to chemerin has been the focus of study. CMKLR1 is found in highest concentrations in leukocytes, especially macrophages and dendritic cells.² Despite research, little is still known about the signal transduction pathway of CMKLR1. Its activation is known to result in intracellular Ca²⁺ flux and a decrease in cAMP which is consistent with activation of G_i proteins.³

2.3.2 Chemerin peptides as CMKLR1 antagonists

In 2008, Cash et al. determined that upon proteolytic cleavage, chemerin-derived peptides showed potent inhibition of CMKLR1 and anti-inflammatory properties.⁷ To confirm this finding, a series of peptides were designed based on the C-terminus of prochemerin, and only those with identical sequence to that of prochemerin exerted inhibitory effects at picomolar concentrations. These results were confirmed *in vivo*, by injecting mice with C15(A¹⁴⁰-A¹⁵⁴) before zymosin challenge, which resulted in decreased neutrophil and monocyte recruitment but

had no effects on CMKLR1 knockout mice. Additionally, the anti-inflammatory effects of C15 were also countered by injection of anti-chemerin antibody before the challenge.

Subsequently, Chemerin-9, a C-terminal nonapeptide, was determined to be the smallest peptide that retained nanomolar potency to CMKLR1.¹¹⁴ However, due to its susceptibility to proteolytic cleavage, its biological activity is significantly affected. Thus in 2009, Shimamura and Matsuda determined a stable chemerin form by determining the sites of proteolytic cleavage and replacing the affected amino acids by unnatural amino acids.¹¹³ In summation: the replacement of Phe¹⁵⁵ with 1,2,3,4-tetrahydroisoquinoline-3-carboxylic acid (Tic) and Ala¹⁵⁴ with D-Ala¹⁵⁴, to prevent Ala¹⁵⁴-Phe¹⁵⁵ cleavage; the extension of the N-terminus to prevent Phe¹⁴⁸-Leu¹⁴⁵ cleavage; the replacement of Pro-Gly sequence with Pro-D-Ser, to maintain the Type II β -turn. The final construct can be summarized as: D-Tyr¹⁴⁷[DSer¹⁵¹-DAla¹⁵⁴-Tic¹⁵⁵]chem¹⁴⁸⁻¹⁵⁶. This analogue, schemerin9, had increased metabolic stability *in vitro*, when incubated with human plasma, as well as an increased half-life *in vivo* in mice. It was also shown to retain the anti-lipolysis activity of chemerin9 in mouse primary adipocytes, resulting in reduced plasma free fatty acid levels.

Chemerin and CMKLR1 appear to play an important role in inflammation and thus in numerous chronic inflammatory diseases. The anti-inflammatory effects of the chemerin peptides could be a promising therapeutic tool and investigative tool, since much is still unknown about the CMKLR1 receptor. Furthermore, its functionality can perhaps be enhanced by the usage of ganglioside GM1 as a lipid tether. Here, I present a synthetic route, beginning with natural ganglioside GM1, purified from bovine brain, towards a modified maleimide-functionalized GM1, which can be coupled to peptides via a free thiol, present at the end of a polyethyleneglycol (PEG) linker.

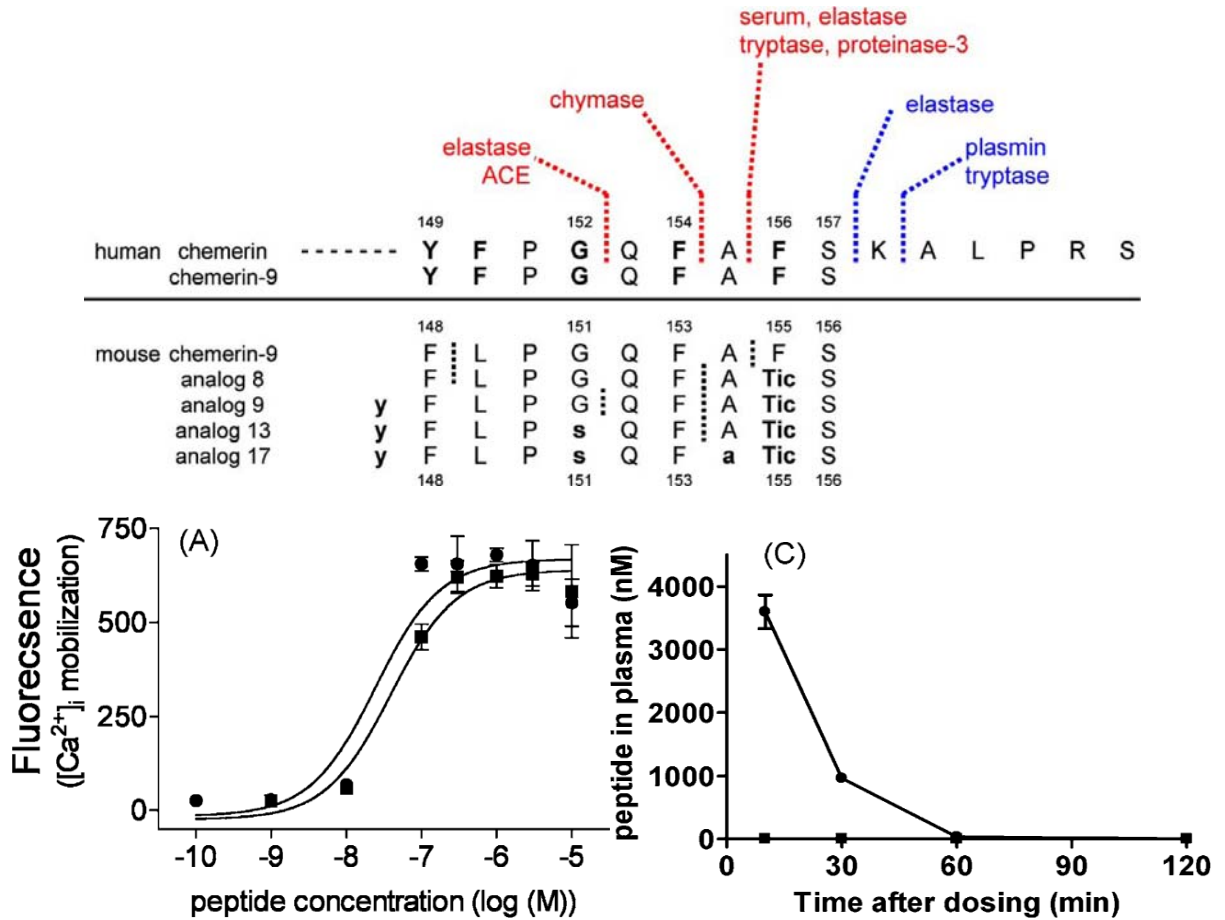


Figure 9. (Top) The protease cleavage sites on natural chemerin; blue sites are activating and red sites are deactivating. Analogue 17 is the sequence shown to be biostable and bioactive. (Bottom left) Analogue 17 versus natural human chemerin and the effect on [Ca²⁺]_i mobilization (circles are Analogue 17; squares are natural chemerin). (Bottom Right) The biostability of Analogue 17 versus natural chemerin *in vivo* (circles are Analogue 17; squares are natural chemerin).
 [Reprinted with permission from Elsevier.]

CHAPTER 3: EXPERIMENTAL PROCEDURES AND FUTURE DIRECTIONS

3.1 General Synthesis, Detection and Purification Conditions

Silica gel chromatography was carried out on 60Å 230-400 mesh silica gel.

Compounds were visualized on thin-layer chromatography, using a 60:40:9 chloroform: methanol: water solvent system, using phosphomolybdic acid stain (PMA, 10 g in 100 mL ethanol) and subsequent heating.

HPLC purifications were done using a two-solvent system labeled A (99% water, 1% acetonitrile, 0.1% trifluoroacetic acid) and B (10% water, 90% acetonitrile, 0.07% trifluoroacetic acid). Semi-preparative HPLC purifications were performed at a flow rate of 2.5 mL/min using a Vydac C₁₈ reverse phase column (Column #13, 10 mm x 250 mm, 10-15 µm). Analytical HPLC analyses were performed at a flow rate of 1.5 mL/min using a Vydac C₁₈ reverse phase column (Column #53, 4.5 mm x 250 mm, 5 µm). Elution of the product was monitored by UV absorption at 230 nm and MALDI-TOF MS.

NMR spectra (¹H and ¹³C) were obtained on Bruker DPX-300 NMR and Bruker Avance III 500 MHz NMR instruments. Chemical shifts are given in ppm (δ), with TMS (¹H) and CDCl₃ (¹³C) as internal standards. The multiplicities are indicated by: s (singlet), d (doublet), t (triplet), q (quartet), and m (multiplet).

Mass spectra were recorded on an LTQ-Finnigan ESI Mass Spectrometer in the negative ionization mode. Data from the mass spectrometer was processed using XCalibur software.

MALDI-TOF MS were obtained using Bruker Microflex TOF MS.

3.2 Final synthesis and purification procedures

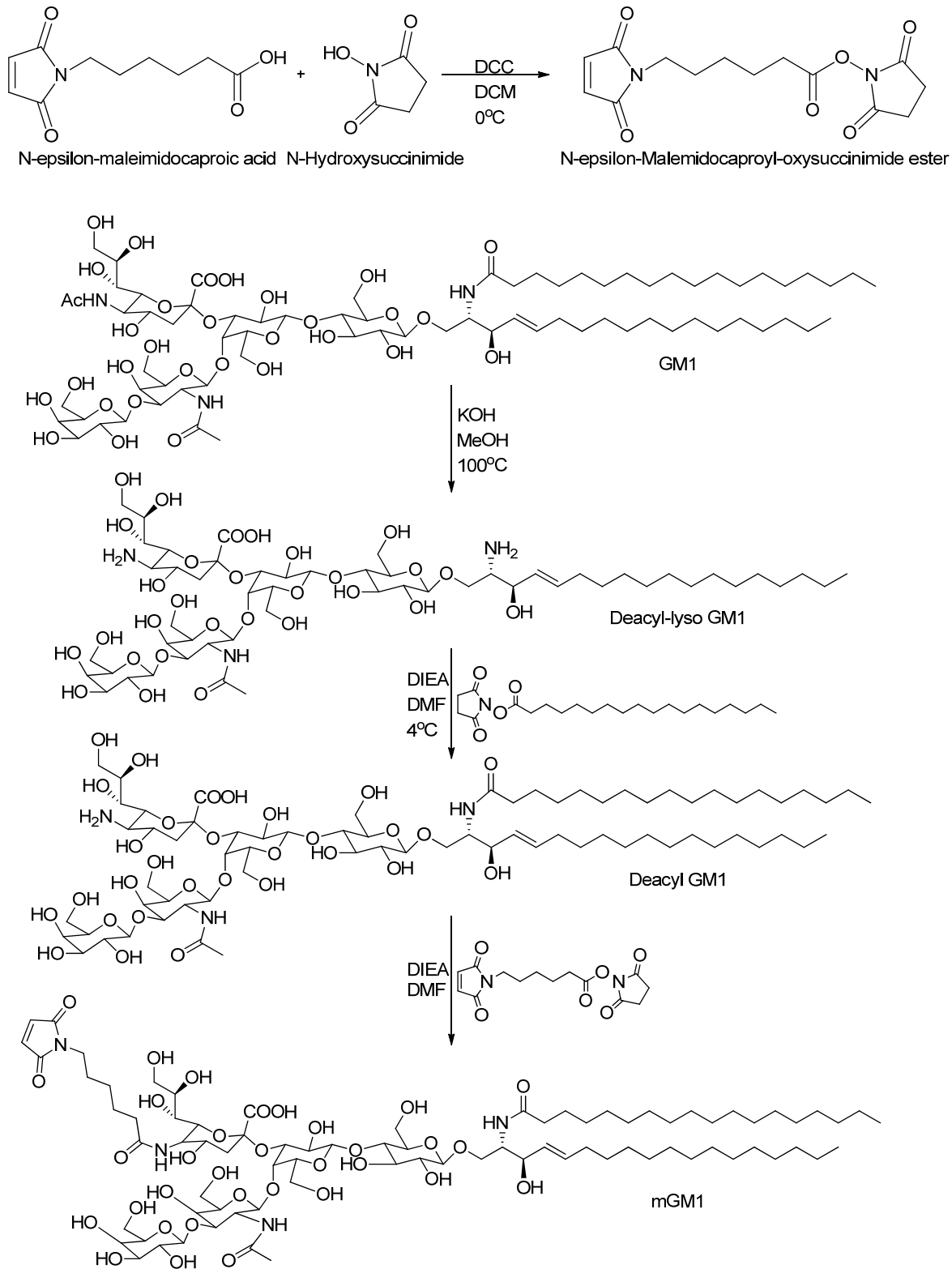
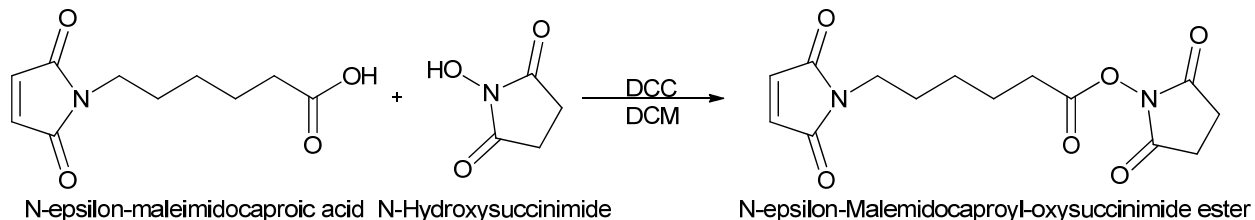


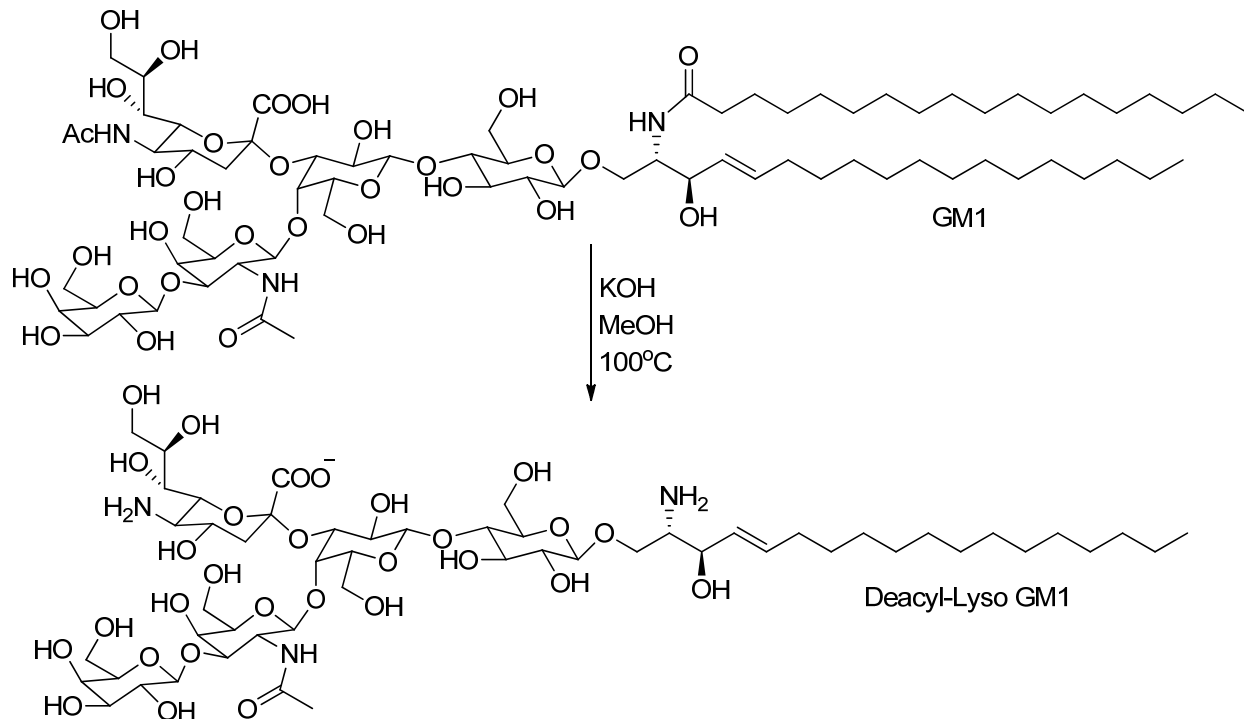
Figure 10. Synthesis of maleimide-GM1 from natural GM1 and EMCA

3.2.1 Synthesis and Purification of *N*-(ϵ -Maleimidocaproyloxy) succinimide ester (EMCS)



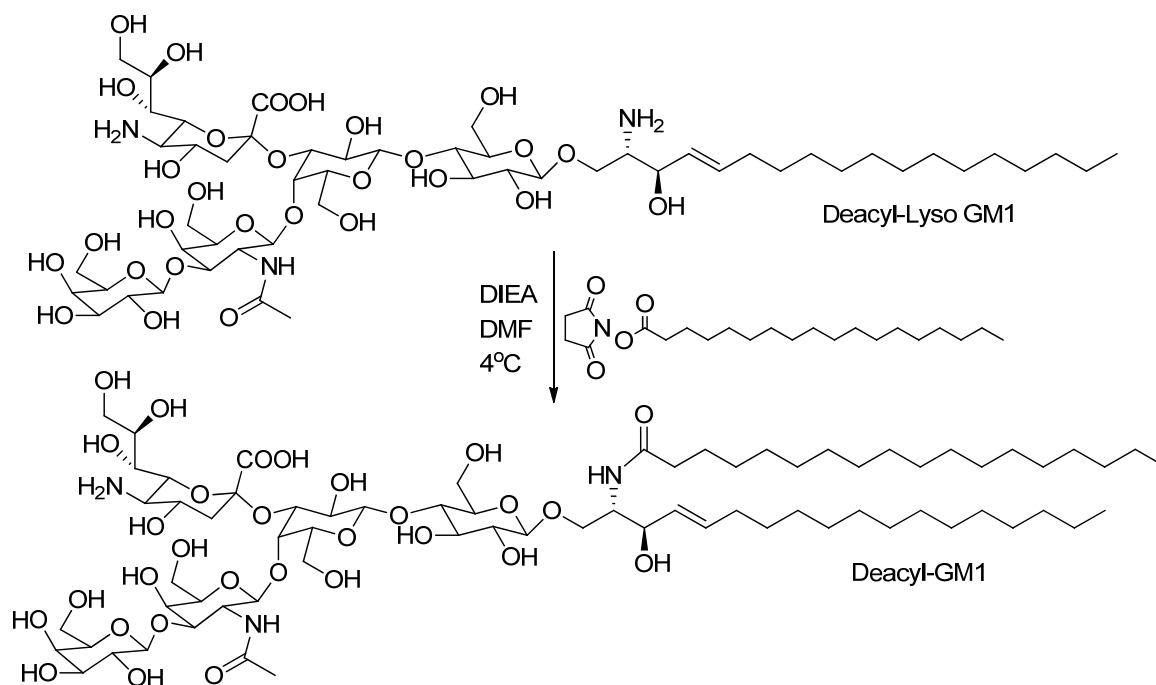
In 10 mL of dry tetrahydrofuran ϵ -Maleimidocaproic Acid (180 mg, 1 eq, 0.85 mmol) and *N*-Hydroxysuccinimide (160 mg, 1.5 eq, 1.37 mmol) were dissolved. *N,N'*-Dicyclohexylcarbodiimide (345 mg, 2 eq, 1.67 mmol) was added and the reaction was stirred at 0°C for two hours. The solvent was removed in vacuo and the reaction completion was confirmed by ¹H NMR. The crude reaction mixture was purified by preparative thin-layer chromatography using 1:1 ethyl acetate: hexane solvent system. The product band was visualized by UV. The product was extracted from the silica gel to yield 185 mg of product (70% yield).

3.2.2 Synthesis and Purification of Deacyl-Lyso GM1



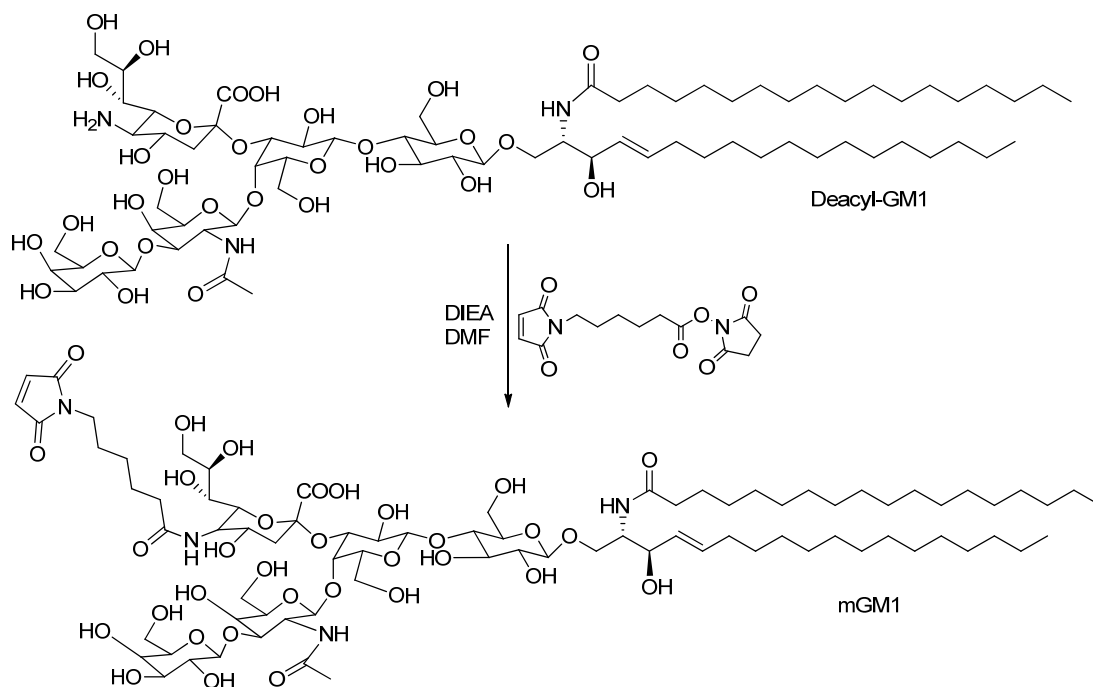
To 50 mL of dry methanol, potassium hydroxide was dissolved (1.7800 g, 100 eq., 32 mmol). Ganglioside GM1 (500 mg, 1 eq., 0.32 mmol) was added and the reaction was heated to 100°C in an oil bath, under pressure, and stirred for two days.¹¹⁵ The reaction progress was monitored by MALDI-TOF MS and thin layer chromatography; the reactant had an R_f value of 0.25 and the product had an R_f value of 0.05 (Solvent: 60:40:9 chloroform: methanol: water). The solvent was removed in vacuo and the resulting residue was neutralized to pH 7.0 with acetic acid and then dialyzed against water (2 X 1.0 L). The resulting solution was lyophilized to yield the crude product. The crude reaction mixture was purified by silica gel column chromatography (2:2:1 butanol: methanol: water). The elution was monitored using thin layer chromatography and MALDI-TOF MS. The product was collected and the solvent was removed in vacuo, yielding 163 mg (40% yield).

3.2.3 Synthesis and Purification of Deacyl-GM1



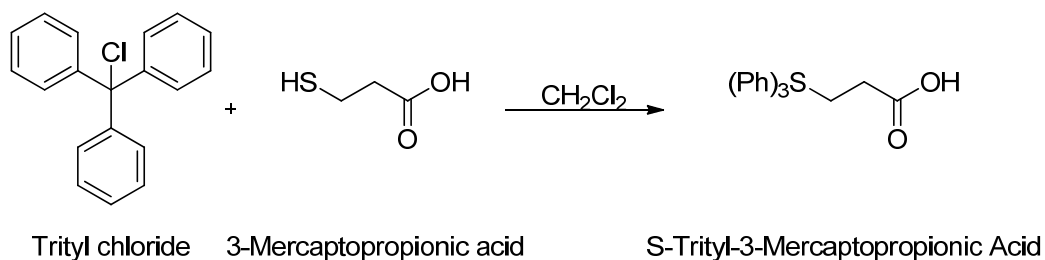
Deacyl-lyso GM1 (27 mg, 1 eq, 22 μmol) and stearic acid-NHS ester (ZL-III-140, 8 mg, 1 eq, 21 μmol) were placed in an oven-dried flask and dried on the high oil pump for a half hour and purged with argon. The starting materials were dissolved in 3 mL of dry dimethylformamide (7 μM with respect to Deacyl-lyso GM1), and the reaction mixture was cooled on ice for 5 minutes before adding 20 μL of N,N-diisopropylethylamine. The reaction was stirred on ice overnight and the reaction progress was monitored by thin layer chromatography; the product had an R_f value of 0.13 (Solvent: 60:40:9 chloroform: methanol: water). The solvent was removed in vacuo yielding the crude product. It was purified using silica gel chromatography (60:40:5 chloroform: methanol: water) and elution was monitored using thin layer chromatography (60:40:9 chloroform: methanol: water) and MALDI-TOF MS. Solvent was removed in vacuo to yield 19 mg of product (50% yield).

3.2.4 Synthesis and Purification of Maleimide-GM1 (mGM1)



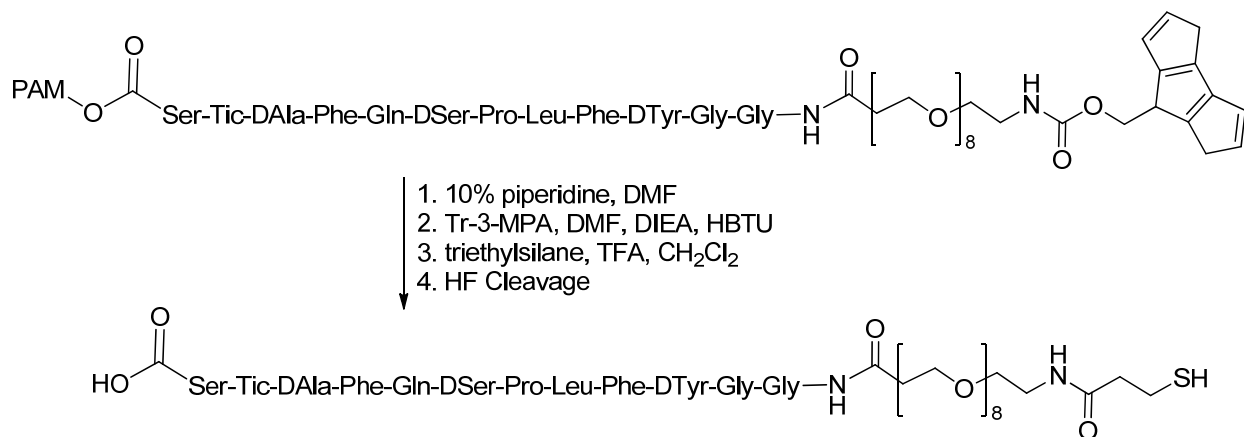
Deacyl-GM1 (25.0 mg, 1 eq, 16.6 μmol) and EMCS (28.0 mg, 5 eq, 90.9 μmol) were added to dry flask and dissolved in 1 mL of dry dimethylformamide (17 mM with respect to Deacyl-GM1). The reaction was stirred overnight at room temperature and the reaction progress was monitored by MALDI-TOF MS and thin layer chromatography; the product had an R_f value of 0.4 (Solvent: 60:40:9 chloroform: methanol: water). The solvent was removed in vacuo. The crude product was purified by preparative thin layer chromatography (60:40:5 chloroform: methanol: water). The product band was visualized by UV, confirmed by MALDI-TOF MS, and extracted from the silica using 50:50 chloroform: methanol. The product was then further purified by dialysis (3 X 1.0 L) and the resulting solution was lyophilized. To remove chloroform soluble impurities, the resulting product was redissolved in water and washed with chloroform resulting in 5 mg of pure product, confirmed by ^1H NMR (20% yield).

3.2.5 Synthesis and Purification of S-Tryl-3-Mercaptopropionic Acid (Tr-3MPA)



Trityl chloride (1.1600 g, 1.6 eq, 4 mmol) and 4Å molecular sieves were added to a dry flask and dissolved in methylene chloride. 3-mercaptopropionic acid (220 µL, 1 eq, 2.5 mmol) were added and the reaction was stirred overnight at room temperature, resulting in yellow solid formation. The solvent was removed in vacuo and the remaining residue was washed with methylene chloride and hexane until the yellow color was removed. The solid was suspended in diethyl ether and collected by vacuum filtration to yield 870 mg (100% yield).

3.2.6 Synthesis and Purification of *s*-Chemerin9-PEG8-3-Mercaptopropionic Acid (*s*Chem9-PEG8-MPA)



s-chemerin9-PEG8-Fmoc was pre-synthesized in the lab on PAM resin. *s*chemerin9-PEG8-Fmoc (75 mg, 1 eq, 0.025 mmol) was swelled in dimethylformamide for one hour. 10% piperidine (2 mL) was added and allowed to react for 10 minutes. A positive Kaiser test was used to confirm reaction completion. S-trityl-3-mercaptopropionic acid (34.8 mg, 4 eq, 0.100 mmol), and N,N,N',N'-Tetramethyl-O-(1H-benzotriazol-1-yl)uronium hexafluorophosphate (36.0 mg, 3.8 eq, 0.095 mmol) were dissolved in 1 mL of dimethylformamide (to yield 0.1 M concentration of the peptide) and 26 μ L of diisopropylethylamine (6 eq, 0.150 mmol) was added. This solution was added to the resin and allowed to react for 1.5 hours. A negative Kaiser test was used to determine reaction completion. To remove the trityl group, triethylsilane (40 μ L, 10 eq, 0.250 mmol) was added to 4 mL of 1:1 methylene chloride: trifluoroacetic acid. This solution was added to the resin and allowed to react overnight. The resin was washed with dimethylformamide, methylene chloride, and diethyl ether, transferred to an HF cleavage vessel and dried overnight in vacuo. Following HF cleavage, the resin was washed with cold ether and then the peptide was eluted using 100 mL of 10% acetic acid (aqueous). The solvent was removed in vacuo and the remaining residue was freeze dried yielding 46.1 mg of crude product

(51% yield). The peptide was purified by semi-preparative HPLC using 30%-44% Solvent B over 45 minutes, yielding 7.5 mg (30% yield from previous step). Purity was confirmed by Analytical HPLC using 25%-45% Solvent B over 45 minutes, and identity was confirmed by MALDI-TOF MS.

3.2.7 Spectral Data of Compounds

N-(ϵ -Maleimidocaproyloxy) succinimide ester (EMCS): white solid (185 mg, 70%);

^1H NMR (500 MHz, CDCl_3) δ 6.69 (s, 2H), 4.11 (q, 2H, $J_1=15$ Hz, $J_2=5$ Hz), 2.82 (s, 4H), 2.59 (t, 2H, $J=7.5$ Hz), 1.80-1.74 (m, 2H), 1.66-1.60 (m, 2H), 1.43-1.37 (m, 2H)

^{13}C NMR (125 MHz, CDCl_3) δ 170.80, 169.04, 168.35, 134.06, 37.47, 30.78, 28.04, 25.84, 24.08

Deacyl-Lyso GM1: white solid (163 mg, 40%); MALDI-TOF MS: m/z [$\text{C}_{53}\text{H}_{94}\text{N}_3\text{O}_{29}$] $^-$ calcd: 1236.60, found: 1235.601, m/z [$\text{C}_{55}\text{H}_{98}\text{N}_3\text{O}_{29}$] $^-$ calcd: 1264.63, found: 1263.595.

Deacyl-GM1: white solid (19 mg, 50%); MALDI-TOF MS: m/z [$\text{C}_{71}\text{H}_{128}\text{N}_3\text{O}_{30}$] $^-$ calcd: 1502.86, found: 1501.869 m/z [$\text{C}_{73}\text{H}_{132}\text{N}_3\text{O}_{30}$] $^-$ calcd: 1531.83, found: 1529.886

Maleimide-GM1 (mGM1): white solid (5 mg, 20%);

MALDI-TOF MS: m/z [$\text{C}_{81}\text{H}_{139}\text{N}_4\text{O}_{33}$] $^-$ calcd: 1695.93, found: 1696.412 m/z [$\text{C}_{83}\text{H}_{143}\text{N}_4\text{O}_{33}$] $^-$ calcd: 1723.96, found: 1723.402

ESI MS (ms2 1695.55@30.00) m/z [$\text{C}_{81}\text{H}_{139}\text{N}_4\text{O}_{33}$] $^-$ calcd: 1695.93, found: 1695.36, m/z [$\text{C}_{62}\text{H}_{113}\text{N}_2\text{O}_{23}$] $^-$ calcd: 1253.77, found: 1253.36, m/z [$\text{C}_{48}\text{H}_{90}\text{NO}_{13}$] $^-$ calcd: 888.64, found: 888.45 (ms2 1724.00@29.00) m/z [$\text{C}_{83}\text{H}_{144}\text{N}_4\text{O}_{33}$]: calcd: 1724.97, found: 1724.45, m/z [$\text{C}_{64}\text{H}_{118}\text{N}_2\text{O}_{23}$] $^-$ calcd: 1282.81, found: 1281.36, m/z [$\text{C}_{50}\text{H}_{95}\text{NO}_{13}$] $^-$ calcd: 917.68, found: 916.38.

S-Trityl-3-Mercaptopropionic Acid: white solid (870 mg, 100%)

^1H NMR (500 MHz, $\text{C}_2\text{D}_6\text{OS}$) δ 12.15 (s, 1H), 2.27 (t, 2H, $J=5$ Hz), 2.15 (t, 2H, $J=5$ Hz)

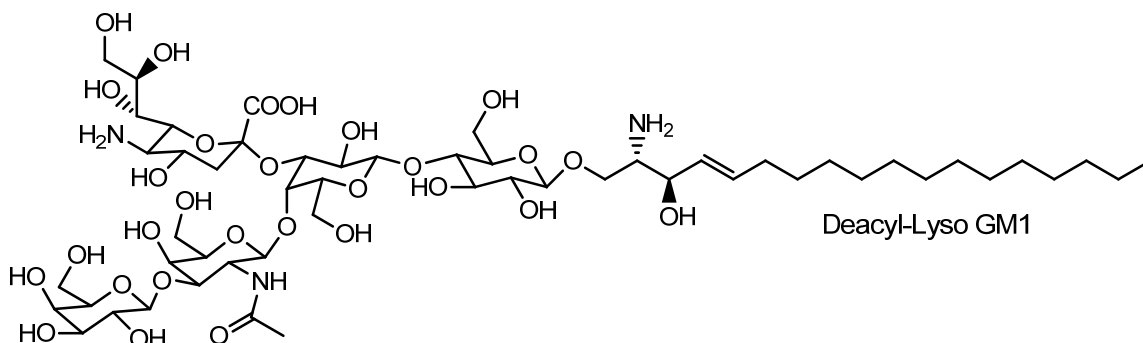
^{13}C NMR (125 MHz, $\text{C}_2\text{D}_6\text{OS}$) δ 173.13, 144.84, 129.56, 128.51, 127.21, 66.65, 33.37, 27.16

s-Chemerin9-PEG8-3-Mercaptopropionic Acid: white solid (7.5 mg, 30%);

MALDI-TOF MS: m/z [$\text{C}_{88}\text{H}_{126}\text{N}_{14}\text{O}_{27}\text{S} + \text{Na}$] $^+$ calcd: 1867.07, found: 1866.256

3.3 Optimization of Reactions

3.3.1 Optimization of purification of Deacyl-Lyso GM1



Prior to silica gel purification with 2:2:1 butanol: methanol: water, solvent systems of chloroform:methanol:water were used. Specifically, 60:40:5 chloroform:methanol:water ended up being not polar enough, but allowed the removal of less polar impurities. The polarity of the solvent was increased to 60:40:9 chloroform:methanol:water and once the product began to come out, changing the solvent system to 60:40:9 chloroform:methanol: 1M ammonium hydroxide(aq) allowed for quicker elution. Oftentimes, TLC was not sensitive enough to detect the elution of product and ESI-MS or MALDI-TOF MS were much more apt in detecting product elution. However, even after multiple purifications, it was still difficult to achieve purity. Changing the solvent system to butanol:methanol:water allowed for much better purification of GM1 compounds. For deacyl-lyso GM1, 2:2:1 butanol:methanol:water was sufficient to achieve good ^1H NMR purity. The purification with butanol at this step also makes subsequent purifications easier. Additionally, the crude product was loaded dry onto the column.

3.3.2 Optimization of overall synthesis of Maleimide-GM1 (mGM1)

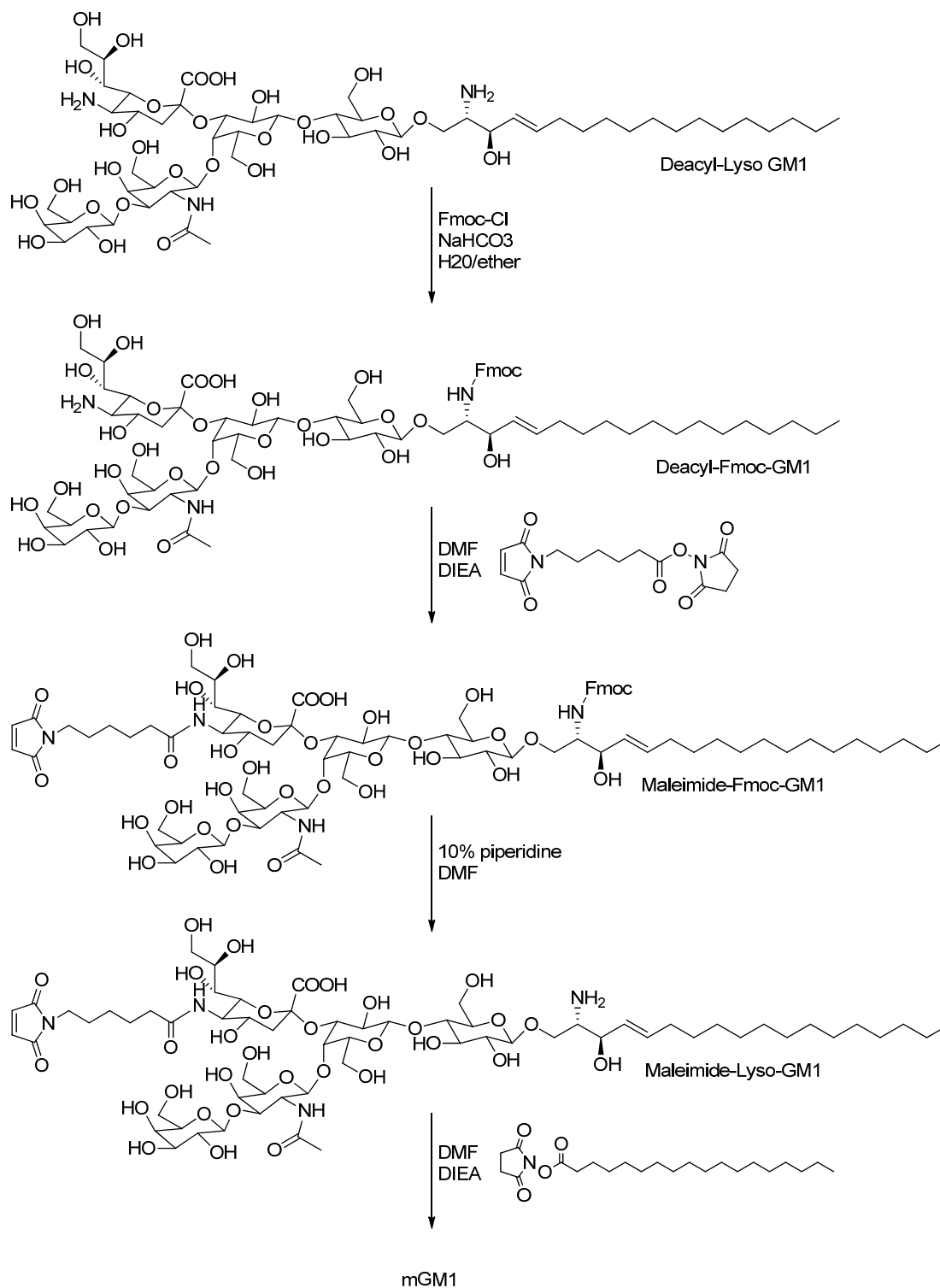


Figure 11. Initial Reaction scheme for the synthesis of mGM1.

The initial reaction scheme for mGM1 was adapted from Schwarzmann and Sandhoff's synthesis paper on preparing labeled gangliosides.¹¹⁵ In this reaction scheme, to modify the sialic acid amine after base methanolysis of both stearic acid and acetic acid, the free amine on the sphingosine was first protected with fluorenylmethyloxycarbonyl (Fmoc). The advantage of this synthesis scheme is that the protection with Fmoc is a two phase reaction with the Deacyl-lyso-GM1 in the aqueous layer and Fmoc-Cl in the ether layer. The aqueous layer is first frozen and allowed to slowly melt at 4°C along with continuous stirring to allow for the slow mixing of the two layers and reaction. If there is exactly 1 equivalent of Fmoc-Cl, it will selectively add to the free amine on the sphingosine, because as it is the less sterically hindered site; it is the kinetic product, which is favored at low temperatures. This protection, then allows for an excess of whatever desired molecule is to be attached to the sialic acid, which in this case would be EMCS. The Fmoc protecting group is then removed through typical piperidine protonation and subsequent cleavage of an aromatically stable leaving group. However, upon deprotection of the Fmoc protecting group, the maleimide was found to be unstable in the basic conditions, due to piperidine, and thus a different method of synthesis had to be formulated. The reaction was monitored by TLC every 10 minutes, until a new spot appeared at 40 minutes. However, upon concentration in vacuo and preparative thin layer chromatography in 50:50:10 (chloroform:methanol:water), the product could not be found in any of the fractions by MALDI-TOF MS and the hydrolyzed maleimide peak is evident by ¹H NMR.

The modified reaction scheme is described in the above section. To avoid Fmoc protection and subsequent deprotection by piperidine, the stearic acid was immediately coupled to Deacyl-lyso-GM1. To ensure specificity, the reaction was carried with exactly 1 equivalent of stearic acid-NHS ester to Deacyl-lyso-GM1 and at 4°C to allow for the kinetic product to form

preferentially. Once again, attachment at the sphingosine free amine is more favorable due to the lack of steric hindrance. Additionally, specificity may also have been promoted due to hydrophobic interactions between the two lipid moieties. This modification to the synthesis also aided in higher yield overall because it shortened the total number of steps from five to three steps. From this step, the EMCS can be coupled to the Deacyl-GM1 as previously described, and as in the initial reaction scheme, it can be added in excess because there is only one reactive amine. It is important to add excess of EMCS because the sialic acid free amine is more sterically hindered.

3.3.2 Optimization of synthesis and purification of Deacyl-GM1

As previously mentioned the reaction was carried out at 4°C to favor synthesis of the kinetic product. The reaction was also carried out under dilute conditions to favor only a single-coupled product. The reaction was found to run to nearly completion after six hours, although overnight made no difference in reaction yield. While there was still evidence of Deacyl-lyso-GM1 starting material by both thin layer chromatography and MALDI-TOF-MS, adding more stearic acid-NHS ester resulted in lower yield due to double-coupling to the free amine of sialic acid. Even with 1:1 equivalents of Deacyl-lyso-GM1 to Deacyl-GM1, there was still some amount of the double-coupled product that formed, although this was higher running by thin layer chromatography and was easy to purify out. For purification of Deacyl-GM1, silica gel column chromatography with 60:40:9 chloroform: methanol: water was too polar to adequately purify the product; 60:40:5 chloroform: methanol: water was much more effective in purification. Preparative thin layer chromatography was also tried with 50:50:10 chloroform: methanol: water, but this resulted in lower yields.

3.3.3 Optimization of synthesis and purification of Maleimide-GM1 (mGM1)

As previously mentioned, this reaction with deacyl-GM1 and EMCS is less favorable due to the steric hindrance of the pentasaccharide head. Initially, one equivalence of EMCS was not enough to cause product formation within four hours; two more equivalences were added and allowed to react overnight, but product was still not observed. When five equivalences were added at the beginning, product formation was observed overnight. However, this reaction is not stable in dimethylformamide for extended periods of time; when left for 48 hours the solution turns a bright red no product formation is observed. Thus, even though starting material, Deacyl-GM1, is still observed after an overnight reaction, it results in lower yield if more EMCS is added and the reaction is allowed to continue. For purification, preparative thin layer chromatography with 60:40:1 chloroform: methanol: water was sufficiently effective. Silica gel column chromatography with 60:40:1 butanol: methanol: water eluted the product too quickly; chromatography with 80:20:1 butanol: methanol: water eluted the compound too slowly and resulted in band widening. A gradation from 80:20:1 to 60:40:10 butanol: methanol: water was effective, but more time consuming than preparative thin layer chromatography and thus not efficient. By both preparative thin layer chromatography and silica gel chromatography, impurities, specifically hydrophobic impurities were still evident by ^1H NMR. In some cases, dialysis followed by a wash with chloroform was effective in removing them. High performance liquid chromatography was also used to purify the product, the following conditions led to baseline separation: isocratic elution of 46.7: 46.7: 7 isopropanol: hexane: water over 40 minutes. However, it was not entirely effective in removing hydrophobic impurities. This could be due to vesicle formation of GM1-derived constructs in aqueous solution and the trapping of hydrophobic impurities.

3.3.4 Optimization of overall synthesis of Chemerin9-PEG8-3-Mercaptopropionic Acid (sChem9-PEG8-MPA)

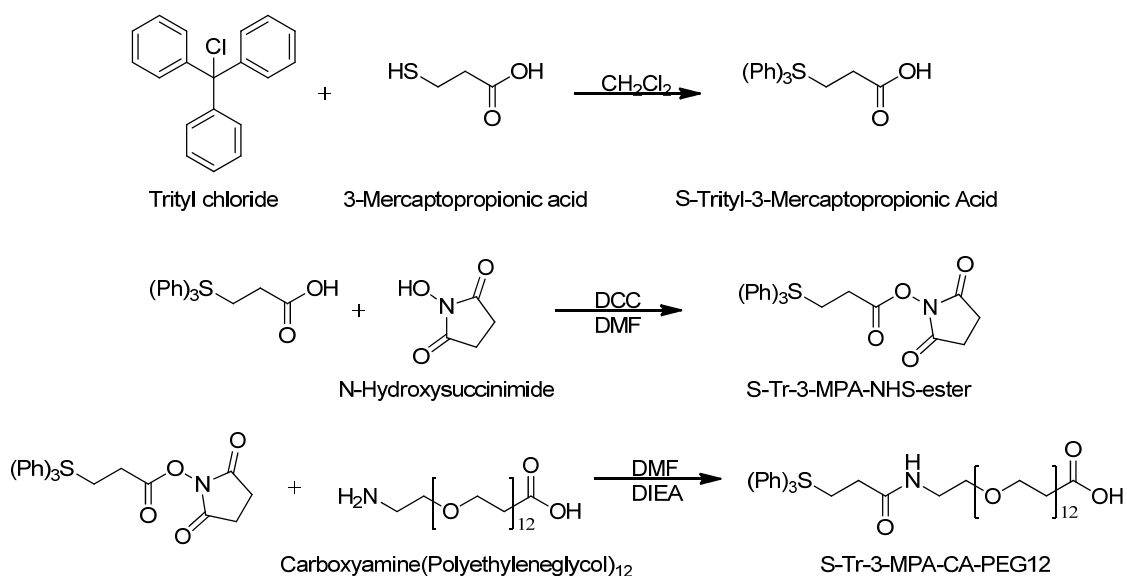


Figure 12. Initial reaction scheme for synthesis of S-Trityl-3-mercaptopropionic acid-carboxyamine(polyethyleneglycol)₈

First, the PEG synthesis was carried out by fully synthesizing the 3-mercaptopropionic acid-trityl-CA(PEG)₈ before solid phase coupling to schemerin9. The 3-mercaptopropionic acid is necessary for the thiol functionality which will be used to couple the peptide to the lipid anchor. The (polyethyleneglycol)₈ is the flexible linker between the peptide ligand and lipid anchor. Finally, the 3-mercaptopropionic acid is initially tritylated because during peptide coupling, the thiol will be under basic conditions due to diisopropylethylamine and the trityl protection prevents disulfide formation. However, the synthesis and purification over these three steps was time consuming. Rather, this was modified to the procedure described above, in which the 3-mercaptopropionic acid was trityl protected, but then the carboxyamine(polyethyleneglycol)₈ and S-Trityl-3-mercaptopropionic acid were added onto schemerin9 through solid phase peptide coupling. This led to significant reduction in synthesis time because no purification was necessary between tests, and yield was also improved.

3.3.5 Optimization of maleimide-thiol coupling reaction

The sample reaction used to mimic S-Tr-3-MPA-PEG8-schemerin9 and mGM1 was glutathione with N-ethyl-maleimide. These compounds are good mimics, because N-ethyl-maleimide (NEM) is soluble in dimethylformamide but not in aqueous buffer and glutathione (GSH) is soluble in aqueous buffer but not in dimethylformamide. This mimics GM1 derivatives which are soluble only in dimethylformamide and schemerin9 which is soluble in the aqueous buffer but not dimethylformamide. The aqueous buffer is necessary to maintain the optimal pH of 7.4 necessary for this reaction; at a lower pH the thiol will not be nucleophilic enough to carry out the reaction, at a higher pH you have the disulfide formation competing with the thiol-maleimide reaction. To further prevent competing disulfide formation, adding Tris (2-Carboxyethyl) phosphine Hydrochloride (TCEP-HCl) was thought to be an option. Additionally, the literature showed that typically the maleimide is added in excess of the thiol, but considering the limited amount of mGM1 available, the thiol was added in excess of the maleimide.

First a TCEP-HCl pH 7.4 phosphate buffer was prepared by adding the literature ratios of monobasic: dibasic stock solution and then titrating with 1M NaOH after addition of TCEP. From this buffer, two sample reactions were setup. The first was a control reaction with NEM dissolved in 1:1 dimethylformamide: phosphate buffer to a concentration of 5 mM. The second reaction was 1:2.5 equivalences of NEM: GSH in 1:1 demthylformamide: phosphate buffer to a concentration of 5 mM. An aliquot was immediately taken for ^1H NMR in D_2O . In both reactions, there were the peaks for NEM at $\delta 0.98$ ppm and $\delta 3.41$ ppm, but not at $\delta 6.67$ ppm, which are the reactive peaks, implying that the NEM was reactive with both the TCEP and maybe the GSH. To confirm reactivity, a third control was made with NEM in 1:1

dimethylformamide: TCEP-free phosphate buffer, which showed the full expected spectrum of NEM confirming reaction with TCEP.

Thus two more control reactions were setup as before but without TCEP and ^1H NMR in D_2O was taken at time 0 hours and time 24 hours. At time 0 hours, the NMR for the control reaction showed no signals, which can be expected since NEM is not soluble in water. At time 24 hours, the NMR showed the appearance of peaks, potentially corresponding to hydrolyzed NEM (reaction below), which would be soluble in water. The reaction with NEM and GSH showed product at both time 0 and time 24 hours.

Finally, one last time-course experiment was taken in which the reaction was carried out in NMR tubes. Deuterated sodium phosphate buffer was made by first making 2M monobasic and dibasic stock solution, adding them in the appropriate ratios and then diluting 200-fold to 0.1M with D_2O . The same two reactions were carried out but with 1:1 $\text{D}_2\text{O}:\text{CD}_3\text{OD}$. ^1H NMR was taken at: 5 minutes, 30 minutes, 4 hours, 9 hours and 24 hours. Over 24 hours, the control reaction with only NEM showed hydrolysis by both water and methanol. The NEM:GSH reaction showed consumption of NEM at time zero and no formation of hydrolyzed NEM, shown from the rightward shift in the quartet at 3.53 ppm. This this implies that even though the NEM and GSH were not soluble in the same solvent, a mixture solvent could allow for their reaction at pH 7.4, without TCEP, and at 1:2.5 maleimide: thiol.

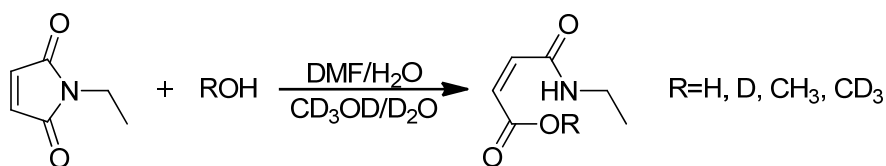


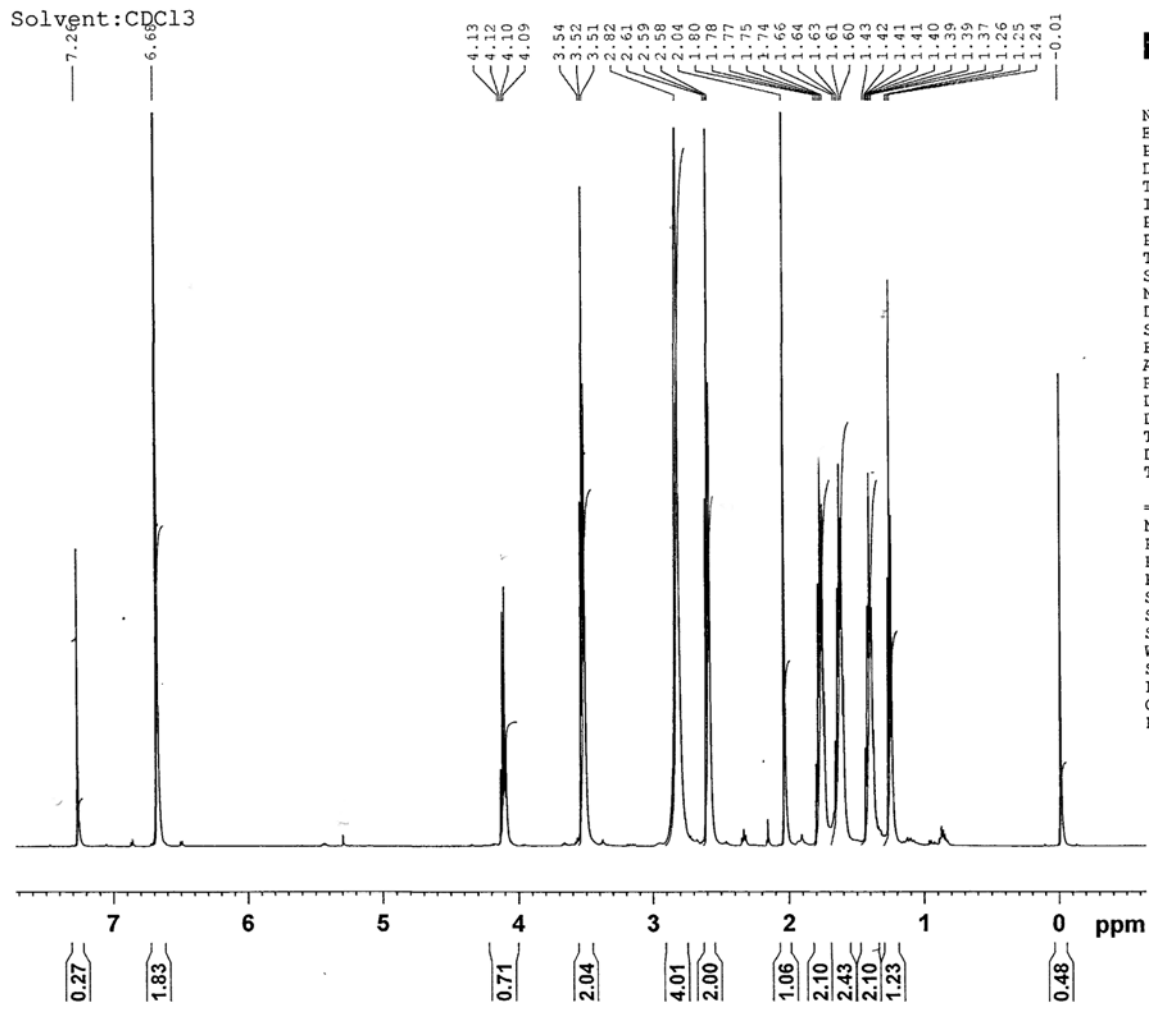
Figure 13. Hydrolysis of N-ethylmaleimide.

3.4 Future Directions

Future directions for this project will include the coupling of mGM1 to schem9-PEG₈-3MPA and optimizing both the reaction conditions and purification conditions, although the NEM and GSH model reaction provide a promising starting point. Afterwards, cellular studies using the luciferase assay previously described will allow determination of both the efficacy and specificity of this construct relative to the soluble ligand. If this proves to be promising, it would be important to see if this is a generalizable technique to other ligands and their cognate GPCRs. Another advantage of using ganglioside GM1 is its specific intracellular trafficking pathway. Being able to use ganglioside GM1 as a lipid transporter to intracellular vesicles could allow for the targeting of intracellular receptors.

G protein coupled receptors are the largest class of proteins in the human proteome. As such, they play a critical role in both basic biology and in medicinal chemistry. Finding effective methods of targeting such receptors is a key role in elucidating their roles and constructing therapeutics. In the past decade, membrane tethered ligands have shown to be potent agonists and antagonists. Pepducins have successfully made use of lipid tethering of peptides to the intracellular leaflets, and using ganglioside GM1 has shown promise in targeting peptides to the extracellular leaflet to act as orthosteric agonists and antagonists. Here, the synthesis of a maleimide-functionalized derivative of GM1 is presented to allow for the attachment of peptides via reaction with a free thiol. Furthermore, the synthesis of a thiol-functionalized, stable chemerin9 with a polyethyleneglycol flexible linker is also presented. Due to the relevance of chemokine-receptor-like-1 (CMKLR1) in inflammation, having a potent and biostable antagonist like ganglioside GM1 tethered stable chemerin9 could be important as both an anti-inflammatory therapeutic and analyzing the signaling pathways of CMKLR1.

APPENDIX



M E T H I L D E N S E N S I T I V E

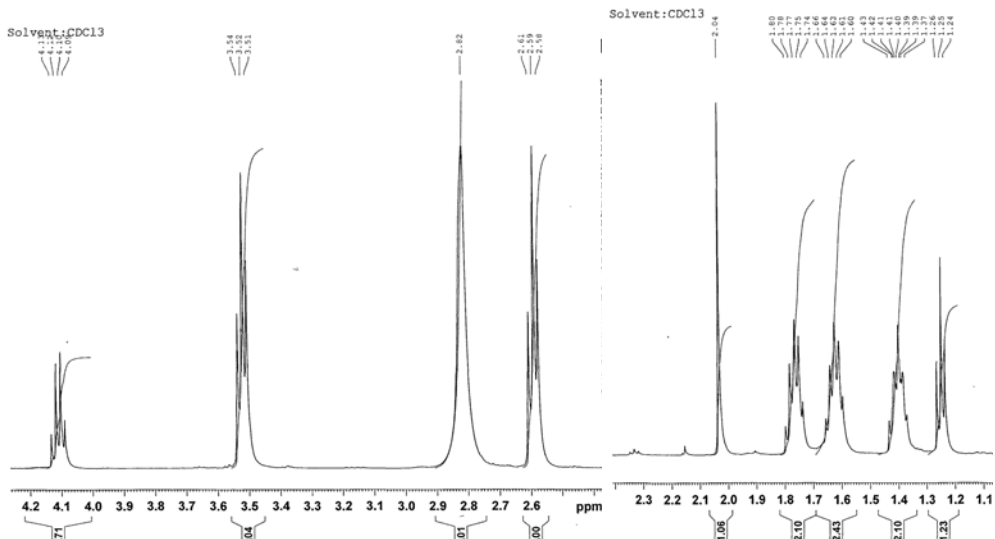


Figure A1.1. ¹H NMR Spectrum of EMCS

DeAc Lysc GM1
Solvent: MeOD

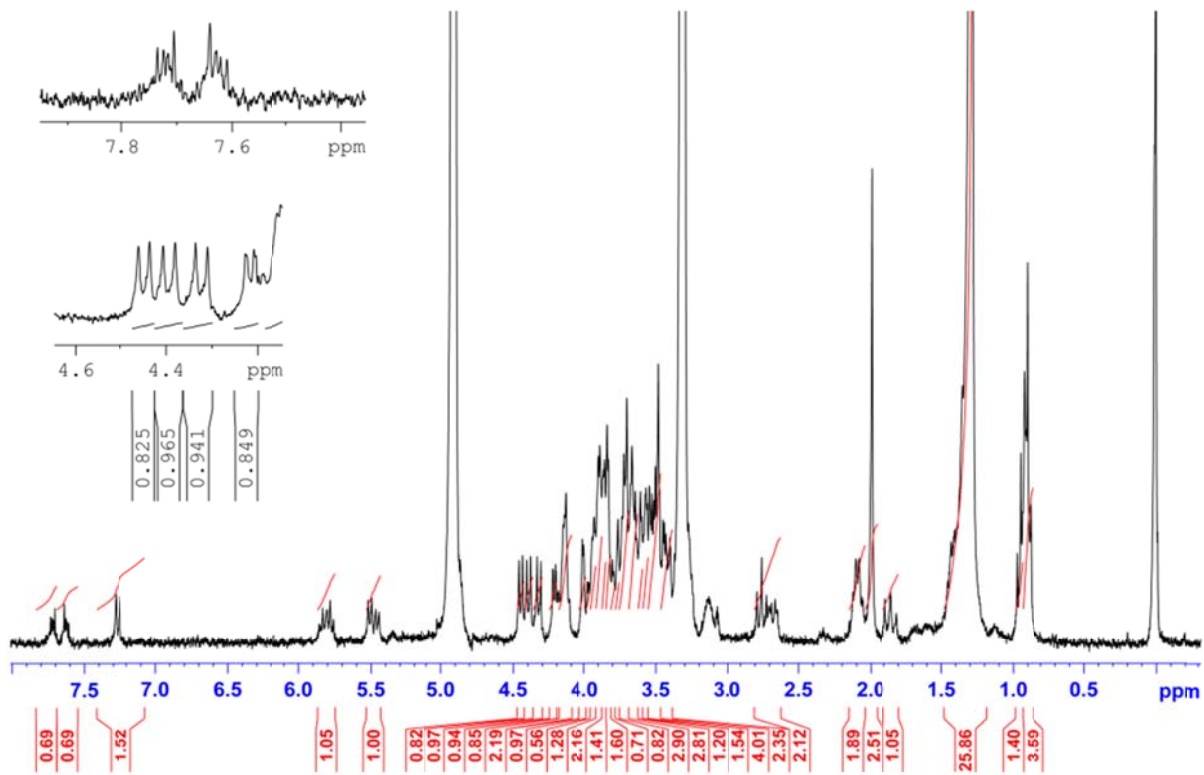
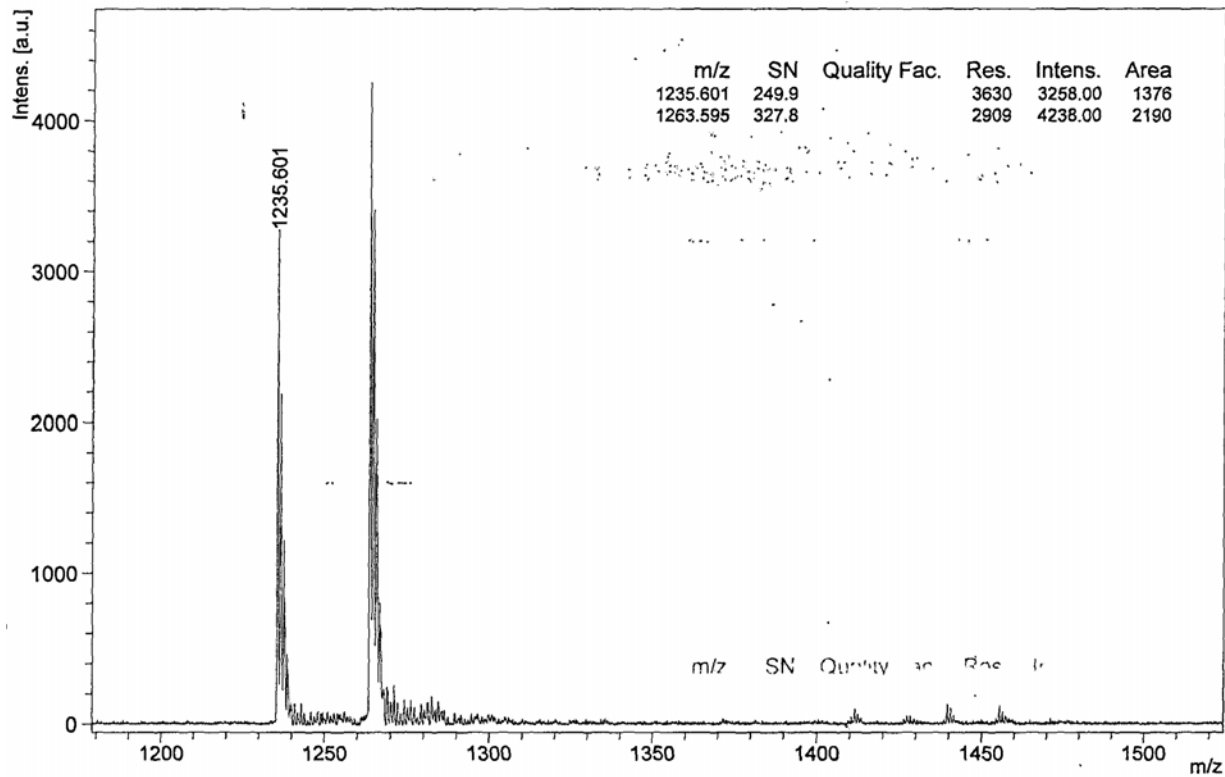


Figure A.1.3. ^1H NMR Spectrum of Deacyl-lyso GM1. The peaks at 7.5 ppm are due to solvent impurities in butanol.



FigureA.1.4. MALDI-TOF MS Spectrum of Deacyl-Lyso GM1

DeAc GM1
Solvent: MeOD

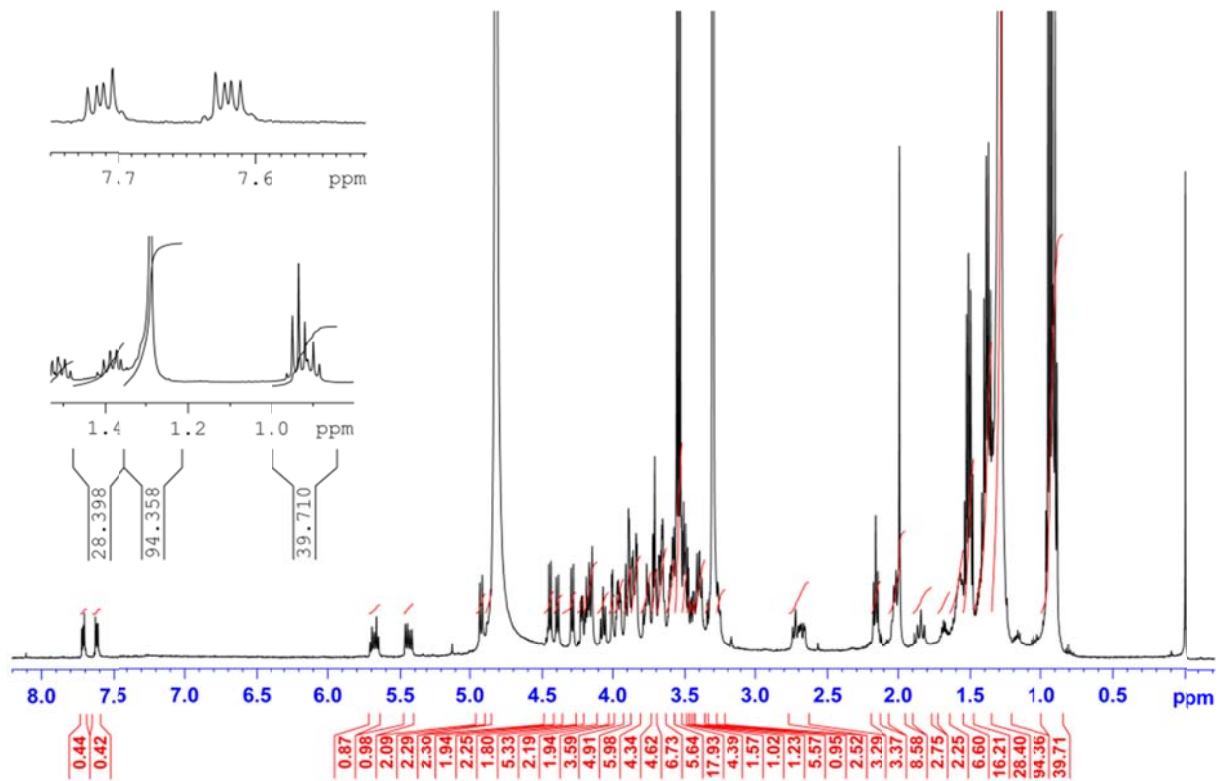


Figure A.1.5. ¹H NMR Spectrum of Deacyl GM1. The peaks at 7.5 ppm are due to solvent impurities in butanol.

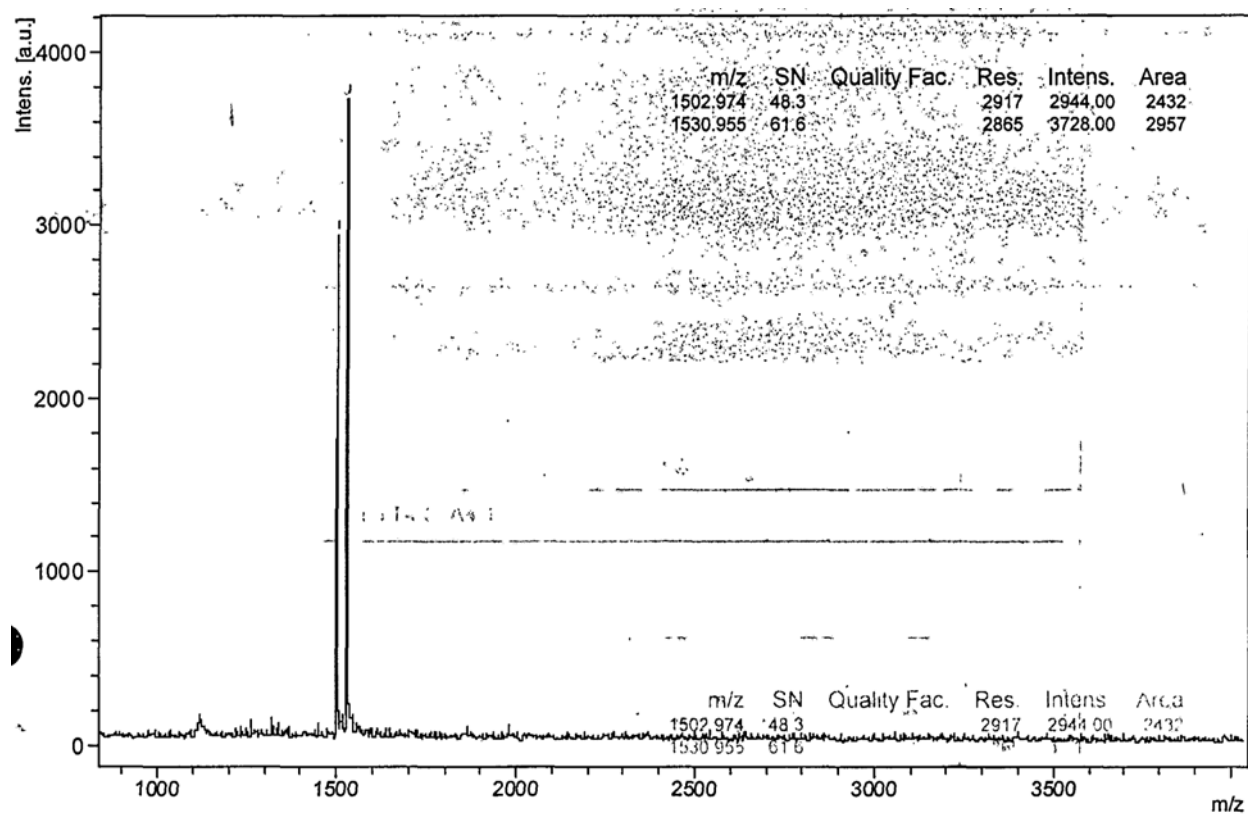


Figure A.1.6. MALDI-TOF MS Spectrum of Deacyl GM1.

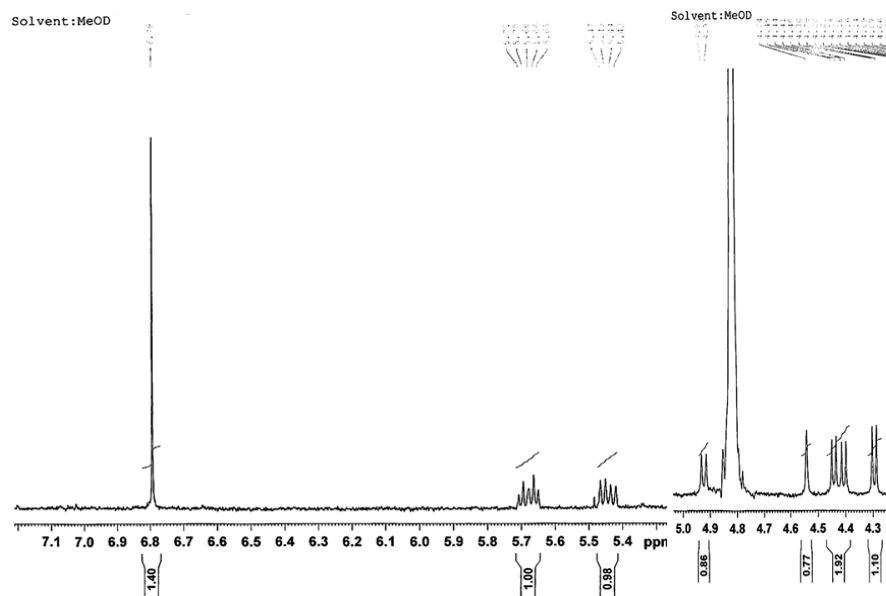
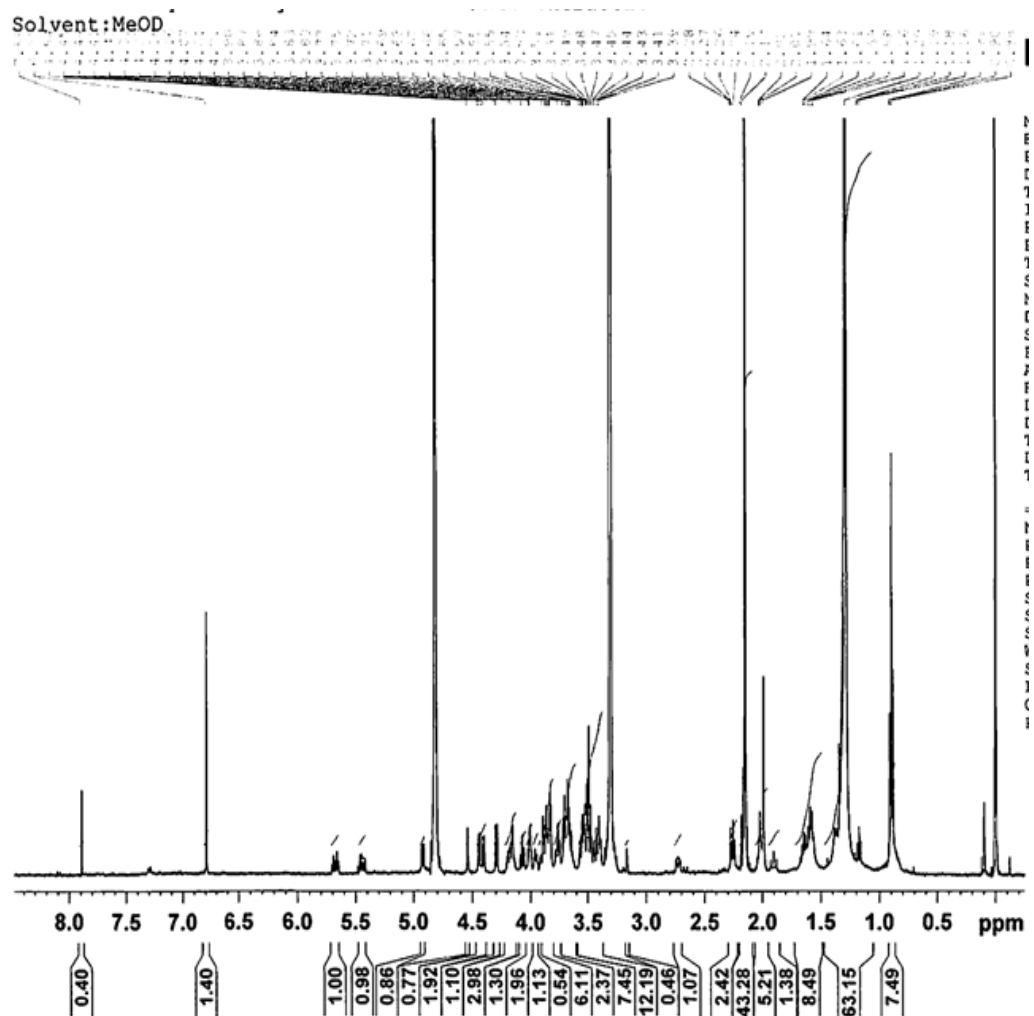
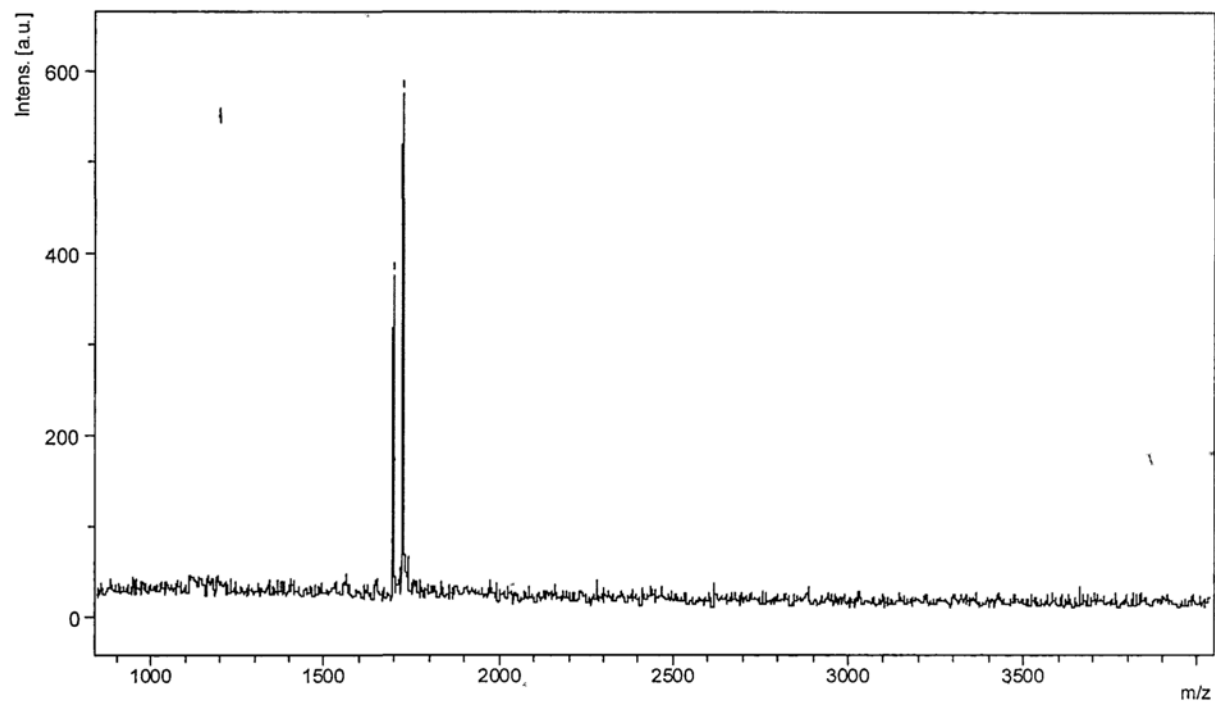


Figure A.1.7. ^1H NMR Spectrum of maleimide GM1.



m/z	SN	Quality Fac.	Res.	Intens.	Area
1697.042	14.1		5993	372.25	268
1725.091	21.1		3080	554.25	462

Figure A.1.8. MALDI-TOF MS Spectrum of maleimide GM1.

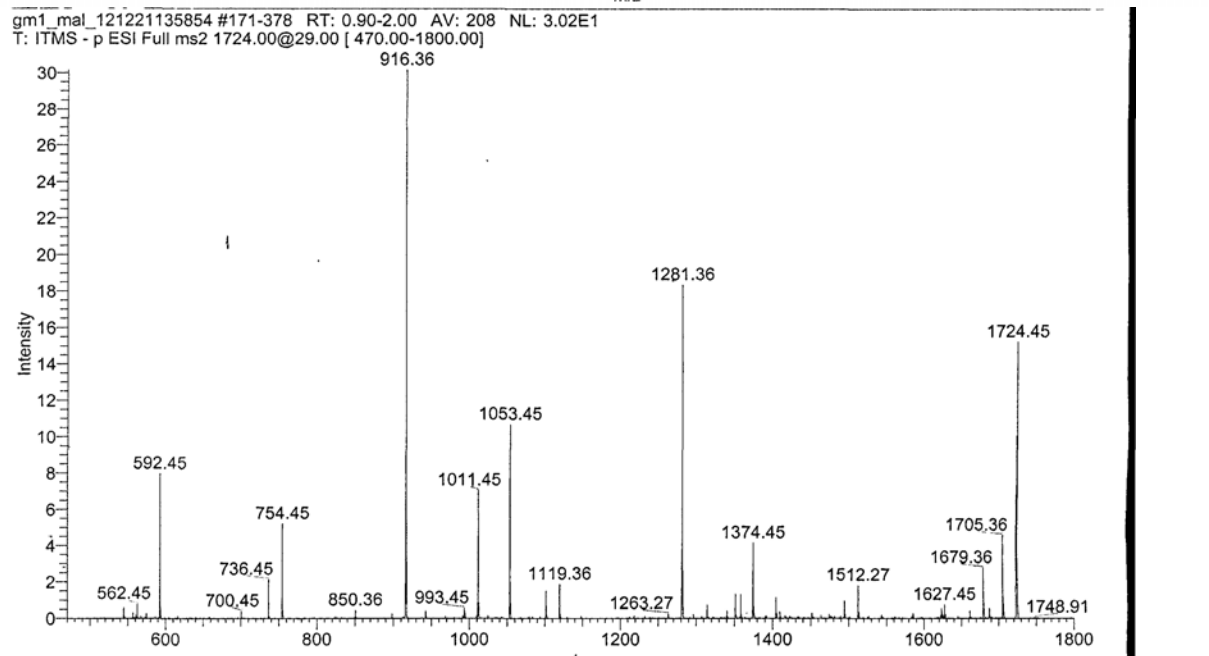
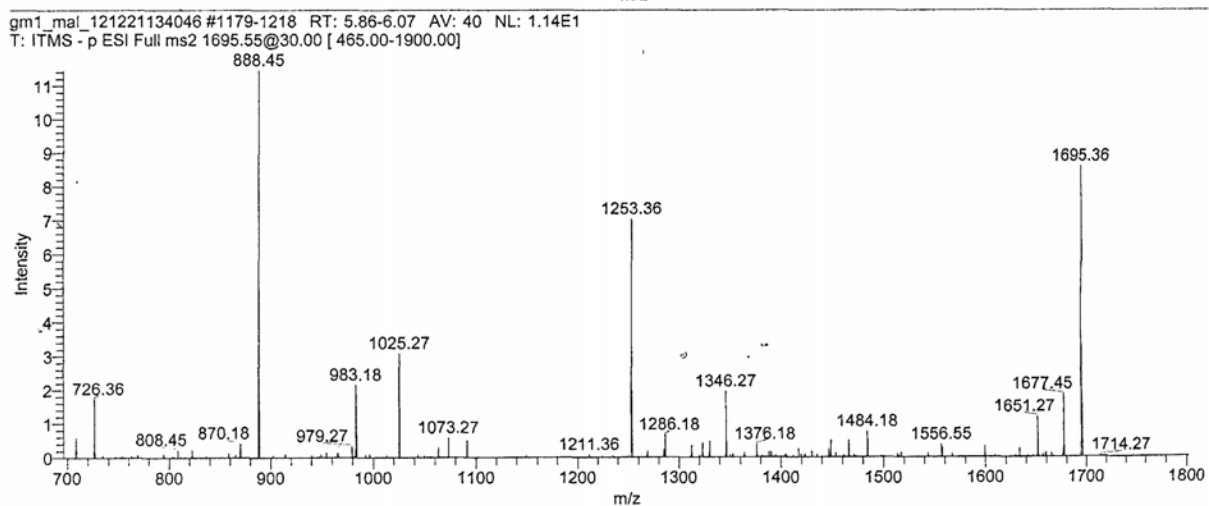
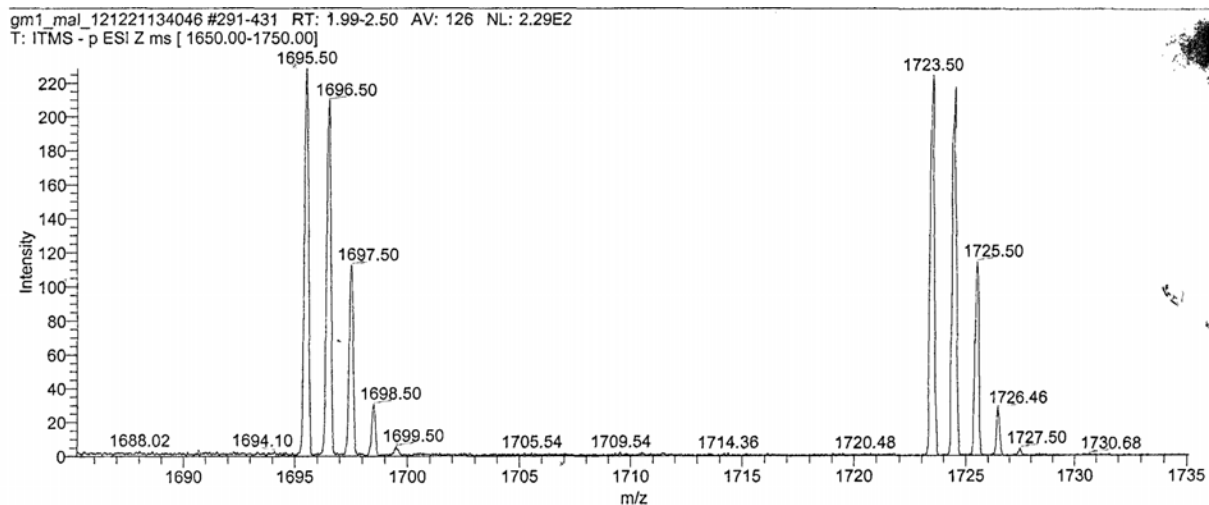


Figure A.1.9. ESI MS Spectrum of maleimide GM1.

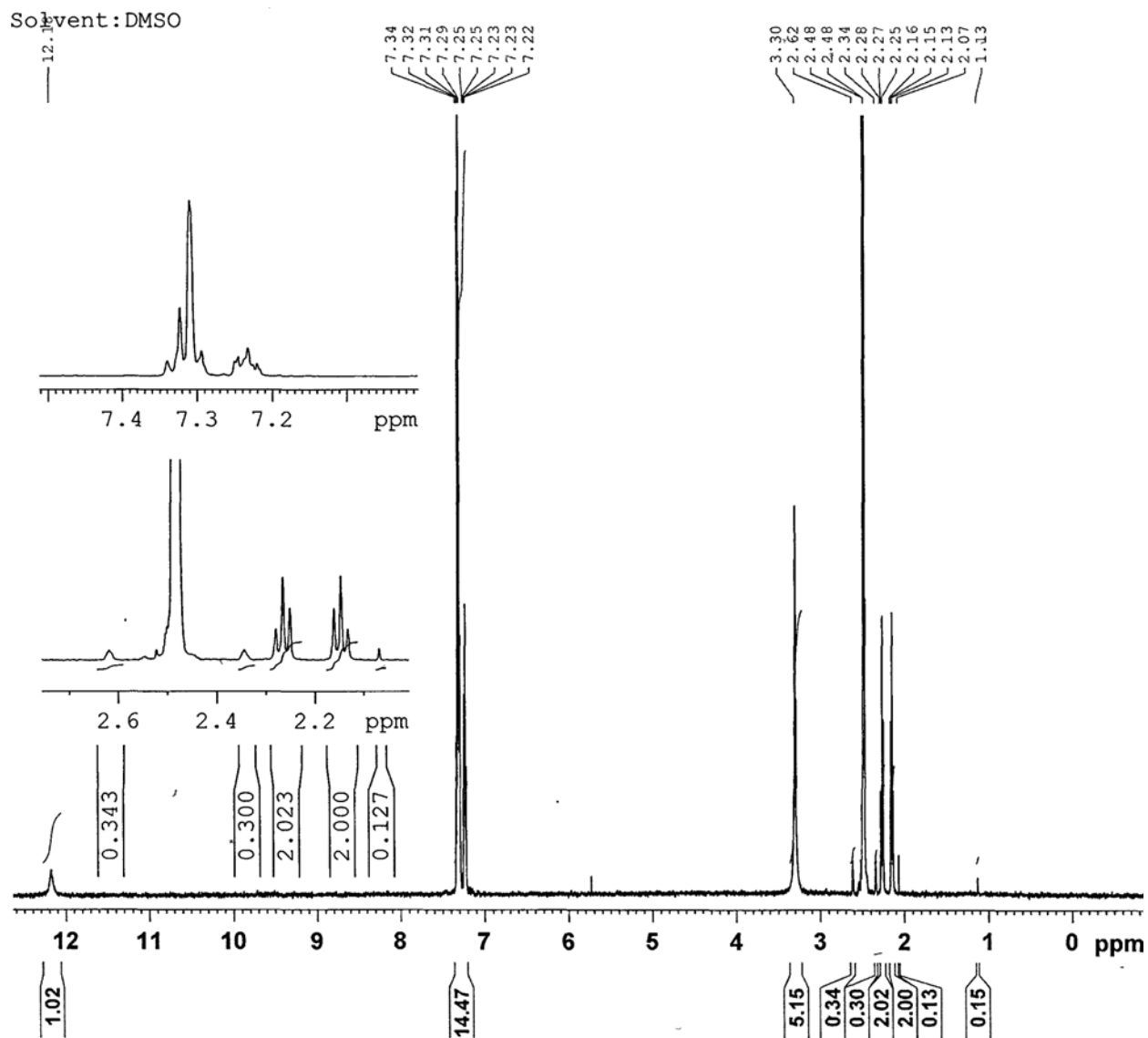


Figure A.1.10. ^1H NMR Spectrum of S-Trityl-3-Mercaptopropionic Acid.

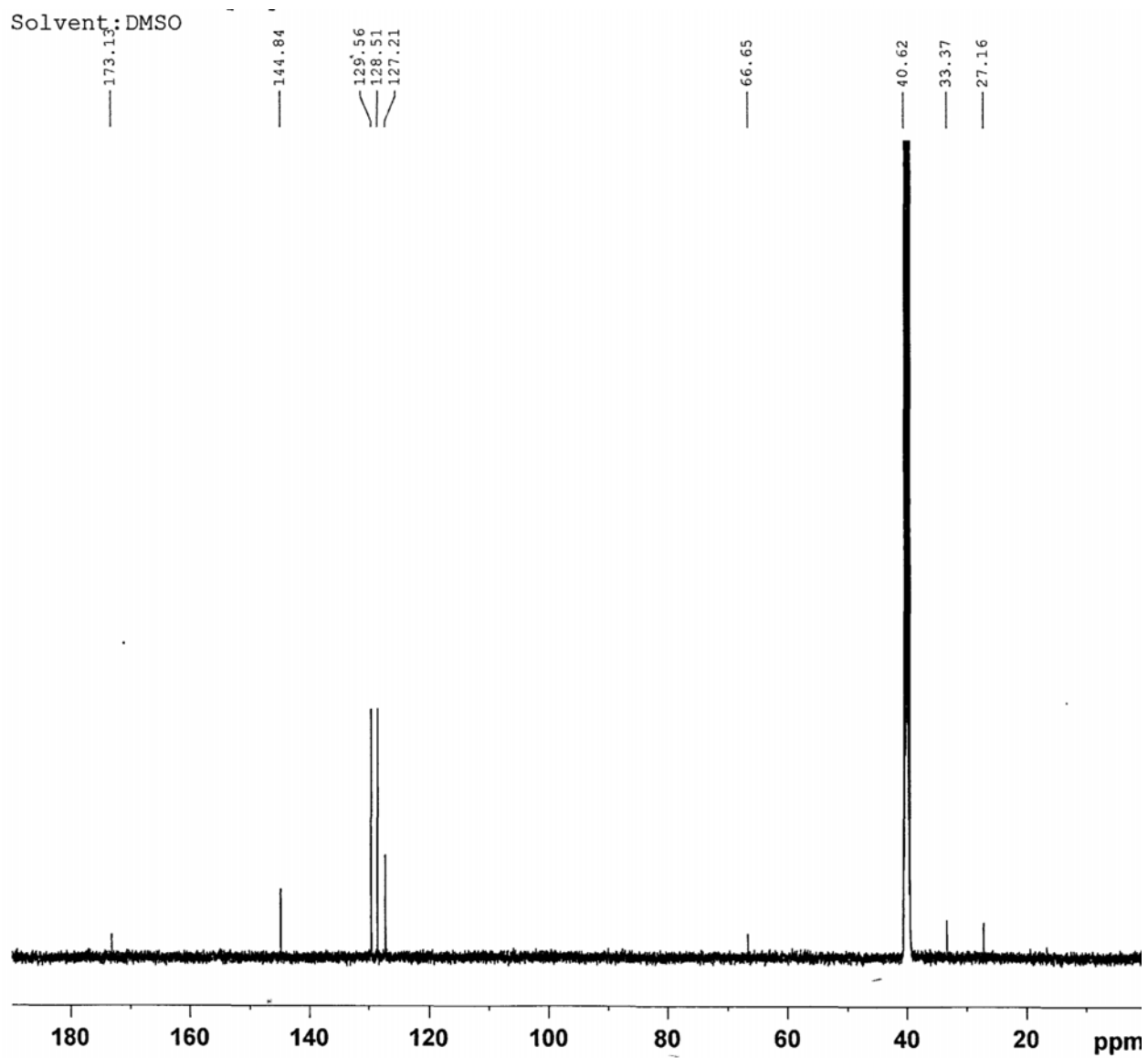


Figure A.1.11. ^{13}C NMR Spectrum of S-Trityl-3-Mercaptopropionic Acid.

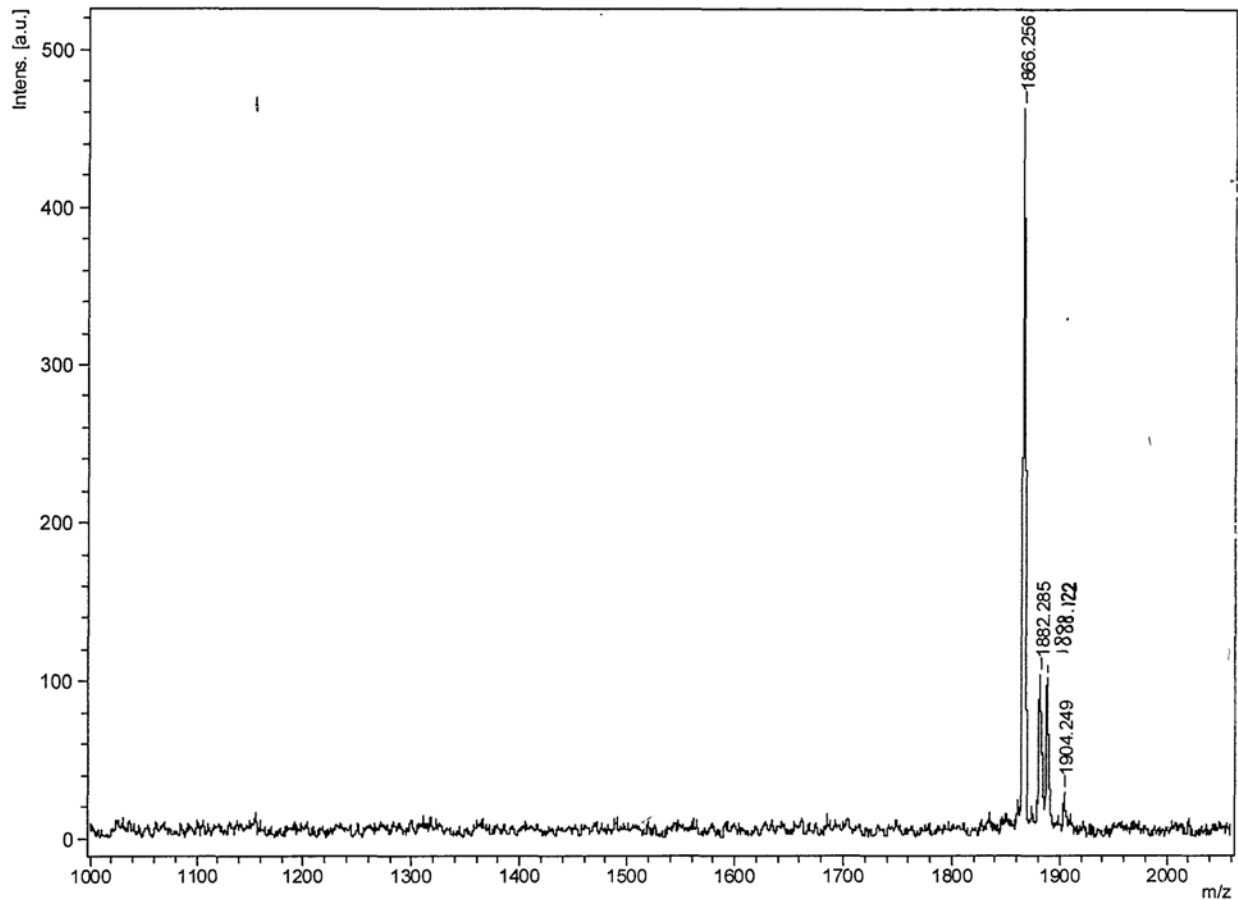


Figure A.1.12. MALDI-TOF MS Spectrum of s-Chemerin9-PEG8-3-Mercaptopropionic Acid.

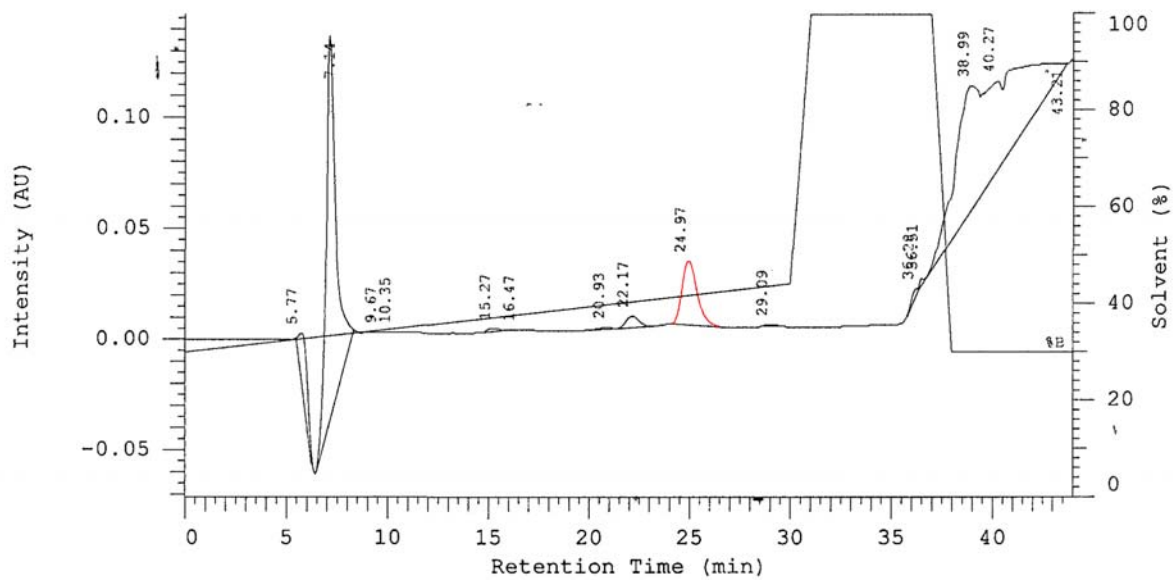


Figure A.1.13. RP-HPLC chromatogram of s-Chemerin9-PEG8-3-Mercaptopropionic Acid. Gradient is 30 to 45 percent Solvent B. Elution of product at 24.97 min. Peak of interest is highlighted in red.

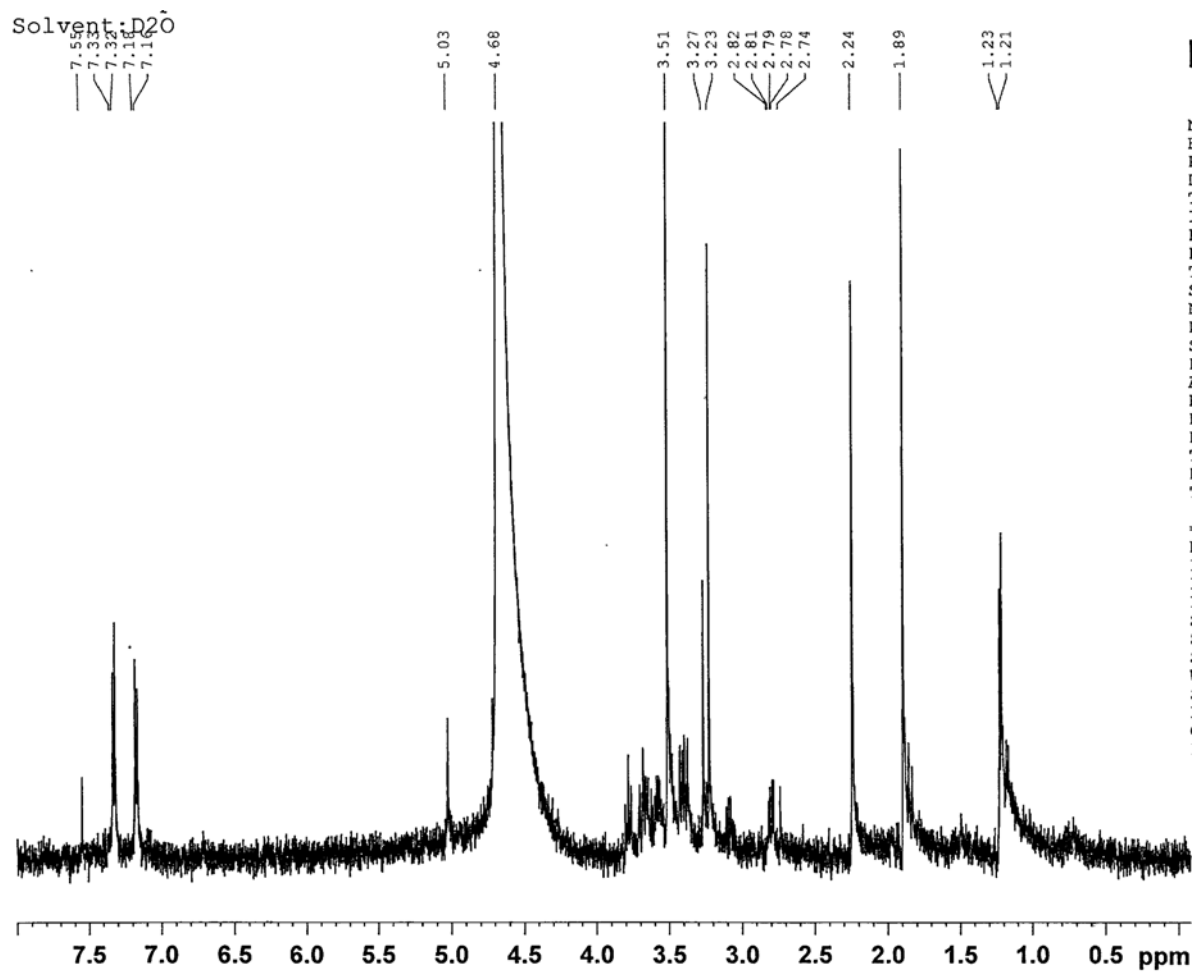


Figure A.1.14. ^1H NMR Spectre of reaction with piperidine resulting in hydrolyzed maleimide lyso GM1.

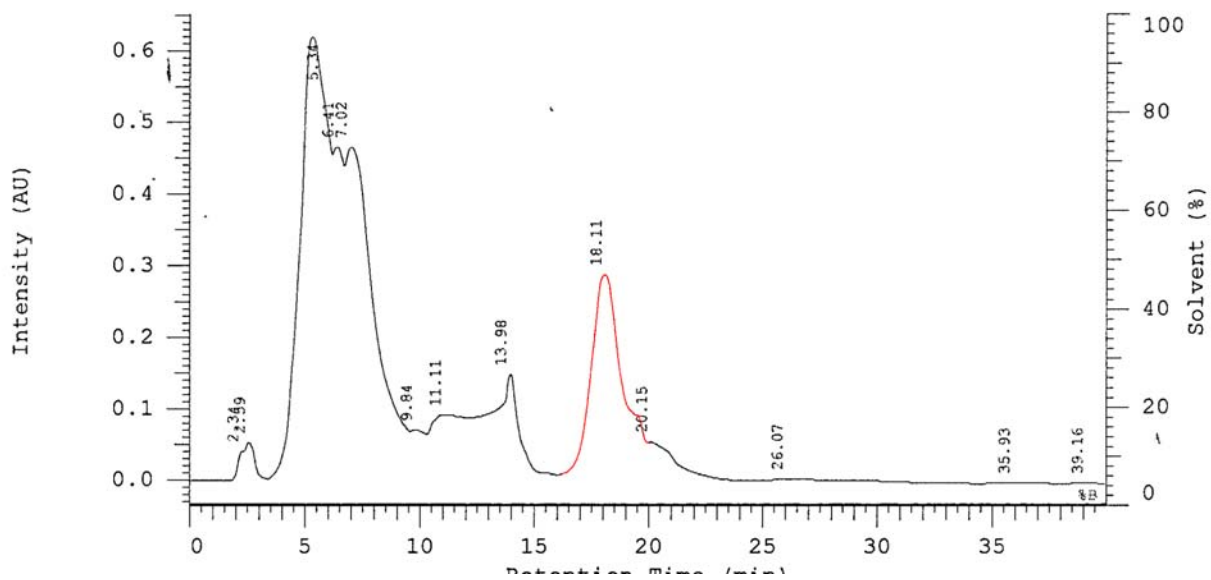


Figure A.1.15. NP-HPLC Chromatogram of maleimide-GM1. Isochratic in 46.7:46.7:7 Isopropanol: hexane: water. Elution of maleimide GM1 at 18.11 min. Peak of interest is highlighted in red.

Solvent: D2O

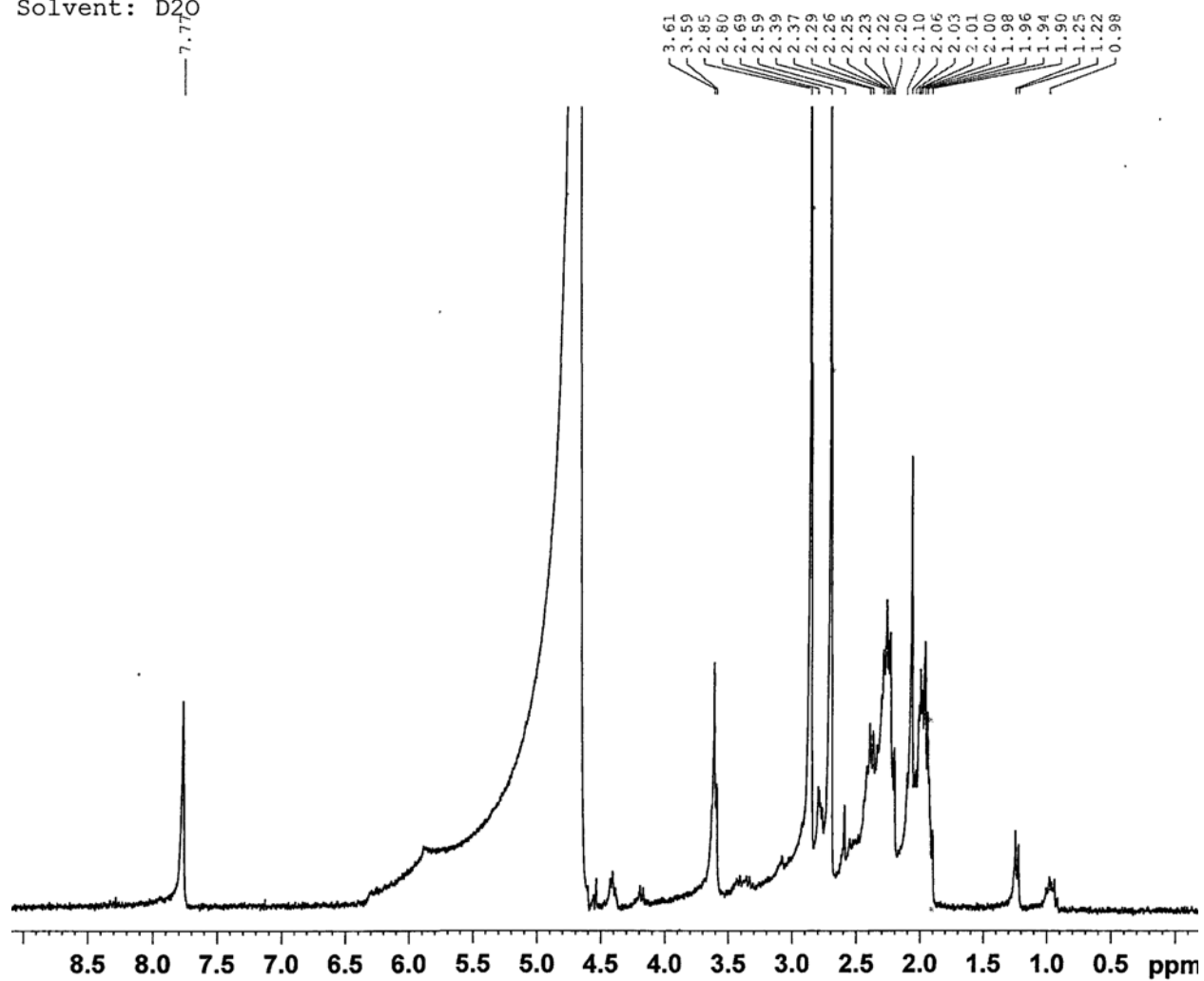


Figure A.1.16. ^1H NMR Spectrum of N-ethylmaleimide and glutathione reaction with TCEP at time zero.

Solvent: D2O

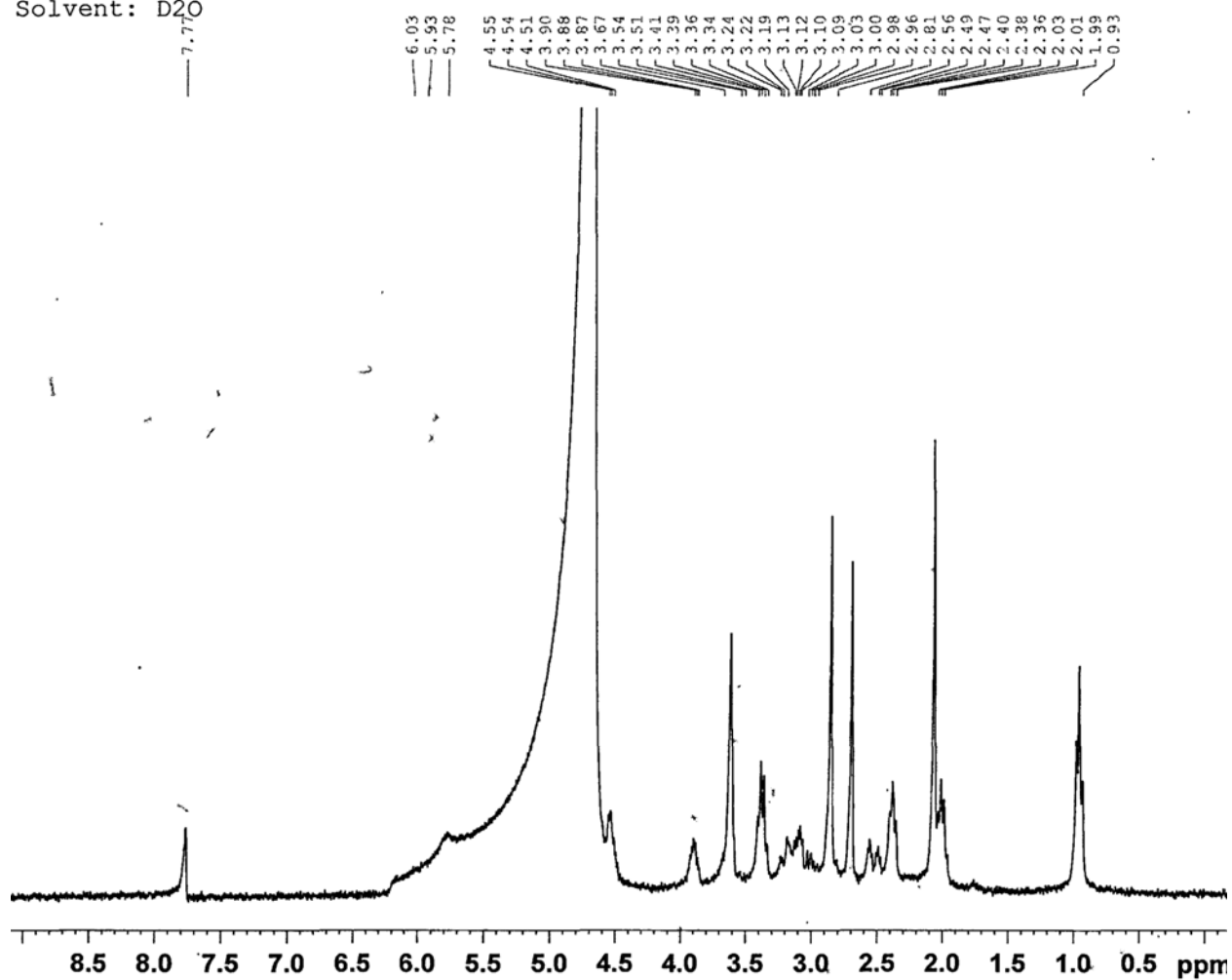


Figure A.1.17. ^1H NMR Spectrum of N-ethylmaleimide and glutathione reaction without TCEP at time zero.

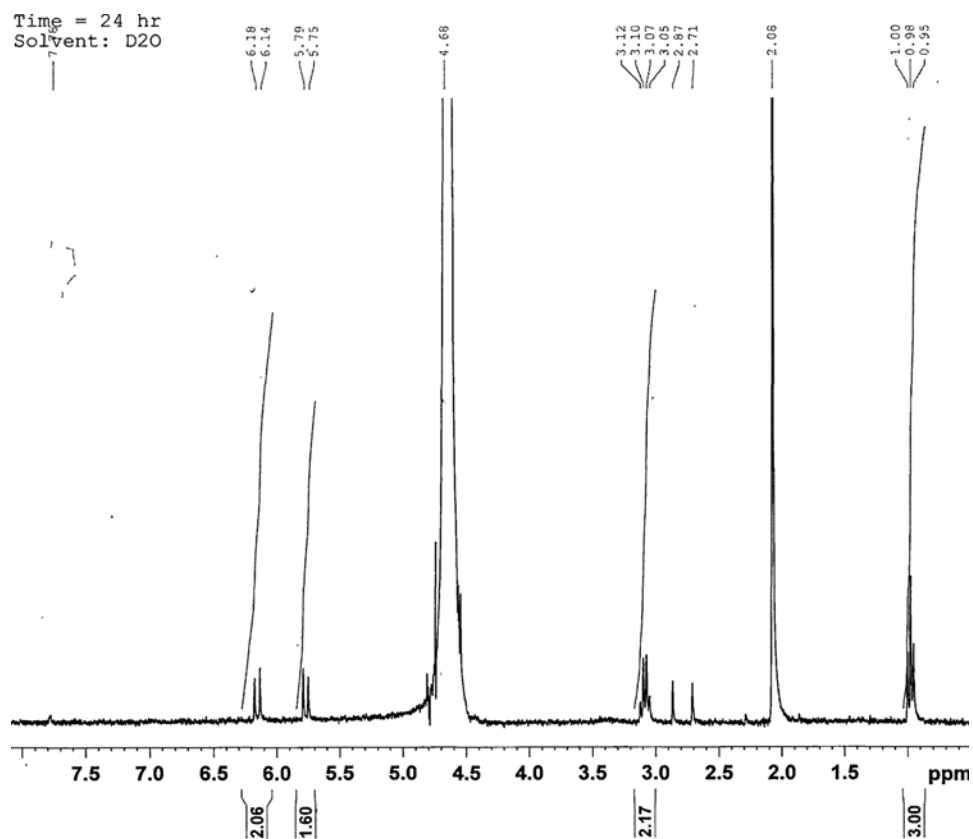
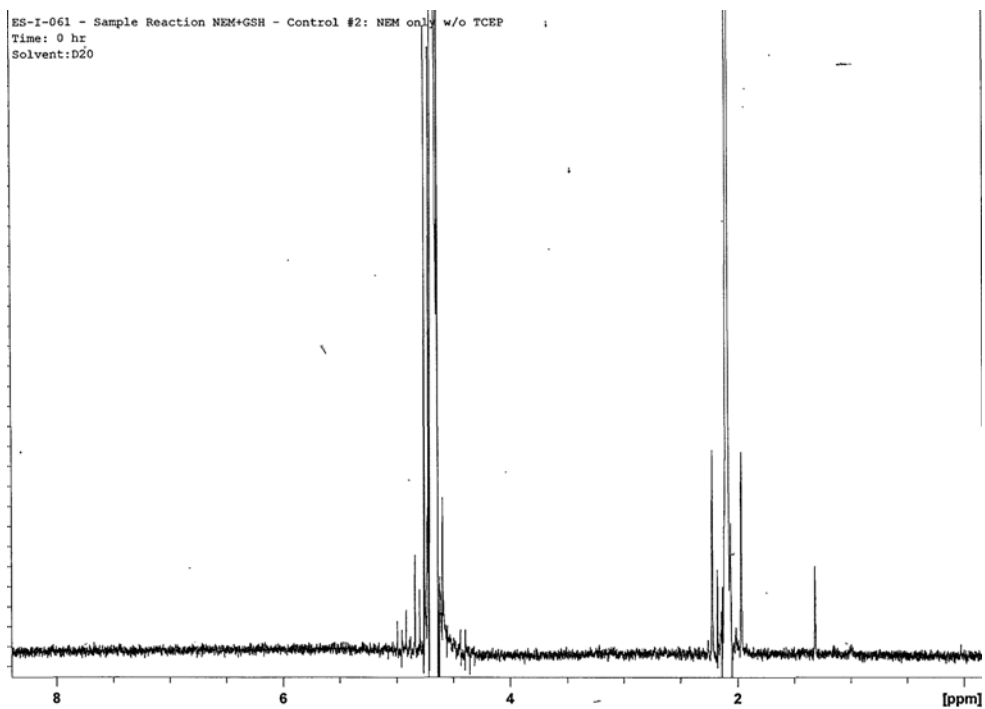


Figure A.1.18. ^1H NMR Spectrum of N-ethyl maleimide control without TCEP at time zero and 24 hours.

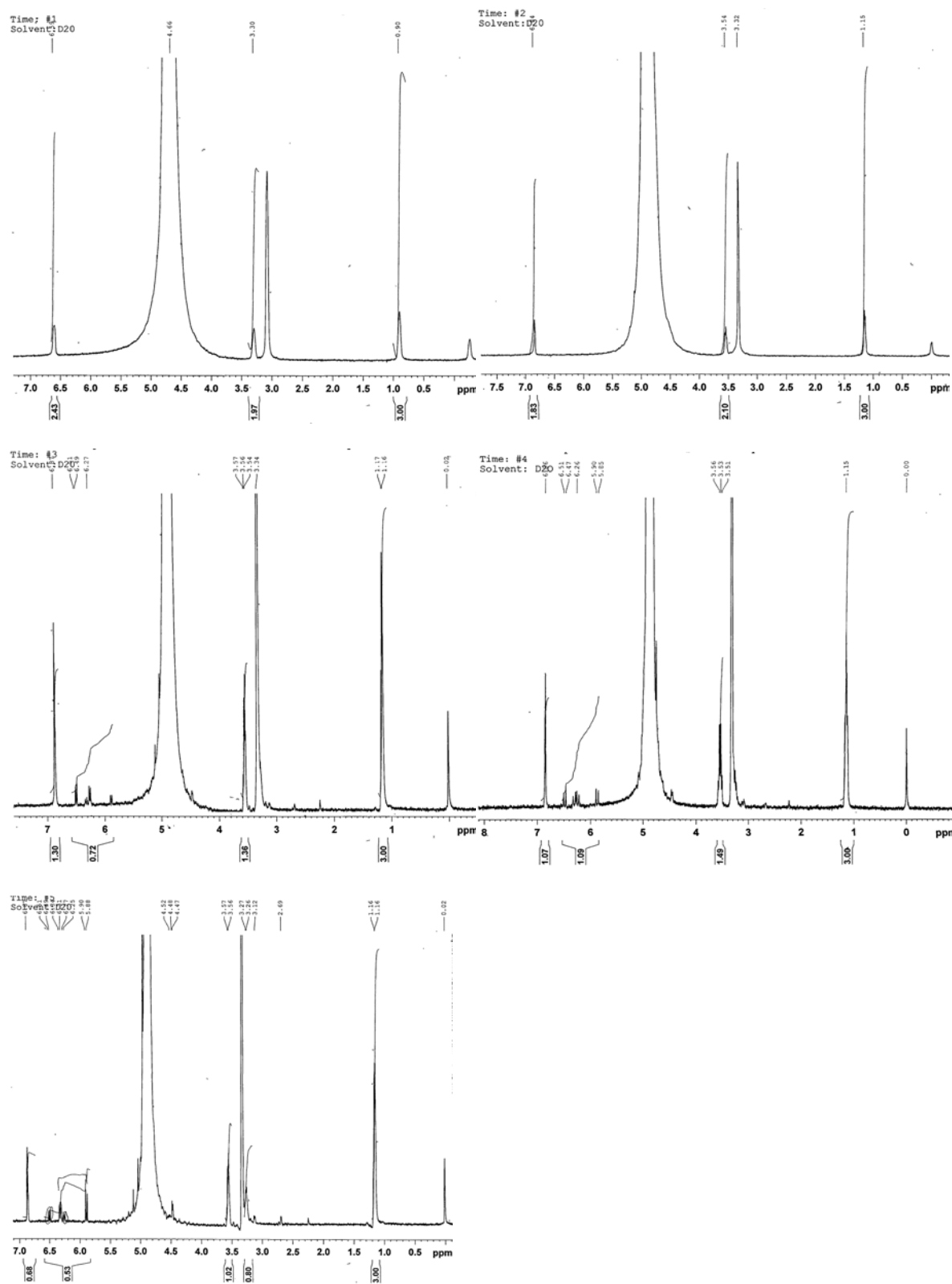


Figure A.1.19. ^1H NMR Spectrum of N-ethyl maleimide control time course experiment over 24 hours at time: 5 minutes, 30 minutes, 4 hours, 9 hours and 24 hours.

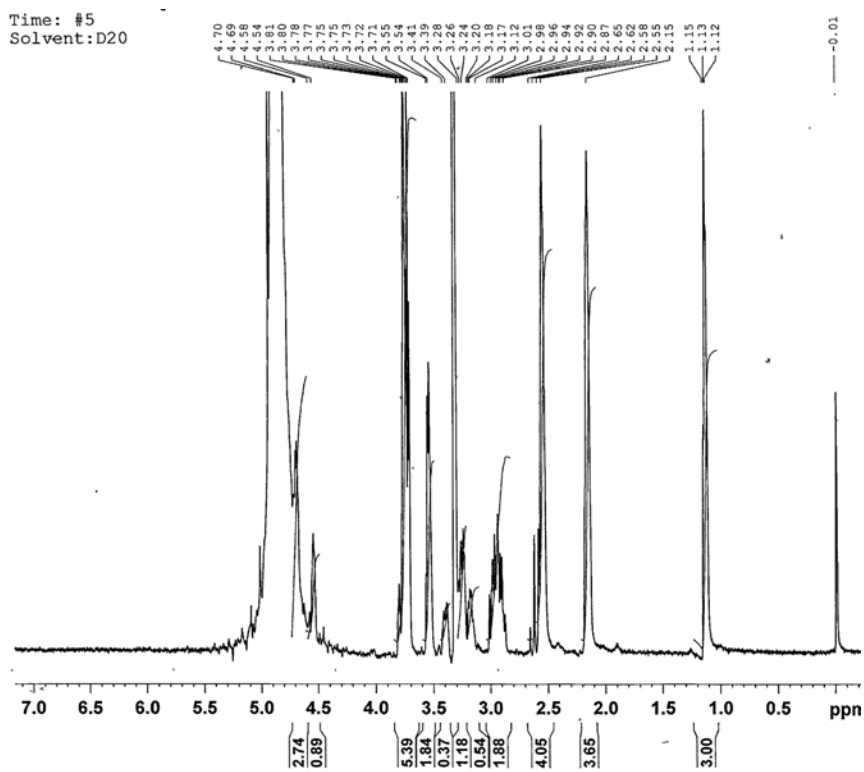
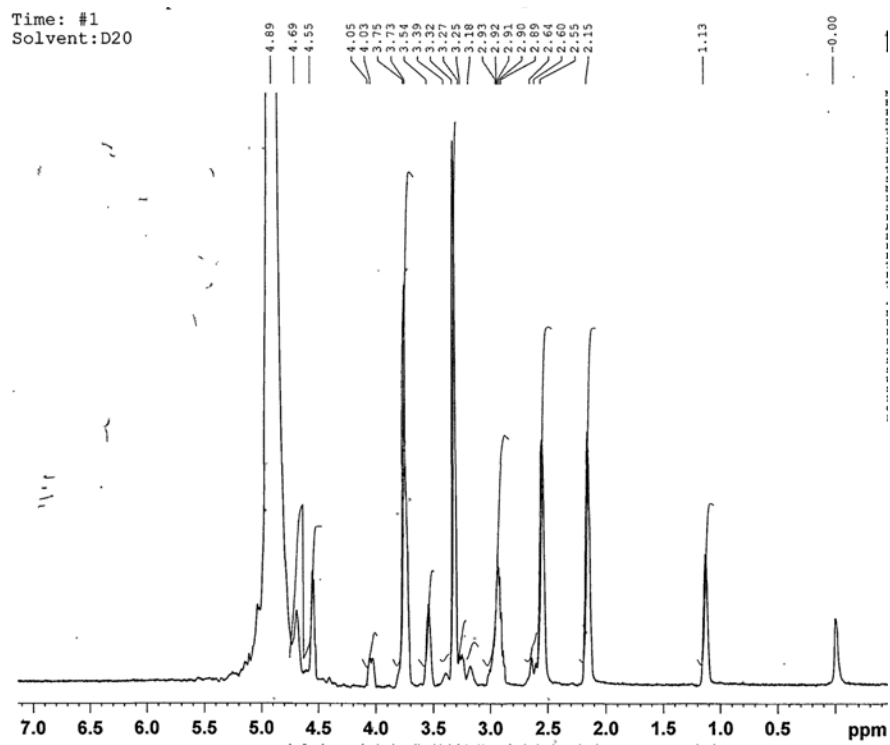


Figure A.1.20. ^1H NMR Spectrum of N-ethylmaleimide and glutathione reaction without TCEP over 24 hours at time 5 minutes and 24 hours.

BIBLIOGRAPHY

1. Kostenis, E., Conklin, B. R. & Wess, J. Molecular basis of receptor/G protein coupling selectivity studied by coexpression of wild type and mutant m2 muscarinic receptors with mutant G alpha(q) subunits. *Biochemistry* **36**, 1487–95 (1997).
2. Rourke, J. L., Dranse, H. J. & Sinal, C. J. Towards an integrative approach to understanding the role of chemerin in human health and disease. *Obesity reviews : an official journal of the International Association for the Study of Obesity* **14**, 245–62 (2013).
3. Wittamer, V. *et al.* Specific recruitment of antigen-presenting cells by chemerin, a novel processed ligand from human inflammatory fluids. *The Journal of experimental medicine* **198**, 977–85 (2003).
4. Berg, V. *et al.* Human articular chondrocytes express ChemR23 and chemerin; ChemR23 promotes inflammatory signalling upon binding the ligand chemerin(21-157). *Arthritis research & therapy* **12**, R228 (2010).
5. Pachynski, R. K. *et al.* The chemoattractant chemerin suppresses melanoma by recruiting natural killer cell antitumor defenses. *The Journal of experimental medicine* **209**, 1427–35 (2012).
6. Roh, S. *et al.* Chemerin--a new adipokine that modulates adipogenesis via its own receptor. *Biochemical and biophysical research communications* **362**, 1013–8 (2007).
7. Cash, J. L. *et al.* Synthetic chemerin-derived peptides suppress inflammation through ChemR23. *The Journal of experimental medicine* **205**, 767–75 (2008).
8. Covic, L., Gresser, A. L., Talavera, J., Swift, S. & Kuliopulos, A. Activation and inhibition of G protein-coupled receptors by cell-penetrating membrane-tethered peptides. *Proceedings of the National Academy of Sciences of the United States of America* **99**, 643–8 (2002).
9. Covic, L., Misra, M., Badar, J., Singh, C. & Kuliopulos, A. Pepducin-based intervention of thrombin-receptor signaling and systemic platelet activation. *Nature medicine* **8**, 1161–5 (2002).
10. Altenbach, C., Kusnetzow, A. K., Ernst, O. P., Hofmann, K. P. & Hubbell, W. L. High-resolution distance mapping in rhodopsin reveals the pattern of helix movement due to activation. *Proceedings of the National Academy of Sciences of the United States of America* **105**, 7439–44 (2008).
11. Yao, X. *et al.* Coupling ligand structure to specific conformational switches in the beta2-adrenoceptor. *Nature chemical biology* **2**, 417–22 (2006).

12. Farrens, D. L., Altenbach, C., Yang, K., Hubbell, W. L. & Khorana, H. G. Requirement of rigid-body motion of transmembrane helices for light activation of rhodopsin. *Science (New York, N.Y.)* **274**, 768–70 (1996).
13. Fortin, J.-P. *et al.* Membrane-tethered ligands are effective probes for exploring class B1 G protein-coupled receptor function. *Proceedings of the National Academy of Sciences of the United States of America* **106**, 8049–54 (2009).
14. Fortin, J.-P., Chinnapen, D., Beinborn, M., Lencer, W. & Kopin, A. S. Discovery of dual-action membrane-anchored modulators of incretin receptors. *PloS one* **6**, e24693 (2011).
15. Davson, H. & Danielli, J. F. *The Permeability of Natural Membranes*. 365 (Cambridge University Press: Cambridge, UK, 1952).
16. Yeagle, P. L. Lipid regulation of cell membrane structure and function. *FASEB journal : official publication of the Federation of American Societies for Experimental Biology* **3**, 1833–42 (1989).
17. Clandinin, M. T., Jumpsen, J. & Suh, M. Relationship between fatty acid accretion, membrane composition, and biologic functions. *The Journal of pediatrics* **125**, S25–32 (1994).
18. Boesze-Battaglia, K. & Schimmel, R. Cell membrane lipid composition and distribution: implications for cell function and lessons learned from photoreceptors and platelets. *The Journal of experimental biology* **200**, 2927–36 (1997).
19. Van Meer, G., Voelker, D. R. & Feigenson, G. W. Membrane lipids: where they are and how they behave. *Nature reviews. Molecular cell biology* **9**, 112–24 (2008).
20. Demel, R. A., Geurts van Kessel, W. S. M. & Van Deenen, L. L. M. The properties of polyunsaturated lecithins in monolayers and liposomes and the interactions of these lecithins with cholesterol. *Biochimica et Biophysica Acta (BBA) - Biomembranes* **266**, 26–40 (1972).
21. Yeagle, P. L. Modulation of membrane function by cholesterol. *Biochimie* **73**, 1303–10 (1991).
22. Danielli, J. F. & Davson, H. A contribution to the theory of permeability of thin films. *Journal of Cellular and Comparative Physiology* **5**, 495–508 (1935).
23. Edidin, M. Lipids on the frontier: a century of cell-membrane bilayers. *Nature reviews. Molecular cell biology* **4**, 414–8 (2003).
24. Langmuir, I. The Constitution and Fundamental Properties of Solids and Liquids. II. Liquids. *Journal of the American Chemical Society* **39**, 1848–1906 (1917).

25. Gorter, E. On Bimolecular Layers of Lipoids on the Chromocytes of the Blood. *Journal of Experimental Medicine* **41**, 439–443 (1925).
26. Singer, S. J. & Nicolson, G. L. The fluid mosaic model of the structure of cell membranes. *Science (New York, N.Y.)* **175**, 720–31 (1972).
27. Bagatolli, L. a, Ipsen, J. H., Simonsen, A. C. & Mouritsen, O. G. An outlook on organization of lipids in membranes: searching for a realistic connection with the organization of biological membranes. *Progress in lipid research* **49**, 378–89 (2010).
28. Shimshick, E. J. & McConnell, H. M. Lateral phase separation in phospholipid membranes. *Biochemistry* **12**, 2351–60 (1973).
29. Jain, M. K. & White, H. B. Long-range order in biomembranes. *Advances in lipid research* **15**, 1–60 (1977).
30. Brown, D. a & Rose, J. K. Sorting of GPI-anchored proteins to glycolipid-enriched membrane subdomains during transport to the apical cell surface. *Cell* **68**, 533–44 (1992).
31. Simons, K. & Ikonen, E. Functional rafts in cell membranes. *Nature* **387**, 569–72 (1997).
32. Tran, D., Carpentier, J. L., Sawano, F., Gorden, P. & Orci, L. Ligands internalized through coated or noncoated invaginations follow a common intracellular pathway. *Proceedings of the National Academy of Sciences of the United States of America* **84**, 7957–61 (1987).
33. Rothberg, K. G., Ying, Y. S., Kamen, B. a & Anderson, R. G. Cholesterol controls the clustering of the glycopospholipid-anchored membrane receptor for 5-methyltetrahydrofolate. *The Journal of cell biology* **111**, 2931–8 (1990).
34. Simons, K. & Gerl, M. J. Revitalizing membrane rafts: new tools and insights. *Nature reviews. Molecular cell biology* **11**, 688–99 (2010).
35. Kenworthy, A. K. *et al.* Dynamics of putative raft-associated proteins at the cell surface. *The Journal of cell biology* **165**, 735–46 (2004).
36. Glebov, O. O. & Nichols, B. J. Lipid raft proteins have a random distribution during localized activation of the T-cell receptor. *Nature cell biology* **6**, 238–43 (2004).
37. Eggeling, C. *et al.* Direct observation of the nanoscale dynamics of membrane lipids in a living cell. *Nature* **457**, 1159–62 (2009).
38. Pike, L. J. Rafts defined: a report on the Keystone Symposium on Lipid Rafts and Cell Function. *Journal of lipid research* **47**, 1597–8 (2006).
39. Lingwood, D. & Simons, K. Lipid rafts as a membrane-organizing principle. *Science (New York, N.Y.)* **327**, 46–50 (2010).

40. Doherty, G. J. & McMahon, H. T. Mechanisms of endocytosis. *Annual review of biochemistry* **78**, 857–902 (2009).
41. Hansen, C. G. & Nichols, B. J. Molecular mechanisms of clathrin-independent endocytosis. *Journal of cell science* **122**, 1713–21 (2009).
42. Steinman, R. M., Mellman, I. S., Muller, W. a & Cohn, Z. a Endocytosis and the recycling of plasma membrane. *The Journal of cell biology* **96**, 1–27 (1983).
43. Grant, B. D. & Donaldson, J. G. Pathways and mechanisms of endocytic recycling. *Nature reviews. Molecular cell biology* **10**, 597–608 (2009).
44. Rodal, S. K. *et al.* Extraction of cholesterol with methyl-beta-cyclodextrin perturbs formation of clathrin-coated endocytic vesicles. *Molecular biology of the cell* **10**, 961–74 (1999).
45. Subtil, a *et al.* Acute cholesterol depletion inhibits clathrin-coated pit budding. *Proceedings of the National Academy of Sciences of the United States of America* **96**, 6775–80 (1999).
46. Conner, S. D. & Schmid, S. L. Regulated portals of entry into the cell. *Nature* **422**, 37–44 (2003).
47. Lajoie, P. & Nabi, I. R. Regulation of raft-dependent endocytosis. *Journal of cellular and molecular medicine* **11**, 644–53 (2007).
48. Sandvig, K. & Van Deurs, B. Selective modulation of the endocytic uptake of ricin and fluid phase markers without alteration in transferrin endocytosis. *The Journal of biological chemistry* **265**, 6382–8 (1990).
49. Damke, H., Baba, T., Van der Blik, a M. & Schmid, S. L. Clathrin-independent pinocytosis is induced in cells overexpressing a temperature-sensitive mutant of dynamin. *The Journal of cell biology* **131**, 69–80 (1995).
50. Swanson, J. A. & Watts, C. Macropinocytosis. *Trends in cell biology* **5**, 424–8 (1995).
51. Palade, G. Fine structure of blood capillaries. *J Appl Phys* **27**, 482–482 (1953).
52. Henley, J. R., Krueger, E. W., Oswald, B. J. & McNiven, M. a Dynamin-mediated internalization of caveolae. *The Journal of cell biology* **141**, 85–99 (1998).
53. Oh, P., McIntosh, D. P. & Schnitzer, J. E. Dynamin at the neck of caveolae mediates their budding to form transport vesicles by GTP-driven fission from the plasma membrane of endothelium. *The Journal of cell biology* **141**, 101–14 (1998).

54. Fra, a M., Williamson, E., Simons, K. & Parton, R. G. De novo formation of caveolae in lymphocytes by expression of VIP21-caveolin. *Proceedings of the National Academy of Sciences of the United States of America* **92**, 8655–9 (1995).
55. Bastiani, M. & Parton, R. G. Caveolae at a glance. *Journal of cell science* **123**, 3831–6 (2010).
56. Hayer, A., Stoeber, M., Bissig, C. & Helenius, A. Biogenesis of caveolae: stepwise assembly of large caveolin and cavin complexes. *Traffic (Copenhagen, Denmark)* **11**, 361–82 (2010).
57. Tagawa, A. *et al.* Assembly and trafficking of caveolar domains in the cell: caveolae as stable, cargo-triggered, vesicular transporters. *The Journal of cell biology* **170**, 769–79 (2005).
58. Cheng, Z.-J., Singh, R. D., Marks, D. L. & Pagano, R. E. Membrane microdomains, caveolae, and caveolar endocytosis of sphingolipids. *Molecular membrane biology* **23**, 101–10 (2006).
59. Pol, A. *et al.* Cholesterol and Fatty Acids Regulate Dynamic Caveolin Cell Surface and Lipid Bodies □. **16**, 2091–2105 (2005).
60. Singh, R. D. *et al.* Gangliosides and beta1-integrin are required for caveolae and membrane domains. *Traffic (Copenhagen, Denmark)* **11**, 348–60 (2010).
61. Chini, B. & Parenti, M. G-protein coupled receptors in lipid rafts and caveolae: how, when and why do they go there? *Journal of molecular endocrinology* **32**, 325–38 (2004).
62. Kozera, L., White, E. & Calaghan, S. Caveolae act as membrane reserves which limit mechanosensitive I(Cl,swell) channel activation during swelling in the rat ventricular myocyte. *PloS one* **4**, e8312 (2009).
63. Le, P. U., Guay, G., Altschuler, Y. & Nabi, I. R. Caveolin-1 is a negative regulator of caveolae-mediated endocytosis to the endoplasmic reticulum. *The Journal of biological chemistry* **277**, 3371–9 (2002).
64. Mayor, S. & Pagano, R. E. Pathways of clathrin-independent endocytosis. *Nature reviews. Molecular cell biology* **8**, 603–12 (2007).
65. Tettamanti, G. Ganglioside/glycosphingolipid turnover: new concepts. *Glycoconjugate journal* **20**, 301–17 (2004).
66. Dickson, R. C. Sphingolipid functions in *Saccharomyces cerevisiae*: comparison to mammals. *Annual review of biochemistry* **67**, 27–48 (1998).

67. Fuller, M. Sphingolipids: the nexus between Gaucher disease and insulin resistance. *Lipids in health and disease* **9**, 113 (2010).
68. Iglesias-Bartolomé, R. *et al.* Differential endocytic trafficking of neuropathy-associated antibodies to GM1 ganglioside and cholera toxin in epithelial and neural cells. *Biochimica et biophysica acta* **1788**, 2526–40 (2009).
69. Keenan, T. W., Morré, D. J. & Basu, S. Ganglioside biosynthesis. Concentration of glycosphingolipid glycosyltransferases in Golgi apparatus from rat liver. *The Journal of biological chemistry* **249**, 310–5 (1974).
70. Merrill, H. Characterization of serine palmitoyltransferase hamster ovary cells. **754**, 284–291 (1983).
71. Michel, C., Echten-deckert, G. Van, Sandhoff, K., Wang, E. & Merrill, A. H. Characterization of Ceramide Synthesis. **272**, 22432–22437 (1997).
72. Ichikawa, S. & Hirabayashi, Y. Glucosylceramide synthase and glycosphingolipid synthesis. *Trends in cell biology* **8**, 198–202 (1998).
73. Linke, T. *et al.* Interfacial regulation of acid ceramidase activity. Stimulation of ceramide degradation by lysosomal lipids and sphingolipid activator proteins. *The Journal of biological chemistry* **276**, 5760–8 (2001).
74. Chinnapen, D. J.-F. *et al.* Lipid sorting by ceramide structure from plasma membrane to ER for the cholera toxin receptor ganglioside GM1. *Developmental cell* **23**, 573–86 (2012).
75. Sack, D. a, Sack, R. B., Nair, G. B. & Siddique, a K. Cholera. *Lancet* **363**, 223–33 (2004).
76. Chinnapen, D. J.-F., Chinnapen, H., Saslowsky, D. & Lencer, W. I. Rafting with cholera toxin: endocytosis and trafficking from plasma membrane to ER. *FEMS microbiology letters* **266**, 129–37 (2007).
77. Merritt, E. a *et al.* Crystal structure of cholera toxin B-pentamer bound to receptor GM1 pentasaccharide. *Protein science : a publication of the Protein Society* **3**, 166–75 (1994).
78. MacKenzie, C. R., Hiramata, T., Lee, K. K., Altman, E. & Young, N. M. Quantitative analysis of bacterial toxin affinity and specificity for glycolipid receptors by surface plasmon resonance. *The Journal of biological chemistry* **272**, 5533–8 (1997).
79. Nichols, B. J. A distinct class of endosome mediates clathrin-independent endocytosis to the Golgi complex. *Nature cell biology* **4**, 374–8 (2002).
80. Kirkham, M. *et al.* Ultrastructural identification of uncoated caveolin-independent early endocytic vehicles. *The Journal of cell biology* **168**, 465–76 (2005).

81. Maccioni, H. J. F., Giraudo, C. G. & Daniotti, J. L. Understanding the stepwise synthesis of glycolipids. *Neurochemical research* **27**, 629–36 (2002).
82. Badizadegan, K., Wheeler, H. E., Fujinaga, Y. & Lencer, W. I. Trafficking of cholera toxin-ganglioside GM1 complex into Golgi and induction of toxicity depend on actin cytoskeleton. *American journal of physiology. Cell physiology* **287**, C1453–62 (2004).
83. Stevens, R. C. *et al.* The GPCR Network: a large-scale collaboration to determine human GPCR structure and function. *Nature reviews. Drug discovery* **12**, 25–34 (2013).
84. Audet, M. & Bouvier, M. Restructuring G-protein-coupled receptor activation. *Cell* **151**, 14–23 (2012).
85. Zhang, X. & Eggert, U. S. Non-traditional roles of G protein-coupled receptors in basic cell biology. *Molecular bioSystems* **9**, 586–95 (2013).
86. Tuteja, N. Signaling through G protein coupled receptors. *Plant signaling & behavior* **4**, 942–7 (2009).
87. Rosenbaum, D. M., Rasmussen, S. G. F. & Kobilka, B. K. The structure and function of G-protein-coupled receptors. *Nature* **459**, 356–63 (2009).
88. Lagerström, M. C. & Schiöth, H. B. Structural diversity of G protein-coupled receptors and significance for drug discovery. *Nature reviews. Drug discovery* **7**, 339–57 (2008).
89. Granier, S. & Kobilka, B. A new era of GPCR structural and chemical biology. *Nature chemical biology* **8**, 670–3 (2012).
90. Ferguson, S. S. G., Zhang, J., Barak, L. S. & Caron, M. G. Molecular mechanisms of G protein-coupled receptor desensitization and resensitization. *Life sciences* **62**, 1561–5 (1998).
91. McCudden, C. R., Hains, M. D., Kimple, R. J., Siderovski, D. P. & Willard, F. S. G-protein signaling: back to the future. *Cellular and molecular life sciences : CMLS* **62**, 551–77 (2005).
92. Wall, M. A., Posner, B. A. & Sprang, S. R. Structural basis of activity and subunit recognition in G protein heterotrimers. *Structure (London, England : 1993)* **6**, 1169–83 (1998).
93. Wedegaertner, P. B., Wilson, P. T. & Bourne, H. R. Lipid modifications of trimeric G proteins. *The Journal of biological chemistry* **270**, 503–6 (1995).
94. Ford, C. E. *et al.* Molecular basis for interactions of G protein betagamma subunits with effectors. *Science (New York, N.Y.)* **280**, 1271–4 (1998).

95. Li, Y. *et al.* Sites for Galpha binding on the G protein beta subunit overlap with sites for regulation of phospholipase Cbeta and adenylyl cyclase. *The Journal of biological chemistry* **273**, 16265–72 (1998).
96. SUTHERLAND, E. W. & RALL, T. W. Fractionation and characterization of a cyclic adenine ribonucleotide formed by tissue particles. *The Journal of biological chemistry* **232**, 1077–91 (1958).
97. BERTHET, J., RALL, T. W. & SUTHERLAND, E. W. The relationship of epinephrine and glucagon to liver phosphorylase. IV. Effect of epinephrine and glucagon on the reactivation of phosphorylase in liver homogenates. *The Journal of biological chemistry* **224**, 463–75 (1957).
98. Ross, E. M. & Gilman, A. G. Resolution of some components of adenylyl cyclase necessary for catalytic activity. *The Journal of biological chemistry* **252**, 6966–9 (1977).
99. Hoffman, B. B. & Lefkowitz, R. J. Adrenergic receptors in the heart. *Annual review of physiology* **44**, 475–84 (1982).
100. Berstein, G. *et al.* Phospholipase C-beta 1 is a GTPase-activating protein for Gq/11, its physiologic regulator. *Cell* **70**, 411–8 (1992).
101. Siderovski, D. P., Hessel, A., Chung, S., Mak, T. W. & Tyers, M. A new family of regulators of G-protein-coupled receptors? *Current biology : CB* **6**, 211–2 (1996).
102. Shi, L. *et al.* Beta2 adrenergic receptor activation. Modulation of the proline kink in transmembrane 6 by a rotamer toggle switch. *The Journal of biological chemistry* **277**, 40989–96 (2002).
103. Swaminath, G. *et al.* Probing the beta2 adrenoceptor binding site with catechol reveals differences in binding and activation by agonists and partial agonists. *The Journal of biological chemistry* **280**, 22165–71 (2005).
104. Overington, J. P., Al-Lazikani, B. & Hopkins, A. L. How many drug targets are there? *Nature reviews. Drug discovery* **5**, 993–6 (2006).
105. Covic, L., Gresser, A. L., Talavera, J., Swift, S. & Kuliopulos, A. Activation and inhibition of G protein-coupled receptors by cell-penetrating membrane-tethered peptides. *Proceedings of the National Academy of Sciences of the United States of America* **99**, 643–8 (2002).
106. Kjelsberg, M. A., Cotecchia, S., Ostrowski, J., Caron, M. G. & Lefkowitz, R. J. Constitutive activation of the alpha 1B-adrenergic receptor by all amino acid substitutions at a single site. Evidence for a region which constrains receptor activation. *The Journal of biological chemistry* **267**, 1430–3 (1992).

107. Luttrell, L. M., Ostrowski, J., Cotecchia, S., Kendall, H. & Lefkowitz, R. J. Antagonism of catecholamine receptor signaling by expression of cytoplasmic domains of the receptors. *Science (New York, N.Y.)* **259**, 1453–7 (1993).
108. Lomas-Neira, J. & Ayala, A. Pepducins: an effective means to inhibit GPCR signaling by neutrophils. *Trends in immunology* **26**, 619–21 (2005).
109. Yoshimura, T. & Oppenheim, J. J. Chemokine-like receptor 1 (CMKLR1) and chemokine (C-C motif) receptor-like 2 (CCRL2); two multifunctional receptors with unusual properties. *Experimental cell research* **317**, 674–84 (2011).
110. Goralski, K. B. *et al.* Chemerin, a novel adipokine that regulates adipogenesis and adipocyte metabolism. *The Journal of biological chemistry* **282**, 28175–88 (2007).
111. Bozaoglu, K. *et al.* Chemerin is a novel adipokine associated with obesity and metabolic syndrome. *Endocrinology* **148**, 4687–94 (2007).
112. Chakaroun, R. *et al.* Effects of weight loss and exercise on chemerin serum concentrations and adipose tissue expression in human obesity. *Metabolism: clinical and experimental* **61**, 706–14 (2012).
113. Shimamura, K. *et al.* Identification of a stable chemerin analog with potent activity toward ChemR23. *Peptides* **30**, 1529–38 (2009).
114. Wittamer, V. *et al.* The C-terminal nonapeptide of mature chemerin activates the chemerin receptor with low nanomolar potency. *The Journal of biological chemistry* **279**, 9956–62 (2004).
115. Schwarzmann, G. & Sandhoff, K. Lysogangliosides: synthesis and use in preparing labeled gangliosides. *Methods in enzymology* **138**, 319–41 (1987).